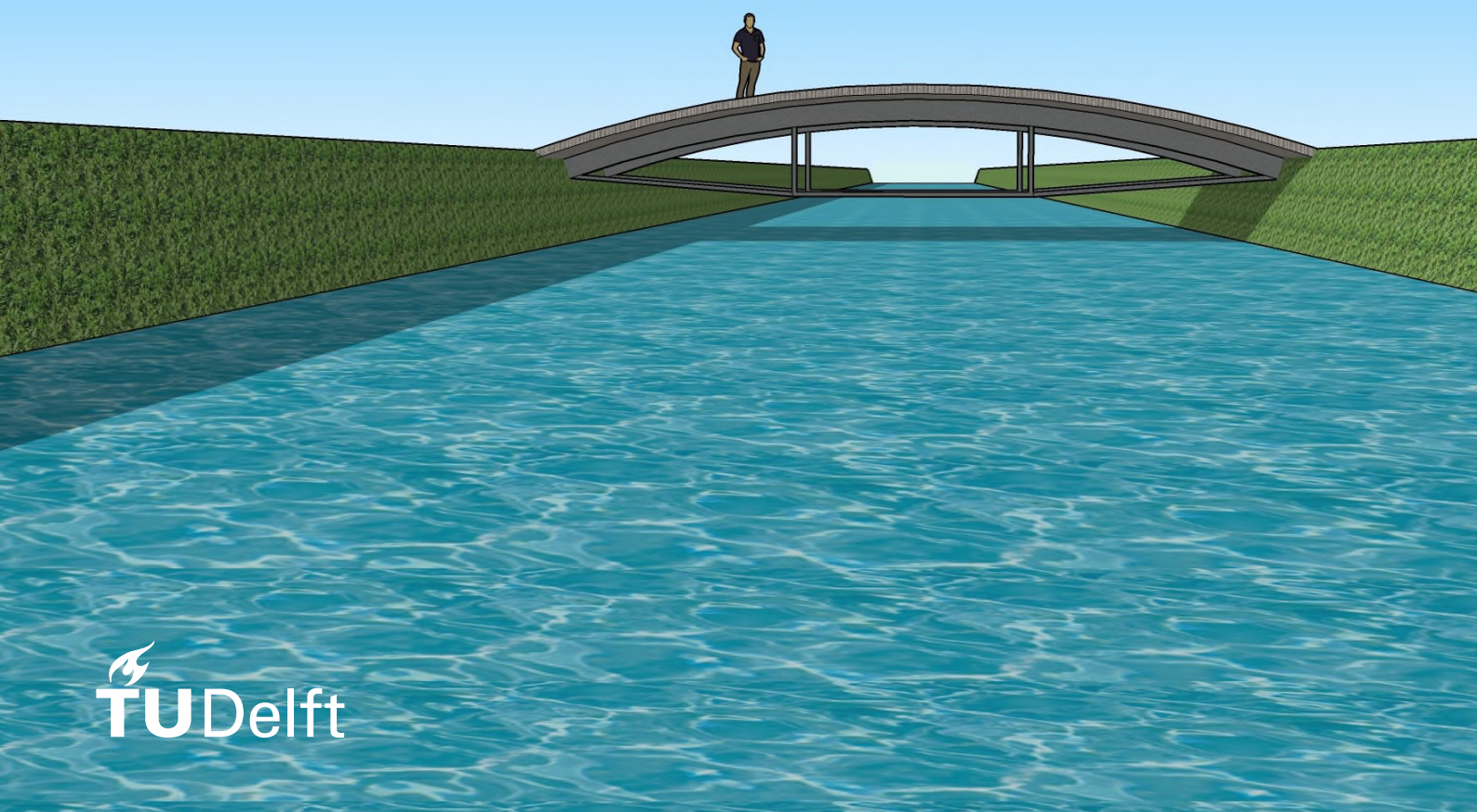


Strain hardening Self-healing concrete Demonstrator Bridge TU Delft

C.E. Roghair



Strain hardening Self-healing concrete

Demonstrator Bridge TU Delft

By

C.E. Roghair

in partial fulfilment of the requirements for the degree of

Master of Science
In Civil Engineering

at the Delft University of Technology,
to be defended publicly on Friday July 7, 2017 at 4:00 PM.

Supervisor:	Dr. H.M. Jonkers	TU Delft
Thesis committee:	Prof. dr. ir. H.E.J.G. Schlangen	TU Delft
	Dr. ir. H.R. Schipper	TU Delft
	Dr. M. Luković	TU Delft

An electronic version of this thesis is available at <http://repository.tudelft.nl/>.

Preface

In this report the result of a research performed in the past year can be found. This research was carried out to obtain the degree Master of Science in Civil Engineering at Delft University of Technology. The research is conducted for the section Materials and Environment. A part of the experiments have been carried out in the Microlab at the section itself, the remaining part of the experiments are performed in the Stevin laboratories.

A lot of people have assisted and supported me while working on my thesis and I would like to thank these people for their support.

First I would like to thank the members of my graduation committee, Dr. H.M. Jonkers, Prof. dr. ir. H.E.J.G. Schlangen, Dr. ir. H.R. Schipper and Dr. M. Luković. It was always possible to ask for some advice about my research or discuss about the questions and problems I had during my research.

Also, I would like to thank the people who explained and helped me by the performance of the experiments, Maiko van Leeuwen, Martin Megalla and Branko Savija. Especially Maiko van Leeuwen who helped me with a lot of experiments and also was there when I did not know how to continue if tests did not go as expected.

Furthermore, I would like to thank Renée Mors for her time to answer my questions and to discuss the results of the tests I have found. We also discussed what was the best manner to show my results in my thesis.

Finally, I want to thank my family, friends and colleagues for their support and advice whenever I needed it.

*C.E. Roghair
Delft, July 2017*

Contents

Abstract	9
1 Introduction	10
1.1. The project	10
1.2. Research	10
1.2.1. Main objective	11
1.2.2. Research questions	11
1.2.3. Expectations	11
1.3. What is SSC?	12
1.3.1. How does SSC work?	12
1.3.2. Concrete cover	13
1.4. Outline report	16
2 Materials & methods	18
2.1. Mixture	18
2.2. Demonstrator Bridge	19
2.2.1. Design parameters	20
2.2.2. Experiments	20
3 Design Demonstrator Bridge	23
3.1. Characteristics SSC vs TC	23
3.2. Structural design SSC	23
3.2.1. Construction	23
3.2.2. Calculation	23
3.3. Structural design TC	25
4 Experimental results	27
4.1. Compressive and flexural strength test	27
4.1.1. Compressive strength	27
4.1.2. Flexural strength	28
4.2. Permeability test	30
4.3. Rapid chloride migration test	33
4.3.1. Uncracked samples	33
4.3.2. Cracked samples	34
4.4. Frost/thaw cycle test	36
4.4.1. First frost/thaw session	36
4.4.2. Frost/thaw session after healing	37
4.5. Young's modulus in compression test	40
4.6. Shrinkage test	41
4.7. Absorption test	42
5 Discussion	43
5.1. Results	43

5.1.1. Compressive and flexural strength test	43
5.1.2. Permeability test	44
5.1.3. Rapid chloride migration test.....	44
5.1.4. Frost/thaw cycle test	46
5.1.5. Young’s modulus in compression test.....	46
5.1.6. Shrinkage test.....	46
5.1.7. Absorption test.....	47
5.2. Demonstrator Bridge	47
5.2.1. Design TC vs. SSC	47
5.2.2. Assumptions structural design	49
6 Conclusions & recommendations.....	52
6.1. Conclusions	52
6.2. Recommendations	53
Bibliography	55
Appendix.....	56

Abstract

In the year 2006, Delft University of Technology started researching 'Strain hardening Self-healing concrete' (SSC). The reason for this research was the desire to increase the durability of concrete. This depends mostly on the reinforcement, which is used to take the tensile forces in the structure.

To ensure a certain lifespan of concrete structures, a minimum cover depth has to be applied on the reinforcement. However, cracks occur in the concrete and cause a significant decrease in durability and thus a decrease in the lifespan of a structure.

Recent research by M. Sierra-Beltran in 2014 resulted in a newly developed SSC that has the capacity to seal these cracks due to the addition of a healing agent to the mixture. Also, fibers are added to the mixture to keep the cracks small and speed up the healing process, because smaller cracks are sealed faster. The expectation is that this will increase the durability of concrete and decrease the need of maintenance due to cracks and corrosion of the reinforcement during the life span.

In this thesis the newly developed SSC is compared with traditional concrete (TC) to show the positive effects of SSC. For this comparison a structural design is made with both materials based on assumed characteristics. Also, tests are performed to check whether those assumed characteristics are right and a short calculation with the results is made.

Some of the tests are performed to research the structural characteristics; compressive strength, flexural strength, Young's modulus and shrinkage. The other tests are to compare the durability of SSC mortar with TC mortar; healing capacity, frost/thaw resistance, chloride migration, and porosity.

When making a structural design with the assumed characteristics for TC and SSC, one finds that it is possible to design more slenderly with SSC than with TC. This is caused by the decrease in cover depth and the absence of extra reinforcement to control the crack width. The only exception is the height of the bridge deck; the height of the bridge deck is slightly smaller in a TC design. This is caused by the low Young's modulus of SSC.

The positive effect of SSC is expected to be most noticeable on the bridge deck at the locations with negative bending moments. The reason for this expectation is that the bridge deck has the highest concentration of chlorides and cracks will form at the surface of the bridge deck at the locations with negative bending moments. These cracks will be sealed in case of SSC. Other locations where the positive effects can be noticed, although less clearly, are at the beams and the tensile bars. Here, only chlorides from the air will affect the construction.

The material costs of the bridge designed with SSC are significantly higher than the material costs of the bridge designed with TC. However, it is expected that the maintenance costs of the SSC bridge are much lower than the maintenance costs of the TC bridge. Looking at the whole lifespan, the SSC bridge is probably cheaper than the TC bridge.

The results of the tests for the structural characteristics show that SSC mortar has a lower compressive strength and a lower Young's modulus than TC mortar. Especially, the lower Young's modulus will affect the structural design as it decreases the structural stiffness significantly. The flexural strength of SSC mortar is higher than the flexural strength of TC. This does not really influence the structural design as the flexural strength of SSC is too low to carry the tensile loads, so the reinforcement will take the tensile forces. The only change is the cracking moment of the structure.

The tests on durability give overall positive results, showing that SSC is more durable than TC. The chloride migration shows that, before healing, the SSC and TC have similar migration coefficients. However, after the healing period the migration coefficient of the SSC is lower than the migration coefficient of TC, at the location of the crack as well as the uncracked surface. Although, the difference is not as large as expected, this might change with longer healing periods, as the permeability test shows that after 42 days the cracks are nearly sealed. Therefore, it is recommended to do more tests with longer healing periods, to see if the differences in durability increase and to be sure that the cover depth can be decreased.

When making a short calculation with the characteristics found in the results of the test, one sees that the height of the bridge deck and the beams increases a bit more than assumed due to the lower Young's modulus. Furthermore, no large changes are found and still a more slender design is made with SSC compared to a design made with TC.

Therefore, it is recommended to research the possibility of changing the mixture in a way that the Young's modulus is increased and more comparable to the Young's modulus of a traditional concrete.

1 Introduction

At Delft University of Technology research is done on the material 'Strain hardening Self-healing concrete' (SSC) since the year 2006. The reason to start researching this new material was the desire to increase the durability of the concrete, which is mostly dependent on the reinforcement.

By traditional concrete (TC), steel reinforcement is used to take the tensile stress, as concrete has a low tensile strength compared to its compressive strength. This causes the concrete to crack under tension after which the steel reinforcement will take over.

To make sure the reinforcement will not corrode, a concrete layer with a minimal thickness should cover the steel. However, due to the cracks and loss of alkalinity due to carbonation, which will increase over time, there will be a moment that the reinforcement will be exposed to the external environment and will start to corrode. Corrosion can cause the construction to be unable to bear the loads anymore and the structure will fail.

As one would guess by seeing the name strain hardening self-healing concrete, this new kind of concrete is able to seal its cracks and other porous parts due to the addition of a healing agent, which should result in a low-permeable concrete. The healing agent consists of bacteria and a food source. It is expected that the healing capacity will make it possible to design thinner constructions with SSC concrete, as the thickness of the cover should be allowed to be smaller. Also, it should be possible to design a structure with a longer life expectancy and less need for maintenance using this material.

In addition to the healing agent, fibers are added to the mixture. The fibers are added to keep the crack width small, because the larger the crack, the more longer it takes to heal.

1.1. The project

The material is already used in some projects, in form of a repair mortar, although this was in a way to solve problems, which occurred after finishing the project. When proposed to design a whole project with SSC the reasons to reject the proposal are costs, but most importantly the lack of a Eurocode for this type of material.

The Eurocode obliges contractors to design a concrete structure in a way that SSC concrete would not be necessary. Should a contractor want to apply SSC in its design in a way that the positive effects of the SSC are considered, the contractor should prove that this is possible using calculations and tests, which would increase the costs of the project significantly.

To show contractors and institutes that it is possible to design and build projects using SSC and to give them a steady reference, the TU Delft has decided to build a Demonstrator Bridge at their campus. The Demonstrator Bridge will be part of a plan to increase the accessibility of the campus for cyclist and pedestrians from multiple directions.

The design of the bridge will be done with the help of multiple faculties of the TU Delft, one of these faculties being Civil Engineering and Geosciences. Besides the TU Delft there will be external companies helping with the design and construction of the Demonstrator Bridge.

1.2. Research

For the design of a bridge or any other civil project, one needs to know the characteristics of the used materials. Although, quite a lot of research about SSC is done, not all the needed characteristics are known yet. This is because after every research the mixture was changed to improve the measured characteristics. Also, until now the material was only used to repair damaged structures and not to design a complete construction to start with.

1.2.1. Main objective

The main objective of this research is to gather the information (characteristics) that are needed to design a pedestrian/bicycle bridge (see figure 1) and to make a structural design, using assumptions which will be checked with the results of the tests afterwards. This design will be carried out for the SSC mortar and a TC mortar type to be able to compare the results. What kind of structure will be used for the bridge will be decided based on assumed characteristics of the material. These assumptions for the characteristics will be based on the expected outcome of the tests.



Figure 1: Pedestrian bow bridge (Constructiebedrijf Hillebrand B.V., 2010)

1.2.2. Research questions

To get to the main objective the following research questions are set:

- What are the structural characteristics of SSC and TC?
 - Compressive strength
 - Flexural strength
 - Young's modulus
 - Shrinkage
- What is the durability of SSC compared to TC?
 - Healing capacity
 - Frost/thaw resistance in combination with de-icing salt
 - Chloride migration
 - Porosity
- What are the differences in costs between a bridge of TC and a bridge designed with SSC?

1.2.3. Expectations

It is expected that by using SSC to design a pedestrian/bicycle bridge instead of a traditional type of concrete, it will be possible to decrease the cover depth. This opens to possibility to use a smaller construction height and create a more elegantly shaped bridge. This will be due to the increased healing capacity and therefore the increase of durability of the material; the increase of the healing capacity is caused by the addition of the bacteria-based healing agent and poly-vinyl-alcohol (PVA) fibers to the mixture of the concrete.

Another expected outcome is that the use of SSC will have higher material costs in comparison to the use of TC, but will become relatively cheaper when taking the service life into account. This relative decrease of costs during the service life of the construction is because of the expectation that less maintenance for crack repair or damage due to corrosion is necessary.

1.3. What is SSC?

Before starting the research, it is necessary to establish what is already known, to decide the best approach to find and explain the results needed for the design of a pedestrian/bicycle bridge. In this paragraph one finds the needed knowledge.

Traditional concrete has of itself a small healing capacity, autogenous healing. When in contact with water it will generate calcite minerals, which seal the cracks (de Rooij, van Tittelboom, de Belie, & Schlangen, 2013). However, this capacity is expected to be very low in comparison to the capacity of newly developed SSC. It is expected that this increased healing capacity will cause a decrease in thickness needed for the cover. The reason for this increased healing capacity, the influence of fibers and knowledge about determination of the cover depth are given below.

It is also expected that, as mentioned earlier, less maintenance is needed and the structure might even have a longer live span than structures constructed using TC.

1.3.1. How does SSC work?

Bio-based healing agent

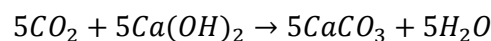
To increase the healing capacity of traditional concrete, an extra component is added to the existing mixture, namely a bio-based agent. The bio-based agent consists of alkali-resistant bacteria and a food source for those bacteria. When this bio-based agent is mixed in the concrete it will have the capacity to produce calcite minerals that fill up the cracks and other porous parts when in contact with water.

The alkali-resistant bacteria in this mixture are spore-forming bacteria and the food resource for the bacteria is calcium lactate. The bacteria and its food resource are either embedded in lightweight aggregates or encapsulated in a bio-degradable polymer matrix before mixed into the concrete.

From earlier researches it can be seen that these bacteria can seal the cracks with both direct and indirect reactions where calcium carbonate (CaCO_3) is formed. The direct reaction to form CaCO_3 is caused by the metabolic conversion according to the following reaction:



The indirect reaction is caused by the metabolically produced CO_2 with the mineral $\text{Ca}(\text{OH})_2$ (portlandite) present in the concrete matrix, as in the following reaction:



This last reaction is comparable to carbonation, which is a slow process that occurs in concrete naturally.

Cracks with a width up to 460 μm can be closed using the bio-based agent. In comparison, in case of autogenous healing, cracks with a width of 50 μm are sealed completely and partially recovery is reached with a crack width of 50-150 μm . Although, it is possible to seal cracks up to 460 μm , smaller cracks will be sealed more easily. For this reason another kind of reinforcement will be used to control the crack width, PVA fibers instead of traditional steel bars (Sierra-Beltran, Jonkers, & Schlangen, 2014). This will give the concrete a deformation capacity without the occurrence of large cracks. The addition of these elements to the mixture will result in a concrete with a better durability than the traditional concrete.

Fibers

As said above PVA fibers are added to the mixture to control the crack width in the concrete. The presence of fibers in combination with a well-designed mixture to increase the interaction between the fibers, concrete matrix and the fiber/concrete interface, causes the material to develop multiple micro-cracks before failure occurs. Due to the fiber bridging properties, the width of the cracks will stay below 0,1 mm with only 2% volume of fibers used. Especially fibers in combination with a high ductility will make it possible to get many small cracks, this instead of a few large cracks. In repair materials for concrete structures, fibers are used to control the drying shrinkage as well as the service load related cracking (Li, 2009).

Besides controlling the crack width, the fibers also will cause the material to act more ductile and have a higher tensile strength than a TC. Instead of a softening phase after the first crack occurs, the SSC first enters a strain hardening phase in which the load that can be taken can increase further. In case of TC, a brittle failure will occur shortly after the first crack appears.

A typical strain-hardening concrete, first has a steep increase in load until the first crack occurs (phase I). This first phase is followed by phase II, the strain hardening phase, where the load keeps increasing slowly. When the peak load is reached, one of the cracks becomes critical and crack localisation will take place. When this happens phase III, the softening phase starts. In figure 2 these phases are shown (Naaman, 2007).

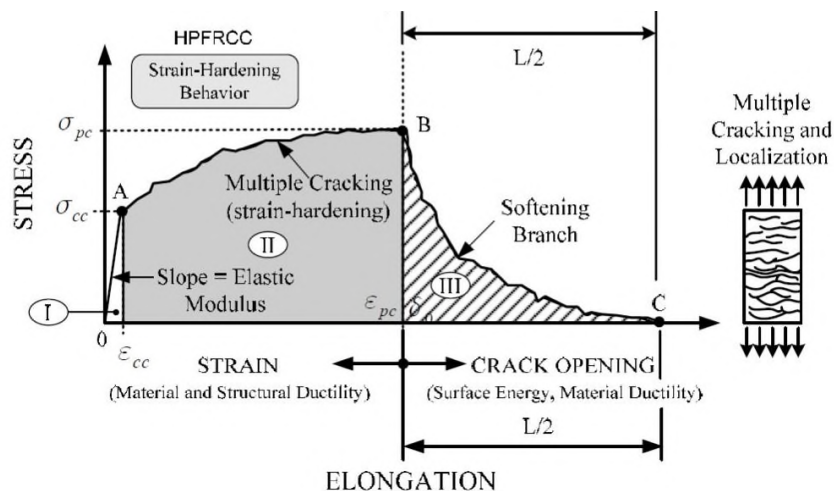


Figure 2: Strain hardening behavior fiber reinforce concrete (Naaman, 2007)

1.3.2. Concrete cover

As mentioned at the start of paragraph 1.2.1 it is expected that using SSC for the design of a structure will result in a thinner cover. The possibility of a thinner cover, is due to the increased healing capacity in combination with the controlled crack width as described above. Due to the expectation of decreasing the cover it is important to know how the thickness of the cover is determined. In this paragraph a look will be taken at how the cover depth is determined in practice using the Eurocode and at the literature about this subject as well.

Eurocode

When designing a structure the cover depth is determined using the Eurocode, in this case NEN-EN 1992-1-1. The Eurocode gives the following formula:

$$C_{nom} = C_{min} + \Delta C_{dev}$$

With

- C_{nom} = Nominal cover depth
- C_{min} = Minimal cover depth
- ΔC_{dev} = Construction tolerance

The minimal cover depth can be determined using the following formula:

$$C_{min} = \max\{C_{min,b}; C_{min,dur} + \Delta C_{dur,\gamma} - \Delta C_{dur,st} - \Delta C_{dur,add}; 10\} \text{ mm}$$

With

- $C_{min,b}$ = Minimal cover depth based on annexation requirements
- $C_{min,dur}$ = Minimal cover depth based on environmental influences
- $\Delta C_{dur,\gamma}$ = Safety margin
- $\Delta C_{dur,st}$ = Reduction cover depth due to stainless steel
- $\Delta C_{dur,add}$ = Reduction cover depth due to extra protection

The values of $C_{min,b}$ and $C_{min,dur}$ can be found in the tables 1 and 2.

Table 1: Minimal cover depth $C_{min,b}$ based on annexation requirements

Bond Requirement	
Arrangement of bars	Minimum cover $C_{min,b}$ *
Separated	Diameter of bar
Bundled	Equivalent diameter (ϕ_e)(see 8.9.1)

*: If the nominal maximum aggregate size is greater than 32 mm, $C_{min,b}$ should be increased by 5 mm.

Table 1 shows that the thickness of $C_{min,b}$ depends on the arrangement of the reinforcement bars in combination with their diameter. Besides these two factors, the aggregate size should be taken into account, if the size of these aggregates is larger than 32 mm, the $C_{min,b}$ should be increased by 5 mm. These factors will only be known when the design is being made, therefore it is not possible to say on forehand what the value of $C_{min,b}$ will be.

Table 2 shows that to be able to determine the thickness of $C_{min,dur}$, one needs to know the environmental class as well as the structural class of the structure. In case of the Demonstrator Bridge the environmental class is XD3 (corrosion induced by chlorides, wet and dry cycles) and the structural class is S4 (life span of 50 years and strength class C40/50). This knowledge makes it possible to see that the thickness of $C_{min,dur}$ will be 45 mm.

Table 2: Minimal cover depth $C_{min,dur}$ based on environmental influences

Environmental Requirement for $c_{min,dur}$ (mm)							
Structural Class	Exposure Class according to Table 4.1						
	X0	XC1	XC2 / XC3	XC4	XD1 / XS1	XD2 / XS2	XD3 / XS3
S1	10	10	10	15	20	25	30
S2	10	10	15	20	25	30	35
S3	10	10	20	25	30	35	40
S4	10	15	25	30	35	40	45
S5	15	20	30	35	40	45	50
S6	20	25	35	40	45	50	55

In some cases $C_{min,dur}$ can be decreased due to extra protection or the use of stainless steel. The decrease of cover depth due to the use of SSC can be seen as extra protection, although it should be proven by for example a chloride migration test.

The highest value of $C_{min,b}$ and $C_{min,dur}$ with corrections will be the needed cover.

Literature

Above is described what requirements the design of a structure should fulfil for cover depth. In the next part, it will be discussed what can be found about this subject in literature.

There are many degradation mechanisms which affect the corrosion of the reinforcement, two of these mechanisms, carbonation and chloride penetration, are emphasized in most investigations. As the tests performed for this research are mainly about chloride penetration, this paragraph will focus on this mechanism.

The model of (Tuutti, 1982) is often used to describe the service life of concrete. According to this conceptual model, the service life of concrete can be divided in two main phases: the initiation phase and the propagation phase. During the initiation phase, the chloride ions will penetrate through the concrete cover, this is caused by an aggressive environment. The duration of the initiation phase depends on the thickness of the cover and the needed concentration of chlorides to start the corrosion process. This concentration is needed due to the protective passive layer that covers the reinforcement by a pH-value > 13, which is caused by the high alkalinity of the pore solution.

At the moment the corrosion starts, the initial phase ends and the propagation phase begins. During the propagation phase the corrosion develops and in the end will lead to local failure of the structure. A schematic view of the development of corrosion is shown in figure 3.

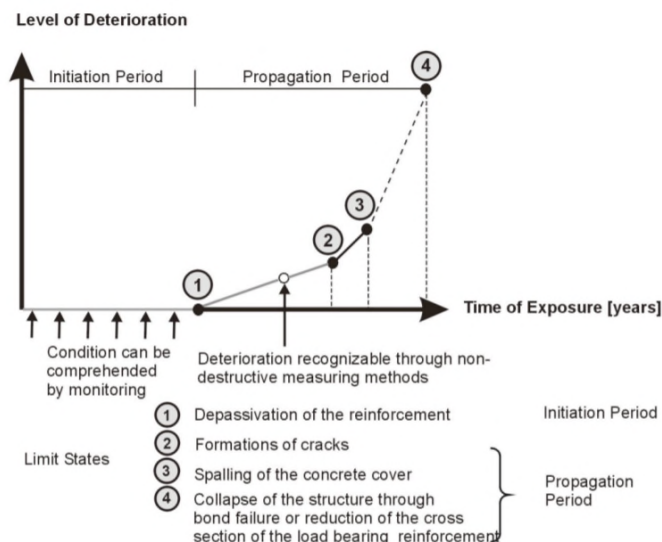


Figure 3: Deterioration process of reinforcement corrosion (fib, 2006)

As said earlier, the propagation phase starts when a certain concentration of chlorides is reached, this is the critical chloride content (C_{crit}). C_{crit} depends on multiple values, which makes it difficult to find an unique value. Also, there are three ways of expressing C_{crit} , using the Cl^-/OH^- ratio, the free chloride threshold level or the total chloride content. In most codes the total chloride content is used, but this still leads to various values for C_{crit} . Nowadays, the mostly used value for C_{crit} lies between 0,2 and 0,4 % of chloride content by cement mass for reinforced concrete. The higher value will be chosen in a moderate environment, while the lower value will be used for aggressive conditions (Blagojevc, 2016).

The theory above describes the chloride penetration for situations with uncracked concrete. As this thesis is about strain hardening self-healing concrete, important is to know what influence the cracks have on the chloride penetration.

It is widely accepted that cracks reduce the protective function of the concrete for the reinforcement and thus decrease the durability. The three main ways why the cracks decrease the durability are:

- The cracks provide vast routes through which harmful substances can penetrate.
- The cracks decrease the protective cover on the reinforcement when looking at the environment and so decrease the initiation phase.
- The cracks can cause differences in the environmental conditions in the concrete, which can lead to the formation of an electrochemical cell.

Since the codes used for designing structures are based on the crack width, most of the research is focused on this factor. However, there is discussion if using the surface crack width is the right factor. It might be that the crack width at the surface of the bar or the crack width proportional to the cover should be used.

In previous research it was mostly aimed to find a so called; threshold crack width. When the crack width is smaller than this value, the cracked concrete will act the same as uncracked concrete. In the literature the found values vary from 0,012 to 0,08 mm. There also are researchers who think there is a crack width above which the increase of crack width will not influence the penetration of chlorides anymore.

In research of (Savija, 2014) it was found that the wider the cracks the faster the chloride penetration. One of the results shows that the chloride penetration depth increases according to a nearly linear relationship with the crack width, however, this is up to a crack width of 0,1 mm. This is probably caused by the increase of crack depth caused by the increasing crack width. It was also found that by the wider cracks chloride penetration parallel to the reinforcement occurs caused by the damage to the concrete/steel interface (Savija, 2014). While it is widely accepted that cracks shorten the initiation phase, a debate is still going on about the effects of cracks on the propagation phase (Blagojevc, 2016).

Although, it is known that cracks influence the durability of the concrete, no exact models which take cracks into account exist yet. However, there are some simplified models which can be used. One of them will be explained below.

The model is developed by (Pacheco Farías, 2015) and uses an effective cover depth. The effective cover depth is determined by reducing the original cover depth with the depth of the crack in the concrete. This means that if a crack reaches the reinforcement the cover depth is assumed to be zero (see figure 4).

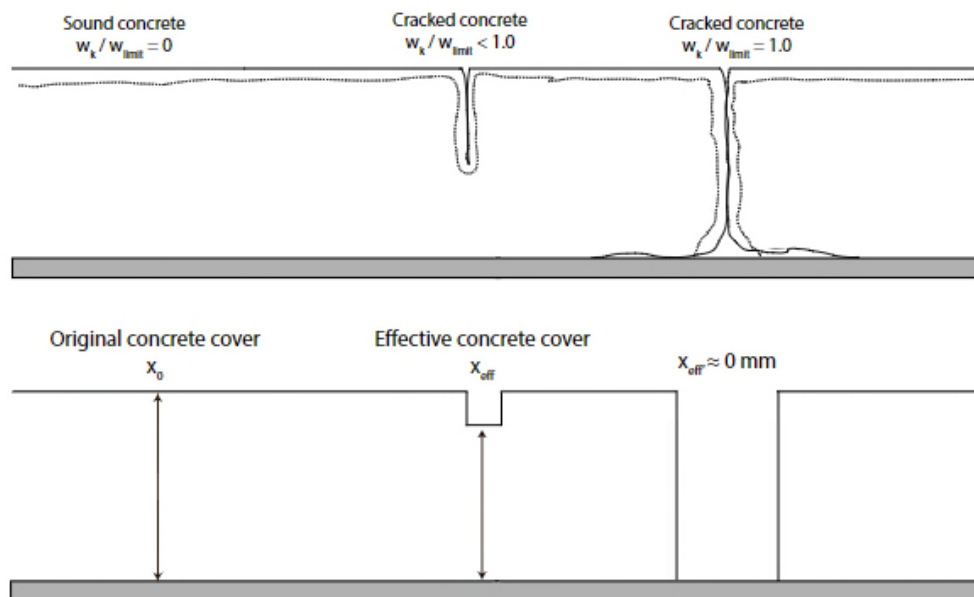


Figure 4: Chloride ingress for sound and cracked concrete using effective cover depth (Pacheco Farías, 2015)

However, to be able to use this method the depth of the cracks has to be known, which often is not the case.

1.4. Outline report

This report consists out of five main elements in the following sequence: 'Materials and methods', 'Structural Design', 'Experimental results', 'Discussion' and 'Conclusions and recommendations'.

Materials and methods

In this chapter, it will be explained which materials will be used and what the compositions of the mixtures for these materials are.

Also, it will be explained which characteristics still have to be researched and what test methods will be used to gain the needed knowledge. Furthermore, the expected outcome is given after some explanation about the Demonstrator Bridge.

Design Demonstrator Bridge

Here, a structural design will be made, using assumed characteristics based on the expectations from the tests that will be performed during the research. To do this, first the most important characteristics of the SSC will be named and compared to those of the TC. Using these values, it will be decided how these can be used in an optimal way.

Besides this, a design will be made using TC. This makes it possible to compare the designs and see what the differences are.

Experimental results

In the chapter 'Experimental results', the outcome of the performed experiments will be listed and clarified. Also, the differences between the characteristics of TC mortar and SSC mortar will be named.

Discussion

In this part of the report, the results displayed in the previous chapter will be discussed. Are the results of the performed experiments as expected and if not, what is the reason? What aspect was not thought about before starting the experiment or went something wrong during the testing procedure?

Also, the differences between the design of the Demonstrator Bridge of SSC and TC will be discussed. Are the effects of the new material as expected and at what locations in the design is the effect most noticeable. Next, the assumptions made for the calculation will be compared with the results. If differences are present it will be discussed what effects this has on the structure and if further research is needed.

Besides this will be discussed how the performed experiments can be improved in the future. How can mistakes be prevented or can forgotten aspects be taken into account.

Conclusions and recommendations

In the final chapter, conclusions will be derived from the results of the structural designs and the results of the tests. Also, recommendations for future research will be given and how the material can be used in an optimal way in a structural design.

2 Materials & methods

As said in chapter 1, there still is a lot of information that needs to be gathered before it is possible to design a complete structure with SSC concrete. Therefore, multiple tests will be done on a SSC mortar and a TC mortar (C40/50). One of the tests will also be done on concrete with a similar strength. The choice for mortar instead of concrete is because it makes it possible to do tests on small samples. The strength (C40/50) is chosen, because this is the expected strength of the SSC mortar found in an article (Sierra-Beltran, Jonkers, & Schlangen, 2014).

In this chapter the mixtures of the used materials will be given. Also, some information about the Demonstrator Bridge will be provided, which will be used to determine the tests that have to be executed. Finally, short descriptions of the tests and the expectations of these tests will be given.

2.1. Mixture

The tests will be performed on samples made of SSC mortar and TC mortar. Due to the size of the samples, it is not possible to use concrete mixtures with normal aggregate sizes for all tests. To get similar results it is therefore chosen to do the tests with comparable mortars instead and only one of the tests will be done on concrete as well.

In table 3 the exact compositions of the mixtures used for the strain hardening self-healing mortar and traditional mortar are shown. The mixture of the used concrete for one of the tests can be found in the test plan in appendix A.

Table 3: Mortar mixtures

Mixture composites	Strain hardening Self-healing mortar (0-2 mm)	Mixture composites	Traditional mortar (C40/50) (0-4 mm)
<i>Cement I 42.5 N (kg/m³)</i>	440	<i>Cement I 42.5 N (kg/m³)</i>	464
<i>Fly ash (kg/m³)</i>	530	-	-
<i>Water (kg/m³)</i>	375	<i>Water (kg/m³)</i>	232
<i>Limestone powder (kg/m³)</i>	410	<i>Sand 2-4 mm (kg/m³)</i>	475
-	-	<i>Sand 1-2 mm (kg/m³)</i>	350
-	-	<i>Sand 0.5-1 mm (kg/m³)</i>	355
-	-	<i>Sand 0.25-0.5 mm (kg/m³)</i>	320
-	-	<i>Sand 0.125-0.25 mm (kg/m³)</i>	180
<i>LWA* (kg/ m³)</i>	69,315	-	-
<i>Super Plasticizer** (kg/m³)</i>	14,4	-	-
<i>PVA fibers 8 mm (kg/m³)</i>	22	-	-

* Lightweight aggregates (55 kg/m³) with carbon source (4 kg/m³), nutrient (0,3 kg/m³), bacteria (0,015 kg/m³) and healing agent (10 kg/m³).

** Cretoplast Col. 35% PL

The mortar for the SSC is chosen based on the results of research already done by M. Sierra-Beltran. This mixture is chosen, because it is the newest mixture she has worked with designing a repair mortar and one wants to know what the potentials are to use it for a complete structure.

The choice for the TC mortar is a mixture that is created using the European Norms as a base for strength and other characteristics.

2.2. Demonstrator Bridge

As mentioned in the introduction, the goal of this research is to gather the information needed to design a pedestrian/bicycle bridge. The Demonstrator Bridge will be part of a plan to decrease the traffic density at a crossroad near the campus of the TU Delft, which is too crowded at the moment due to the many students coming to the university by bike. This crossroad is shown with a red circle in figure 5.

To decrease the traffic density at this crossroad, at multiple locations around the campus of the TU Delft passages will be created for cyclists and pedestrians. One of these passages will be the Demonstrator Bridge as is mentioned in the introduction .

At the moment the exact location of the bridge is not known. However, the bridge will have a similar span as the glass bridge recently built to connect the green village to the rest of the campus (see figure 5).

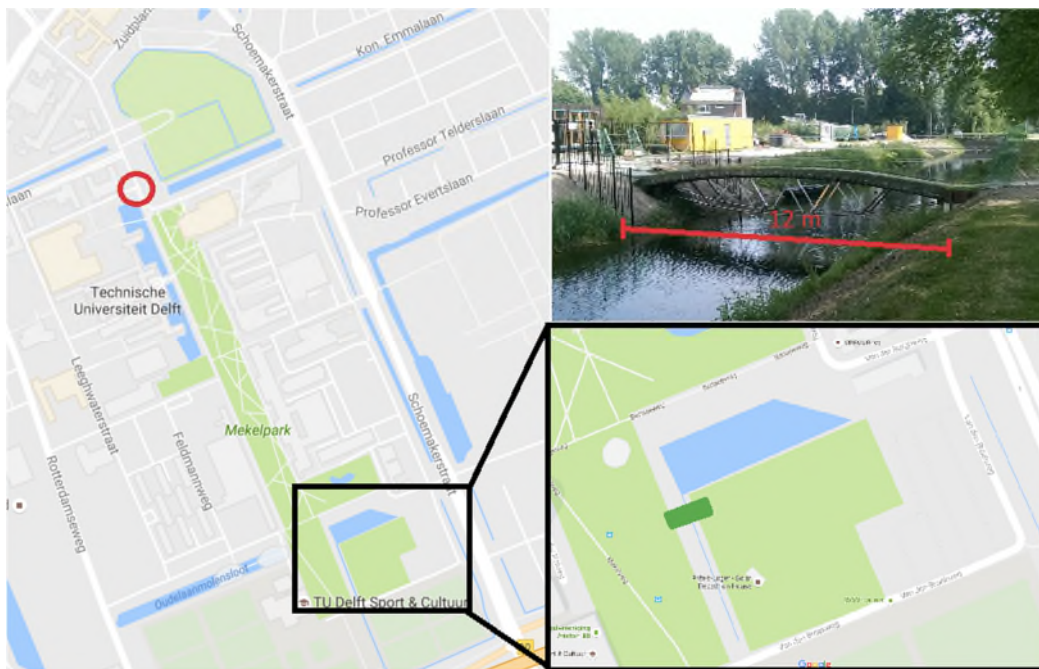


Figure 5: Location and span glass bridge

The figure above shows the location (green rectangle) and the span of the glass bridge (circa 12 m). Therefore, this span will be used for the design of the Demonstrator Bridge in this thesis as well.

2.2.1. Design parameters

As is said before, there is not much information available about the characteristics of SSC and to design a proper bridge, certain information needs to be available. After some reading and discussion, it was decided that using the tests described in the paragraph below, it is possible to gain the characteristics considered necessary (Jonkers, Schlangen, Schipper, & Lukovic, 2016). These characteristics are:

- Compressive strength
- Flexural strength
- Healing capacity
- Chloride migration (salt resistance)
- Frost/thaw resistance in combination with de-icing salt
- Young's modulus
- Shrinkage
- Porosity

As mentioned earlier the tests to gain the characteristics named above will be performed not only on SSC mortar, but on TC mortar as well, to be able to compare the results of both materials. This way it is possible to get a complete view of the differences between the materials. Only the test for the chloride migration will be performed on a traditional concrete as well.

2.2.2. Experiments

To get the characteristics named in the previous paragraph the following tests will be done.

- Compressive and flexural strength test
- Permeability test
- Rapid chloride migration test
- Frost/thaw cycle test
- Young's modulus test
- Shrinkage test
- Absorption test

Below, short descriptions of the tests can be found. For the full explanations of the tests see Appendix A: Test plan.

Compressive and flexural strength test

The aim of this test is to measure the compressive and flexural strength of both TC and SSC mortar.

First, the flexural strength will be measured, using a three-point-bending test. This test is followed by a compression test on the two separated parts. Both tests will be performed until failure. Also, a three-point-bending test will be performed measuring the horizontal deformation of the sample. The test is done according to the standard NEN-EN 13892-2.

Expectation: The TC mortar will have a compressive strength of ± 45 MPa after 28 days. For the SSC mortar a compressive strength of ± 45 MPa is expected after 28 days of curing as well. The flexural strength of TC mortar is about 10% (4,5 MPa) of the compressive strength, although for the SSC mortar it is expected to be higher due to the fiber reinforcement, about 25% (11 MPa) (Sierra-Beltran, 2017).

Permeability test

By the permeability test, the aim is to research the healing capacity of the SSC mortar in comparison to the TC mortar.

Therefore, cylinders will be casted with a diameter of 33,5 mm, which will be split and then put together again with spacers in between, to ensure a crack width of 0.2 mm. Afterwards a permeability test will be done and a photo will be taken every two weeks to see if and how vast the crack is sealed. The first photo and permeability test will be taken at the day the cylinders are cracked, before the healing starts. This test is based on an article by (Palin, Jonkers, & Wiktor, 2015).

Expectation: The results of the test will give that the permeability of the SSC mortar will be smaller than the permeability of the TC mortar at the start of the test. This is due to the addition of fibers to the mixture. Also, it is expected that the permeability of the SSC mortar will decrease faster than the permeability of the TC mortar due to the increased healing capacity.

Rapid chloride migration test

The rapid chloride migration test will be performed to measure the migration coefficient of the mortars and concrete and the influence of cracks on this factor. In this manner, it is possible to say something about the salt resistance.

For the chloride migration test, half of the samples will be cracked after 28 days and will have a healing period of 28 more days. At an age of 56 days all the samples will be subjected to the chloride migration test. By splitting the samples and spraying them with a silver nitrate solution the migration coefficient can be determined measuring the penetration depth. The rapid chloride migration test is executed according to the standard NT BUILD 492.

Expectation: The uncracked samples of the TC mortar, the SSC mortar and the concrete are expected to have similar chloride migration factors. For the cracked and healed samples it is expected that the SSC mortar will have a significant lower non-steady-state migration factor than the TC mortar and the concrete. This is due to the increased healing capacity of the SSC mortar, which is expected to close the cracks.

Frost/thaw cycle test

Using the frost/thaw cycle test, it is aimed to research the frost/thaw resistance in combination with de-icing salt of the mortars and the influence of frost/thaw cycles on the healing-capacity.

To get the results, 6 samples of each mortar will be casted to undergo the frost/thaw cycles with every week a moment where the weight loss of the samples due to scaling will be measured. After the first series of frost/thaw cycles, the samples will have a healing period of 28 days. After the healing period, again the samples will undergo a second series of frost/thaw cycles with every week a measurement of the weight loss. This test is done according to the standard NPR-CEN/TR 15177.

Expectation: The results will show that the SSC mortar will lose less weight due to scaling than the TC mortar. This is expected due to the fibers in the SSC mortar. After the healing period, the difference is expected to be even larger.

Young's modulus in compression test

During the Young's modulus test, measurements will be performed to make it possible to determine the Young's modulus of the mortar.

The test will be performed on samples which are cured for 28 days. The prisms will be placed in the middle of the machine with measurement instruments in vertical direction. First, a basic stress will be applied and the strain will be recorded. Afterwards the samples will be loaded three times until 1/3th of the compressive strength of the mortar. Each time, the basic stress and the compressive stress will be recorded. In the end, when three cycles are performed, the sample will be loaded one more time until failure. Using the recorded stresses and strains the Young's modulus can be calculated. The execution of the test is according to ISO 1920-10.

Expectation: The SSC mortar is expected to act more ductile. Therefore, the expectation is that the Young's modulus of the SSC mortar will be lower than the Young's modulus of the TC mortar. The expected Young's modulus for the TC mortar is 35 GPa and the expected Young's modulus of the SSC mortar is 15 GPa.

Shrinkage test

This test, is performed to determine the shrinkage of both materials. Prisms will be casted with studs in both ends.

After one day of hardening the samples will be demolded. One day after demolding the length will be measured for the first time. The length will be measured as well at 7, 28 and 56 days after demolding. Using these lengths the shrinkage of both materials can be determined. This test is performed according to standard NEN-EN 12617-4.

Expectation: The SSC mortar will have more shrinkage than the TC mortar based on articles of M. Sierra-Beltran and H.M. Jonkers.

Absorption test

With this last test the absorption will be measured and this can be used in a manner to describe the porosity.

This test will be performed on two batches, one batch will be cured for 7 days and the other batch will be cured for 42 days. After curing the samples will be dried in an oven of 40°C and conditioned for 24 hours in the room where the test will take place. Before contact with water, the weight of the samples will be recorded. The water level will be kept at 3 ± 1 mm above the base of the samples. For the first batch, the weight will be recorded after 1 and 7 days in contact with the water. For the second batch, the weight will be recorded after 1, 7 and 28 days in contact with the water. For this test the standard NEN-EN 480-5 is taken as a base for the execution.

Expectation: The absorption of the SSC mortar will be higher than the absorption of the TC mortar, due to the light weight aggregates (Liu, Chia, & Zhang, 2011). However, it is expected that the rate of absorption will decrease over time for both the TC mortar and the SSC mortar.

3 Design Demonstrator Bridge

This chapter shows the designs made with SSC and TC for the Demonstrator Bridge. Also, an explanation about the design process is described.

3.1. Characteristics SSC vs TC

For the characteristics needed for the design assumptions are made, based on the expectations explained in paragraph 2.2.2. These assumptions are made, because at the time the calculation was started not all results were known yet. In the discussion these will be compared with the results of the tests to see if the expectations are right. If not, it will be discussed how does influences the design and if more research is necessary.

The characteristics researched cannot all be used directly in the design. In table 4 the characteristics which will be used in the design are named. These are based on the expected results, if other sources are used it is mentioned below the table.

Table 4: Assumed characteristics for design

Characteristic	TC	SSC
Compressive strength (MPa)	45	45 ³
Flexural strength (MPa)	4,5	11 ⁵
Cover depth (mm)	45 ¹	25 ⁴
Young's modulus (GPa)	35 ²	15 ⁵
Density (kg/m ³)	2400 ²	1860 ⁵

Source assumptions: ¹ (NEN-EN 1992); ² (ENCI B.V., 2015); ³ (Sierra-Beltran, Jonkers, & Schlangen, 2014); ⁴ Literature; ⁵ (Sierra-Beltran, 2017)

Also, based on the literature, it is assumed that no extra reinforcement for crack width control is needed in the design made with SSC, due to the fibers in the mixture. This together with the decrease in cover depth will cause a decrease in profile dimensions.

Finally, the dimensions of the bridge, the expected loads, the environmental class and structural class have to be known as well. These data are shown below:

- Span: 12 m
- Width: 5 m
- Variable load: 4 kN/m²
- Environmental class: XD3
- Structural class: S4

3.2. Structural design SSC

3.2.1. Construction

Table 4 shows that the main differences between the TC and the SSC are the cover depth and the Young's modulus, there is quite a big difference in density as well. To emphasize these differences in a positive manner a cold formed arched bridge deck supported on two beams and trusses is chosen, see figure 6. The explanation why this type of construction is chosen can be found in appendix B.

3.2.2. Calculation

To calculate the bridge, it is split in three elements:

- Bridge deck
- Beams
- Trusses

First, the deck will be calculated by simplifying it to a beam on two supports with cantilevering ends. Afterwards, the calculation will be optimized using a spread sheet program.

For the beams, first a calculation will be made by hand, assuming it is a straight beam on four supports. After checking the shear resistance, this calculation will be optimized using a spread sheet program as well.

As the beams can also be seen as parts of the trusses, the next step is to put the whole trusses into framework software, including the beams. Therefore, an estimate has to be made of the tensile and compressive bars by hand. When all profiles are known, matrixframe can calculate the moments, normal forces and deformation. If one of the values does not satisfy the requirements, the profiles will be adjusted and matrixframe will be used to calculate again. This process will be repeated until all requirements are satisfied. The complete calculation can be found in appendix C. After finishing the calculation it was found that the flexural strength, for which a value is assumed, is not used in the calculation. This is because the value is too low to take the tensile forces caused by the moments, so these forces are taken by the reinforcement.

The final dimensions of the bridge designed with SSC are:

- Bridge deck: $h = 140 \text{ mm}$
- Beams: $b \times h = 140 \times 350 \text{ mm}^2$
- Compressive bars truss: $b \times h = 85 \times 85 \text{ mm}^2$
- Tensile bars truss: $b \times h = 85 \times 120 \text{ mm}^2$

In figure 6 and 7 the result can be seen. A scaled version of figure 7 and the accompanying details can be found in appendix D.

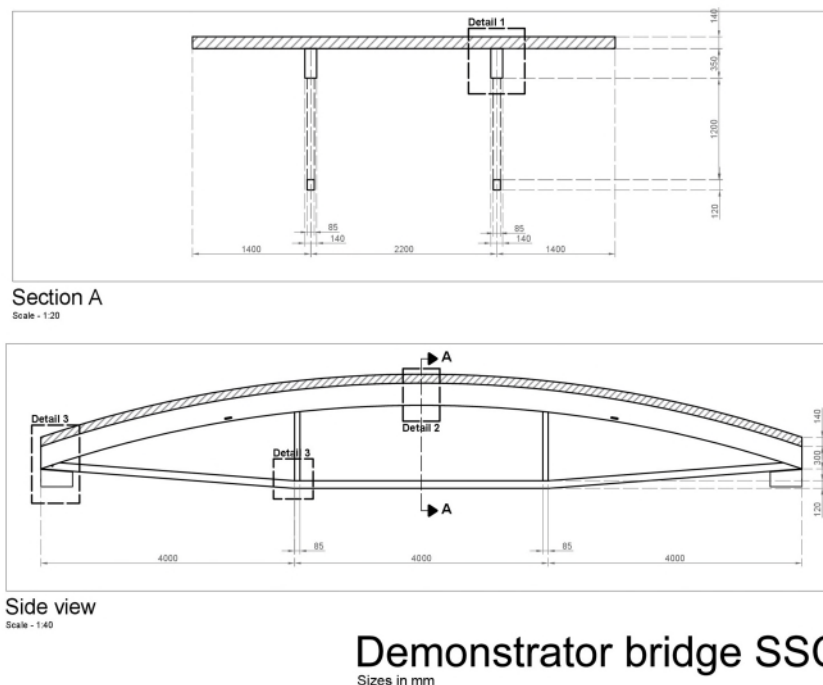


Figure 6: Section and side view SSC design Demonstrator Bridge



Figure 7: Impression SSC design Demonstrator Bridge

3.3. Structural design TC

For the calculation of the bridge designed with TC, the same method as for the design with SSC is used. However, a part about crack width control is added, due to the absence of fibers in the TC. In the figures 8 and 9 the result can be seen. The on scale version of figure 8 and the accompanying details can be found in appendix E.

The final dimensions of the bridge designed with SSC are:

- Bridge deck: $h = 130 \text{ mm}$
- Beams: $b \times h = 200 \times 300 \text{ mm}^2$
- Compressive bars truss: $b \times h = 150 \times 150 \text{ mm}^2$
- Tensile bars truss: $b \times h = 150 \times 180 \text{ mm}^2$

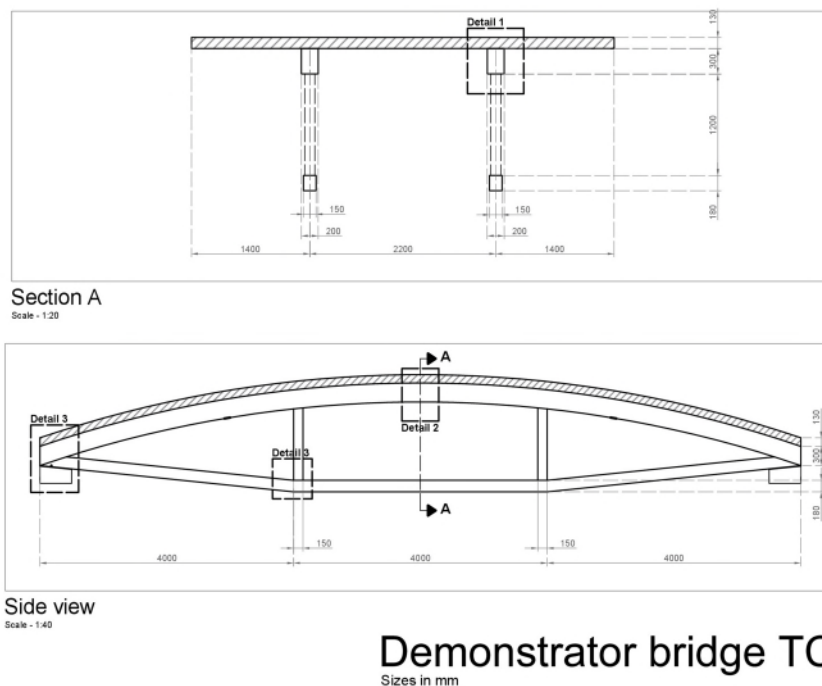


Figure 8: Sideview and cross section TC design Demonstrator Bridge



Figure 9: Impression TC design bridge

4 Experimental results

In this chapter the results of the executed experiments will be presented. In all tests the SSC mortar will be compared with the TC mortar. Only for the RCM test, a comparison will be made with a concrete as well. The samples of the SSC mortar will be named Sx, where the x is a number. The TC mortar samples will be named Tx accordingly and the concrete samples Cx.

4.1. Compressive and flexural strength test

4.1.1. Compressive strength

In table 5 the average values of the compressive strength of both SSC and TC mortar are given. These values are measured at 3, 7 and 28 days after casting. In the figure 10, below the table, these values are shown in a graphical manner, the fit used is a smoothingspline.

Table 5: Development compressive strength

Material	3 days (MPa)	7 days (MPa)	28 days (MPa)
SSC mortar	15,2 ± 0,2	20,6 ± 2,7	32,5 ± 1,9
TC mortar	20,0 ± 1,1	31,9 ± 2,3	42,1 ± 3,8

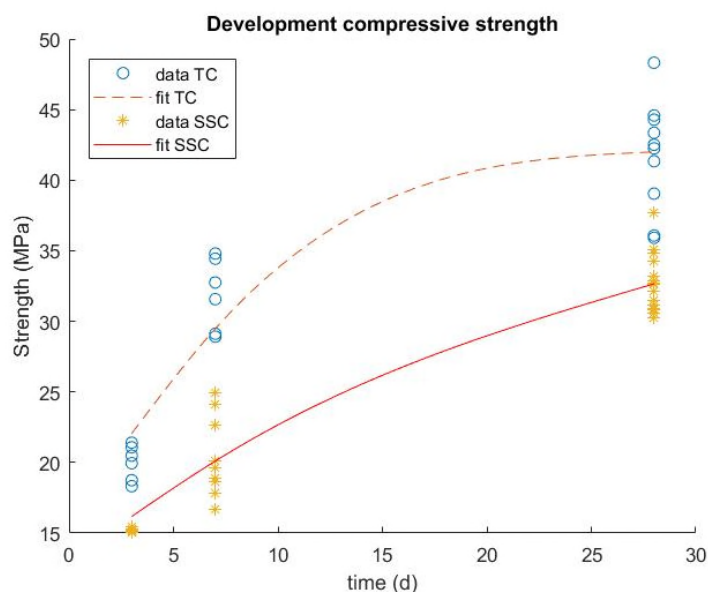


Figure 10: Development compressive strength

In both table 5 and figure 10, it can directly be seen that the TC mortar has a higher compressive strength than the SSC mortar, while it was expected that the mortars would have the same strength. The graph also shows that the rate of strength increase over time of the TC mortar has a clear decrease, whereas there is a minimal decrease in rate of strength increase for the SSC mortar.

4.1.2. Flexural strength

Table 6 shows the average values of the flexural strength of both mortars. Like the compressive strength, these values are taken at 3, 7 and 28 days after casting the samples. Figure 11 shows the same in a graphical way, the fit used is a smoothingspline.

Table 6: Development flexural strength

Material	3 days (MPa)	7 days (MPa)	28 days (MPa)
SSC mortar	8,4 ± 3,8	10,4 ± 0,7	13,0 ± 4,0
TC mortar	4,5 ± 0,1	5,8 ± 0,1	6,3 ± 1,2

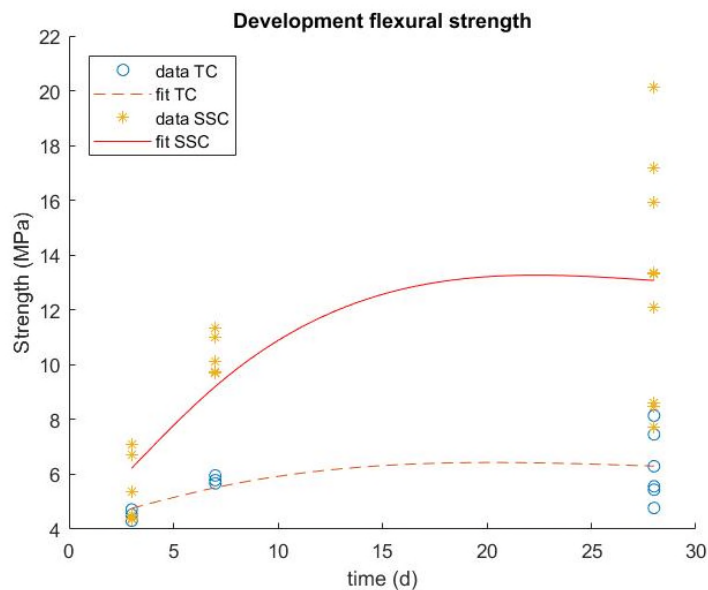


Figure 11: Development flexural strength

When looking at the graph, one can see that the flexural strength of the SSC mortar is significantly higher than the flexural strength of the TC mortar. This is an expected result and is caused by the addition of fibers to the mixture of the SSC mortar. However, it should be noted that there is a large dispersion in the values of the flexural strength of the SSC mortar at 3 and 28 days.

After 28 days of hardening, another three-point-bending test is performed. This time, besides the load, the deformation is measured as well. This makes it possible to see the difference of behaviour between the two mortars clearly when looking at the stress-strain diagram. The result can be seen in the figures below.

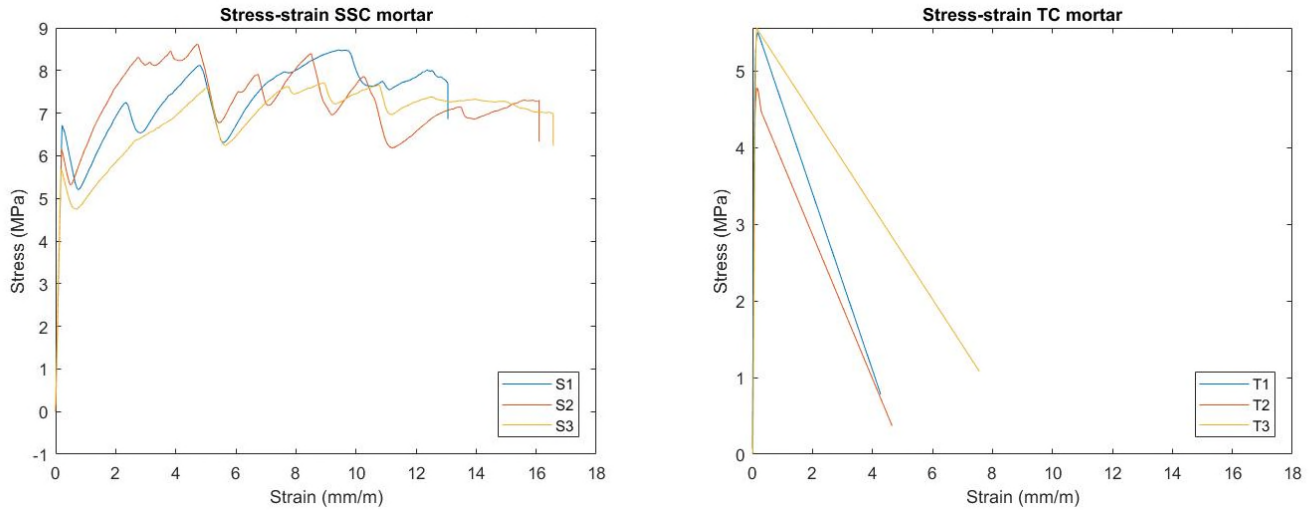


Figure 12: Stress-strain three-point-bending test: left – SSC mortar; right – TC mortar

The figures show a clear difference in behaviour between the materials. The TC mortar shows a brittle failure with a small amount of deformation, whereas the SSC mortar shows strain hardening and lots of deformation. The graph of the SSC mortar ends with a vertical line, because the deformation was larger than the reach of the LVDTs.

4.2. Permeability test

The table below shows the development of the permeability of both the SSC and the TC mortar, in absolute values as well in percentages.

Table 7: Development permeability TC and SSC samples

	<i>Initial crack width (μm)</i>	Initial	14 days		28 days		42 days	
		<i>Weight (g)</i>	<i>Weight (g)</i>	%	<i>Weight (g)</i>	%	<i>Weight (g)</i>	%
T1	590	3327	3401	102	2771	83	2624	79
T2	973	4315	3848	89	3884	90	4432	103
T3	789	3101	2975	96	3012	97	2704	87
T4	348	710	389	55	311	44	301	42
T5	702	2863	2663	93	2626	92	2435	85
T6	721	1958	2119	108	1798	92	2059	105
<i>T_{average}</i>	687	2712	2566	91	2400	83	2425	84
S1	543	556	83	15	264	47	3	1
S2	682	11	13	124	7	68	5	48
S3	380	5	10	225	1	26	2	46
S4	-	101	65	65	11	11	8	8
S5	465	35	12	33	45	129	3	8
S6	299	65	11	16	7	11	4	7
S7	407	33	9	27	65	199	8	25
S8	282	19	9	51	12	66	1	5
<i>S_{average}</i>	437	103	27	70	52	70	4	19

It can be seen that there is a large spread in crack width. Especially the difference in crack widths of the SSC mortar and the TC mortar samples are notable. Bar graphs with these results can be found in appendix F.

The table also shows that the samples of TC mortar have a much higher permeability than the samples of SSC mortar. Although it is difficult to compare due to the difference in crack width. Therefore the samples will be divided in three different categories, in which a comparison will be made. The three categories are:

- 200 – 400 μm (S3, S6, S8, T4)
- 400 – 600 μm (S1, S4, S5, S7, T1)
- 600 – 800 μm (S2, T3, T5, T6)
- > 800 μm (T2)

After the division the samples in the three categories, it is found that one sample, T2, does not fit in any of the categories. Also, it can be seen that the samples in the lower categories are mainly SSC mortar samples and in the higher categories the samples are mostly TC mortar samples. In the figures below, fits are made with the data from the table for the different categories.

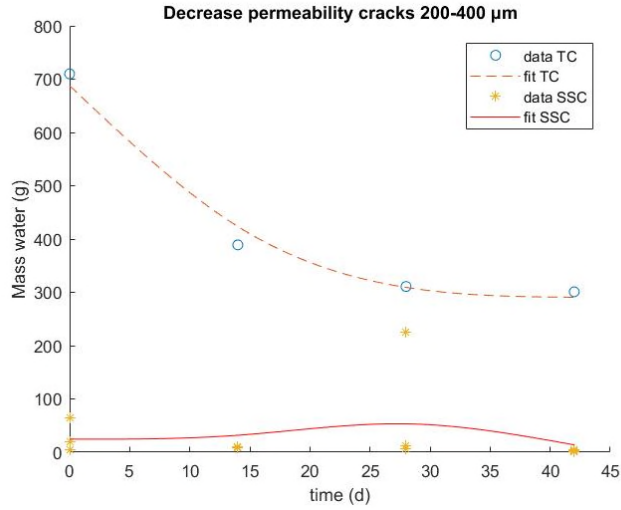


Figure 13: Development permeability samples 200-400 μm

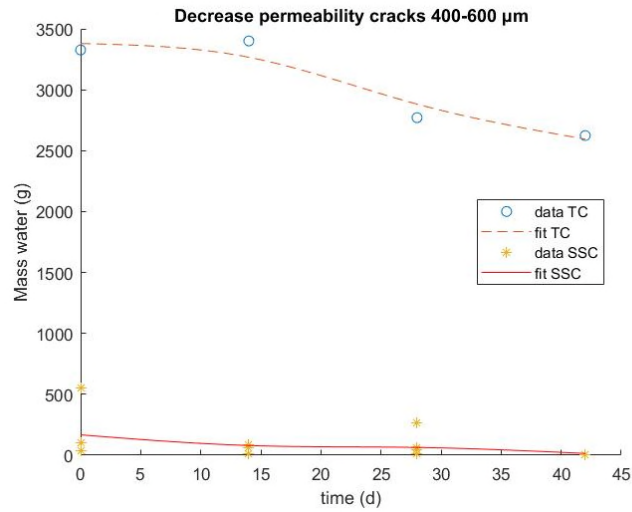


Figure 14: Development permeability samples 400-600 μm

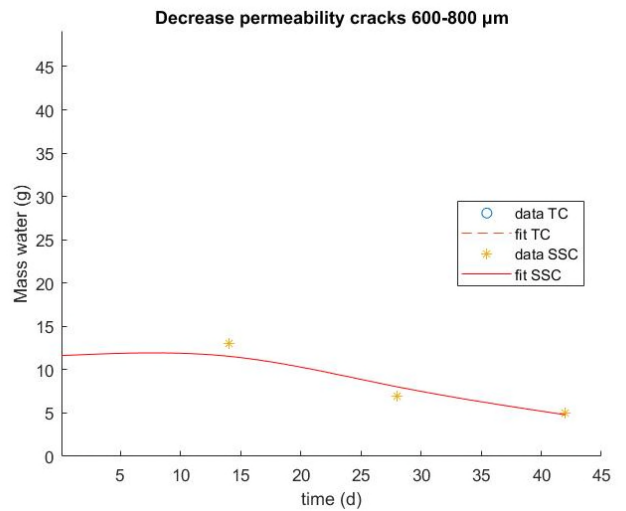
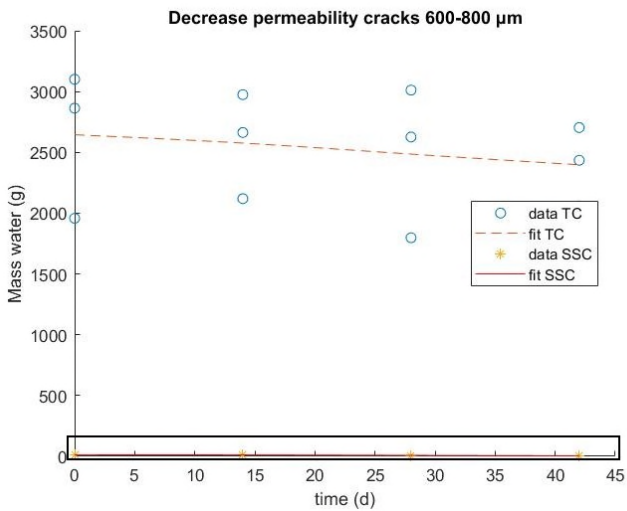


Figure 15: Development permeability samples 600-800 μm : left – TC and SSC; right – Zoom in on SSC

The graphs at the page above, like table 7, show that the SSC samples have a lower permeability at the start. Also, it can be seen that the cracks of the SSC samples are nearly sealed after 42 days, while the permeability of the TC samples only decreased slightly. In the graph for the samples with a crack width of 200-400 µm an increase in permeability can be seen at 28 days.

Before the start of every permeability test, pictures of the samples were taken with a light microscope to see if the healing is visible here as well. In figure 16 and 17 the pictures of the samples T1 and S1 are shown. These samples have a similar crack width and both are in the second category 200-400 µm. In case of the samples S1, the total crack width is the sum of multiple cracks.

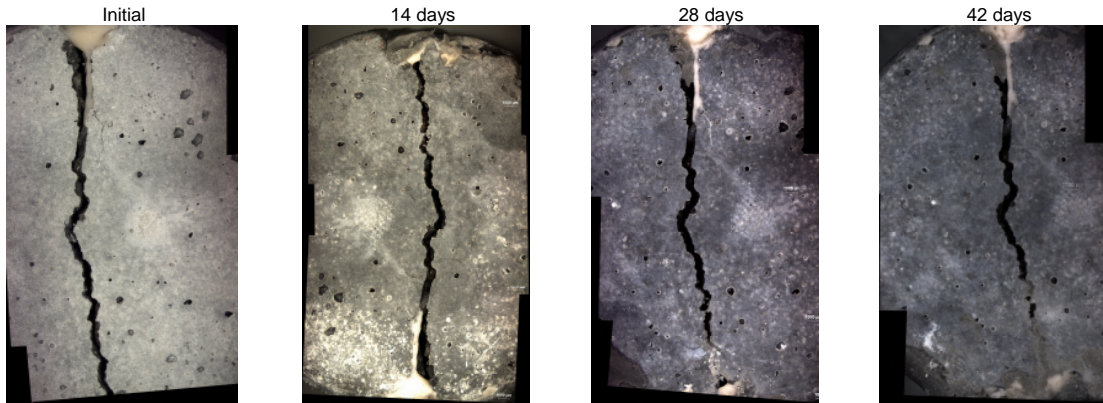


Figure 16: Pictures development permeability T1

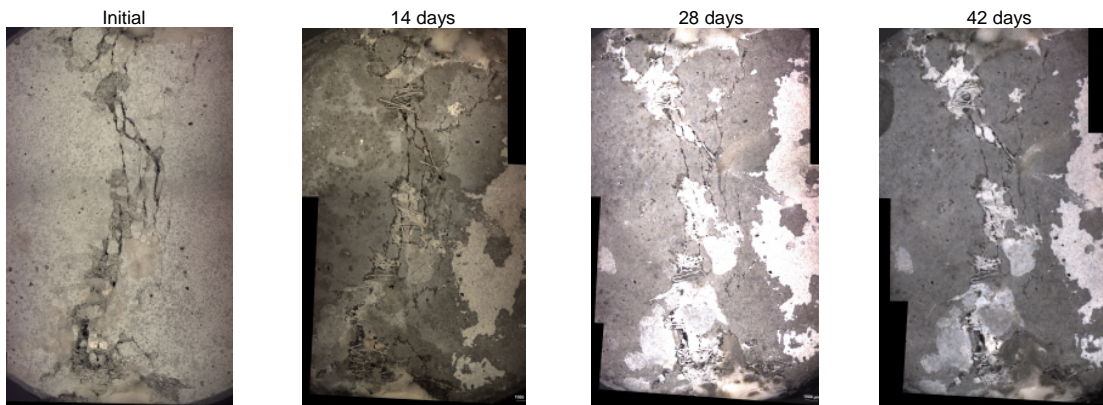


Figure 17: Pictures development permeability S1

In the pictures, it can be seen that T1 has one clear crack, while S1 has multiple small cracks. This behaviour is caused by the fibers in the mortar. When looking at the sealing of the crack, it can be seen that the crack of T1 only closes partly at the bottom of the crack, while the cracks of S1 get less visible over time. This result is in accordance with the measured permeability. The pictures of the other samples can be found in appendix G.

4.3. Rapid chloride migration test

As is explained in paragraph 2.2.2 this test is executed on cracked and uncracked samples of TC, SSC and Concrete. Therefore, an addition is made naming the samples. All cracked samples of TC will get the name TxC and uncracked samples of TC will get the name TxU. The samples of SSC and concrete will be named in the same manner.

4.3.1. Uncracked samples

The tables 8 – 10 show the results of the chloride migration test on the uncracked samples.

Table 8: Non-steady-state migration coefficient uncracked TC mortar samples

Samples TC uncracked	D_{nssm} ($\cdot 10^{-12} \text{ m}^2/\text{s}$)
T1U	14,6
T2U	12,5
T3U	14,0
TU _{average}	13,7 ± 0,9

Table 9: Non-steady-state migration coefficient uncracked SSC mortar samples

Samples SSC uncracked	D_{nssm} ($\cdot 10^{-12} \text{ m}^2/\text{s}$)
S1U	15,2
S2U	12,6
S3U	12,4
SU _{average}	13,4 ± 1,3

Table 10: Non-steady-state migration coefficient uncracked Concrete samples

Samples C uncracked	D_{nssm} ($\cdot 10^{-12} \text{ m}^2/\text{s}$)
C1U	6,2
C2U	5,8
C3U	7,8
CU _{average}	6,6 ± 0,9

The migration coefficient of both the mortars have a similar value as expected. The migration coefficient of the concrete is much lower though; this difference was larger than expected. In the figures below, the penetration of the chlorides in the samples are shown. Pictures of the other samples can be found in appendix H.



Figure 18: Chloride penetration uncracked samples: left – TC; middle – SSC; right – Concrete

4.3.2. Cracked samples

Tables 11 – 13 show the results of the chloride migration test on the cracked samples. The values in the tables are calculated with the penetration depth at the location of the crack and the average penetration depth without the peak. Also the penetration perpendicular to the crack is shown.

Table 11: Non-steady-state migration coefficient cracked TC mortar samples

Samples TC cracked	Crack width (μm)	$D_{\text{nssm,crack}}$ ($\cdot 10^{-12} \text{ m}^2/\text{s}$)	$D_{\text{nssm,average}}$ ($\cdot 10^{-12} \text{ m}^2/\text{s}$)	$D_{\text{nssm,perpendicular}}$ ($\cdot 10^{-12} \text{ m}^2/\text{s}$)
T2C	177	49,4	25,9	26,7
T4C	178	54,8	29,8	27,7
TC_{average}	178 \pm 0,7	52,1 \pm 2,7	27,8 \pm 1,9	27,2 \pm 0,5

Table 12: Non-steady-state migration coefficient cracked SSC mortar samples

Samples SSC cracked	Crack width (μm)	$D_{\text{nssm,crack}}$ ($\cdot 10^{-12} \text{ m}^2/\text{s}$)	$D_{\text{nssm,average}}$ ($\cdot 10^{-12} \text{ m}^2/\text{s}$)	$D_{\text{nssm,perpendicular}}$ ($\cdot 10^{-12} \text{ m}^2/\text{s}$)
S1C	147	43,2	8,3	11,7
S3C	139	21,3	8,2	11,4
S5C	117	48,4	15,5	9,4
S6C	125	42,8	11,5	11,5
SC_{average}	132 \pm 11,7	38,9 \pm 10,4	10,9 \pm 3,0	11,0 \pm 0,9

Table 13: Non-steady-state migration coefficient cracked Concrete samples

Samples C cracked	Crack width (μm)	$D_{\text{nssm,crack}}$ ($\cdot 10^{-12} \text{ m}^2/\text{s}$)	$D_{\text{nssm,average}}$ ($\cdot 10^{-12} \text{ m}^2/\text{s}$)	$D_{\text{nssm,perpendicular}}$ ($\cdot 10^{-12} \text{ m}^2/\text{s}$)
C2C	140	17,2	6,0	9,2
C3C	138	14,0	5,4	5,5
C4C	133	13,6	6,3	7,0
CC_{average}	137 \pm 2,9	14,9 \pm 1,6	5,9 \pm 0,4	7,2 \pm 1,5

Looking at the tables above, one can see that both the migration coefficient at the crack, the migration coefficient perpendicular to the crack and the average migration coefficient without the measurement at the location of the crack are lower for the SSC samples than for the TC, as expected. Although, the migration coefficient of the Concrete samples are even lower, which is unexpected.

When comparing the migration coefficient of the average without the peak with the migration coefficient of the uncracked samples, one can see that the coefficient of the SSC and the Concrete samples have a slightly decreased value, while the coefficient of the TC samples increased significantly.

However, it should be noted that the crack width of the SCC and the Concrete samples are smaller than the crack width of the TC samples.

Figure 19 shows the penetration of the different samples. For all materials a clear peak can be seen at the location of the crack, for one of the SSC samples multiple peaks are visible.

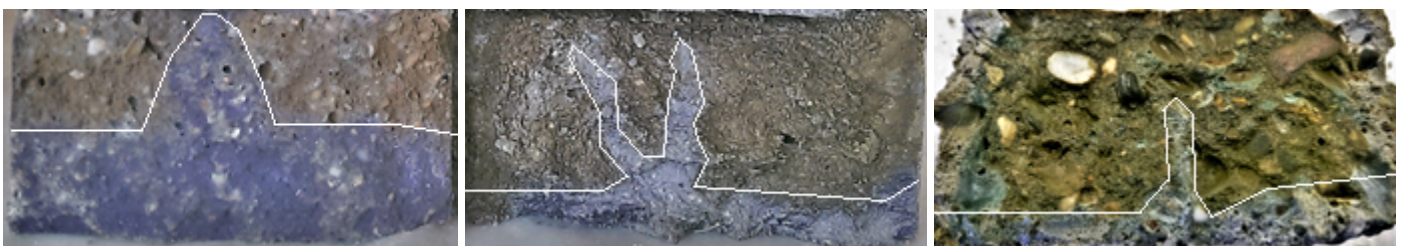


Figure 19: Chloride penetration cracked samples: left – TC; middle – SSC; right – Concrete

In the figures it can be seen that the penetration peak follows the crack in all of the samples. However, the penetration peak in the TC samples is much wider than in the SSC and Concrete samples. Pictures of the other samples can be found in appendix H.

4.4. Frost/thaw cycle test

4.4.1. First frost/thaw session

Tables 14 and 15 show the results of the scaling due to frost/thaw cycles before the healing period.

Table 14: Scaling TC mortar before healing period

Samples	7 cycli, loss (g)	14 cycli, loss (g)	21 cycli, loss (g)	mass/area (g/mm ²)
T1	0,075	0,646	1,218	57,9
T2	0,622	2,128	5,918	281,5
T3	1,416	2,962	5,744	273,2
T4	1,246	3,023	4,242	201,8
T5	0,056	0,062	0,283	13,5
T6	0,648	0,839	1,738	82,7
T _{average}	0,677 ± 0,520	1,610 ± 1,096	3,191 ± 2,218	151,8 ± 106,4

Table 15: Scaling SSC before healing period

Samples	7 cycli, loss (g)	14 cycli, loss (g)	21 cycli, loss (g)	mass/area (g/mm ²)
S1	0,037	0,057	0,100	4,8
S2	0,131	0,224	0,616	29,3
S3	0,096	0,190	0,291	13,8
S4	0,127	0,254	0,432	20,5
S5	0,036	0,075	0,113	5,4
S6	0,160	0,233	0,507	24,1
S _{average}	0,098 ± 0,047	0,172 ± 0,075	0,343 ± 0,194	16,3 ± 9,2

The tables clearly show that the TC mortar samples scale more than the samples of the SSC mortar as expected. Something else that stands out is that some of the samples scale much less than the other samples of the same material, this causes a large dispersion in the results of this test.

In the figure below the same trend can be seen as given in the tables. Also it is noticed that the scaling continues to occur at the same rate.

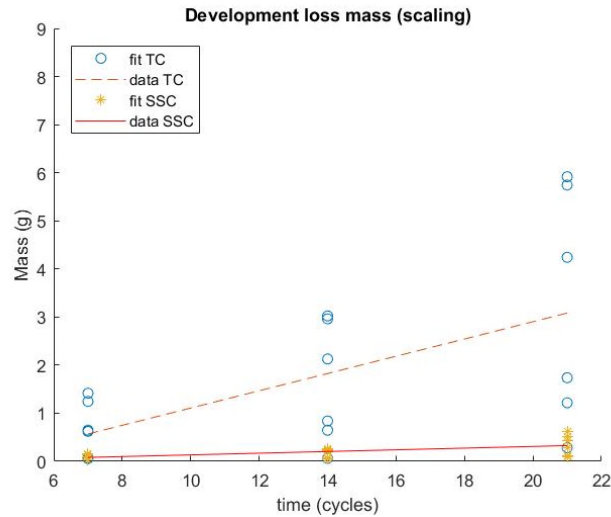


Figure 20: Development scaling before healing period



Figure 21: Surface after 21 frost/thaw cycles before healing period: top – TC mortar; bottom – SSC mortar

In the pictures in figure 21 a difference can be seen as well. The top layer of the TC mortar samples is completely gone, leaving a rough surface. On the surface of the SSC mortar samples cracks can be seen, but the surface is kept together.

4.4.2. Frost/thaw session after healing

In table 16 and 17, one can see the results of scaling due to the period of frost/thaw cycles after the healing period. The tables show that there is clear difference between the amount of scaling, the TC mortar samples scale more than the SSC mortar samples. However, the difference between the two materials have decreased.

Also, it should be mentioned that the standard deviation has increased for both materials compared to the scaling due to the series of cycles before the healing period. Especially the standard deviation of the TC mortar samples have increased.

Figure 22 shows the same trend as is given in tables 1 and 17.

Table 16: Scaling TC mortar after healing period

Samples	7 cycli, loss (g)	14 cycli, loss (g)	21 cycli, loss (g)	mass/area (g/mm ²)
T1	0,122	0,227	0,321	15,3
T2	2,576	5,135	8,053	383,0
T3	0,467	1,540	2,007	95,5
T4	1,045	2,488	3,533	168,0
T5	0,067	0,145	0,258	12,3
T6	0,131	0,462	0,593	28,2
T _{average}	0,735 ± 0,889	1,666 ± 1,759	2,461 ± 2,755	117,0 ± 131,0

Table 17: Scaling SSC mortar after healing period

Samples	7 cycli, loss (g)	14 cycli, loss (g)	21 cycli, loss (g)	mass/area (g/mm ²)
S1	0,051	0,099	0,126	6,0
S2	0,085	0,213	0,565	26,9
S3	0,269	0,408	0,640	30,4
S4	0,149	0,208	0,297	14,1
S5	0,035	0,122	0,270	12,8
S6	0,237	0,271	0,533	25,4
S _{average}	0,138 ± 0,113	0,220 ± 0,103	0,405 ± 0,185	19,3 ± 8,8

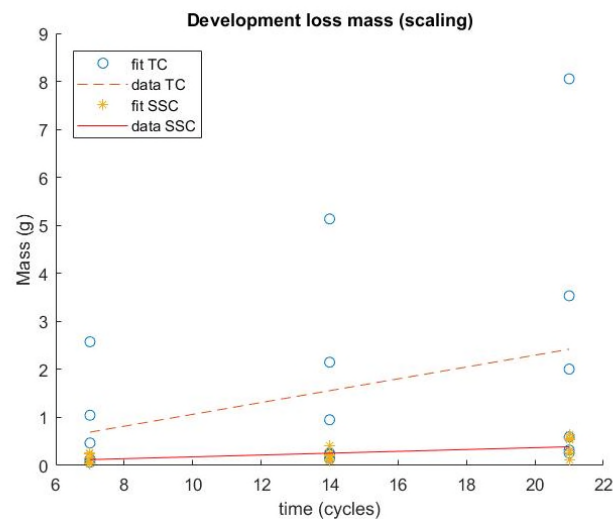


Figure 22: Development scaling after healing period

Also, a difference can be seen when looking at the surfaces of the samples of the materials. The surface of the TC mortar samples has worsened, more gravel is exposed. For the SSC samples more cracks are visible than before the healing period, but the surface is still kept together, this can be seen in figure 23.

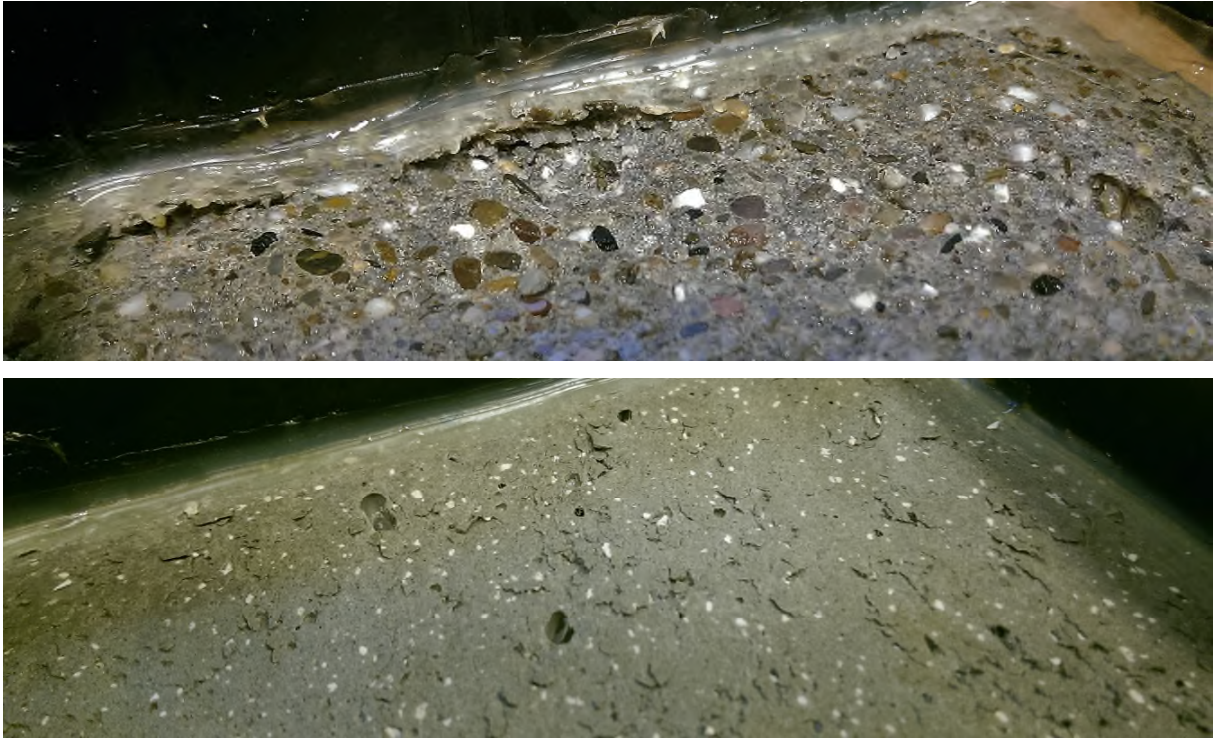


Figure 23: Surface after 21 frost/thaw cycles after healing period: top – TC mortar; bottom – SSC mortar

4.5. Young's modulus in compression test

The table below shows the values of the Young's modulus of the samples of both materials.

Table 18: Young's modulus TC and SSC mortars

Samples	Young's modulus (GPa)	Samples	Young's modulus (GPa)
<i>T1</i>	27,5	<i>S1</i>	10,0
<i>T2</i>	33,5	<i>S2</i>	10,7
<i>T3</i>	27,2	<i>S3</i>	9,8
$\bar{T}_{average}$	$29,4 \pm 2,8$	$\bar{S}_{average}$	$10,2 \pm 0,4$

It can be seen that the Young's modulus of the TC mortar is nearly three times as high as the Young's modulus of the SSC mortar. This is in agreement with the expectation that the Young's modulus of the TC mortar would be the highest of the two. However, for both materials the Young's modulus is slightly lower than the expectation. This result means that the SSC mortar has a more ductile behaviour than the TC mortar. This behaviour can be seen in the stress-strain graphs in figures 24 and 25 as well.

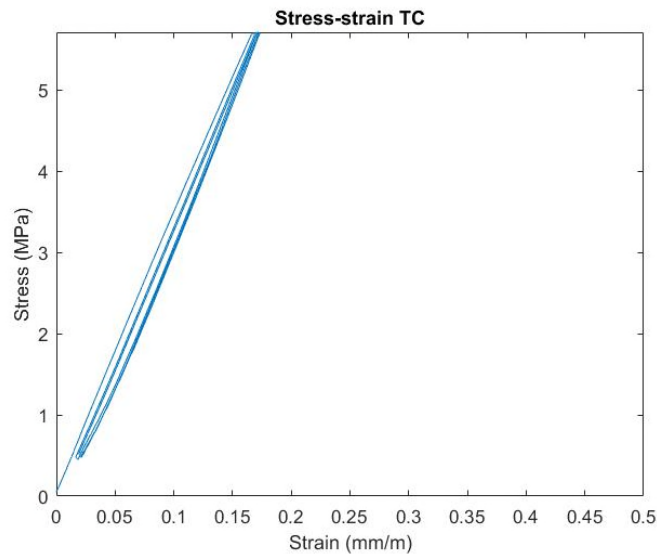


Figure 24: Stress-strain TC mortar under compression

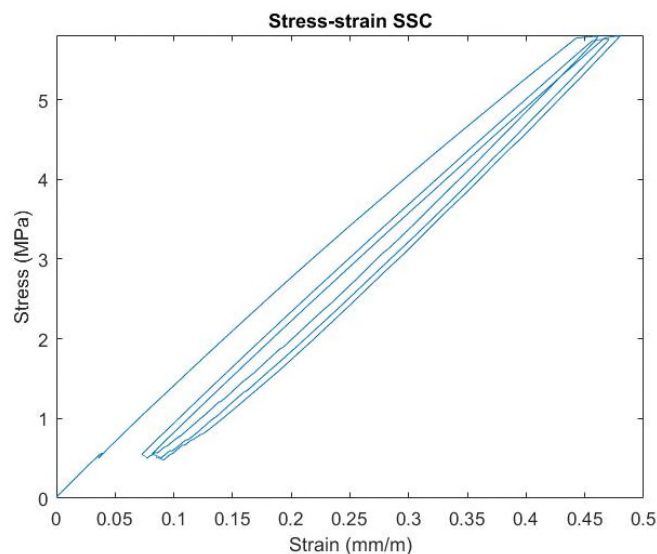


Figure 25: Stress-strain SSC under compression

4.6. Shrinkage test

The table below shows the development of the shrinkage of the TC and SSC mortar samples.

Table 19: Development shrinkage

Samples	3 days Strain (mm/m)	7 days Strain (mm/m)	28 days Strain (mm/m)	56 days Strain (mm/m)
T1	-5,3	-5,3	-5,8	-6,1
T2	-1,7	-1,9	-2,6	-2,7
T3	-1,6	-1,6	-1,9	-2,9
T _{average}	-2,9 ± 1,7	-2,9 ± 1,7	-3,4 ± 1,7	-3,9 ± 2,7
S1	-2,2	-2,7	-3,4	-3,4
S2	-2,0	-2,0	-1,7	-2,3
S3	-2,0	-2,4	-2,5	-2,6
S _{average}	-2,1 ± 0,1	-2,4 ± 0,3	-2,5 ± 0,7	-2,8 ± 0,5

When looking at the table, the shrinkage values of one of the samples immediately comes forward. The shrinkage of the sample T1 is much higher than the shrinkage of the other TC mortar samples and causes the average shrinkage of the TC mortar to be higher than the shrinkage of the SSC mortar samples as well, which is against the expectation. Also, these high values cause a large standard deviation.

If the results of T1 are left out of the comparison, the shrinkage of the SSC mortar samples is larger than the shrinkage of the TC mortar samples, which is as expected.

Figure 26 shows the shrinkage development.

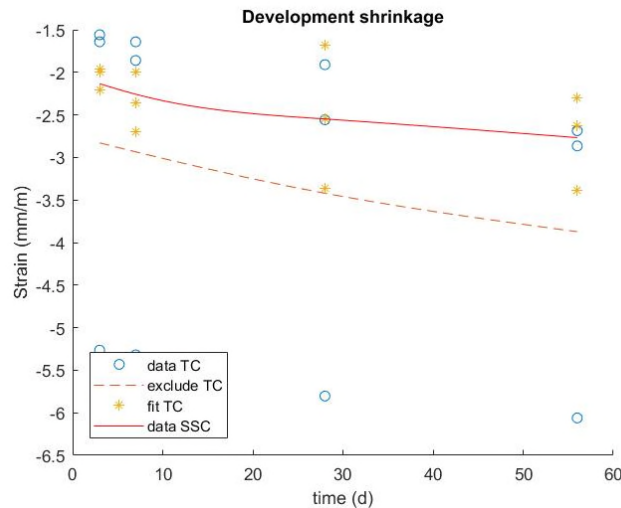


Figure 26: Development shrinkage

In the graph it can be seen that the shrinkage of the TC mortar is higher than the shrinkage of the SSC mortar which is against our expectation. This is probably caused by the high shrinkage values of T1.

4.7. Absorption test

Tables 20 and 21 show the results of the absorption test.

Table 20: Development absorption after 7 days curing

Samples 7 days curing	Start weight (g)	Absorption (g/mm ²) 1 day in water	Absorption (g/mm ²) 7 days in water
T1	566,4	-0,0041	-0,0071
T2	553,9	-0,0049	-0,0081
T3	547,6	-0,0061	-0,0102
T _{average}	556,0 ± 7,8	-0,0050 ± 0,0008	-0,0085 ± 0,0013
S1	442,9	-0,0068	-0,0138
S2	443,8	-0,0068	-0,0137
S3	439,7	-0,0076	-0,0133
S _{average}	442,1 ± 1,8	-0,0071 ± 0,0004	-0,0136 ± 0,0002

Table 21: Development absorption after 42 days curing

Samples 42 days curing	Start weight (g)	Absorption (g/mm ²) 1 day in water	Absorption (g/mm ²) 7 days in water	Absorption (g/mm ²) 28 days in water
T1	563,6	-0,0033	-0,0051	-0,0068
T2	564,3	-0,0036	-0,0059	-0,0075
T3	563,0	-0,0033	-0,0058	-0,0069
T _{average}	563,6 ± 0,5	-0,0034 ± 0,0001	-0,0056 ± 0,0004	-0,0071 ± 0,0005
S1	467,9	-0,0016	-0,0045	-0,0099
S2	464,4	-0,0039	-0,0082	-0,0113
S3	467,5	-0,0029	-0,0073	-0,0128
S _{average}	466,6 ± 1,6	-0,0028 ± 0,0009	-0,0067 ± 0,0016	-0,0113 ± 0,0012

It can be seen that the starting weight of the TC mortar samples is higher than the starting weight of the SSC mortar samples, which is as expected. Besides that, the tables show that both after 7 days of curing and 42 days of curing the SSC mortar samples have a higher absorption rate than the TC mortar samples.

When looking at figure 27, one can clearly see that the rate of absorption decreases over time especially for the TC mortar samples. Also, it can be seen again that the SSC mortar samples absorb water at a higher rate. Another point worth noticing is the fact that the rate of absorption at the start after 7 days of curing is higher than the absorption rate at the start after 42 days of curing for both materials.

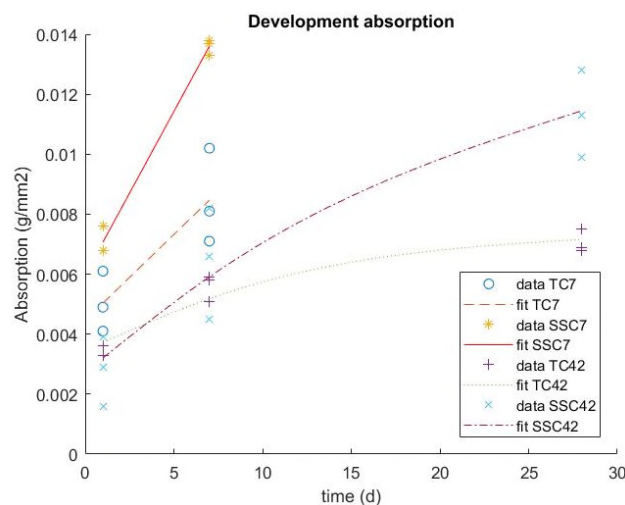


Figure 27: Development absorption

5 Discussion

This chapter discusses the results presented in the previous chapter. The results will be compared with the expectations and if the results are not as expected, the cause of these differences will be discussed.

Also, the design of the Demonstrator Bridge will be discussed. The structural design made with SSC will be compared to the structural design made with TC and the differences will be named. It will also be discussed at what points in the construction the positive effects are most noticeable. The costs to build the bridges will be compared as well.

Finally, the assumptions made for the calculation of the design with SSC will be compared to the results and the differences will be discussed.

5.1. Results

5.1.1. Compressive and flexural strength test

Compressive strength

The results show that the compressive strength of the TC mortar is as expected, see paragraph 2.2.2. Although the compressive strength of the SSC mortar is lower (32,5 MPa) than first expected. This is probably due to the fact that the value for the compressive strength is based on an article about research with an older mixture of SSC. The switch to this newer mixture was made just before starting the tests.

At the moment a modified version of the SSC mortar in this thesis is being researched. This modified version has a compressive strength of 38 MPa. This value is closer to the result, but still higher (Sierra-Beltran, 2017).

Further, in the results it is mentioned that the decrease in rate of strength increase of the SSC mortar is much smaller than the decrease in rate of strength increase of the TC mortar. This would suggest that the strength of the SSC mortar can come closer to the strength of the TC mortar after a longer period. However, the type of fit could influence this view, in this case a 'smoothingspline' in matlab is used. When using a quadratic function to fit, the line of the SSC mortar become nearly horizontal at 28 days. The line of the TC mortar, however, goes down again (see figure 28).

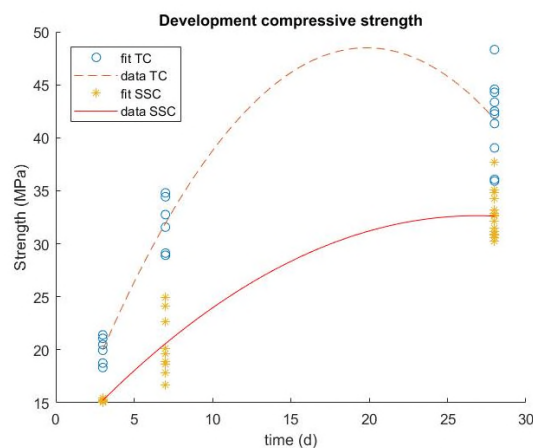


Figure 28: Development compressive strength using a quadratic function fit

Comparing both graphs (figures 10 and 28), the first plot seems more logical. However, it would be interesting to do some compressive strength tests at the age of 56 days, to see if the development of the strength continues.

Flexural strength

The results of the flexural strength tests are close to the expectations. The flexural strength of both materials is slightly higher than expected in absolute values.

When looking at the flexural strength as a percentage of the compressive strength, the value of the flexural strength still is slightly higher than the expected value in case of the TC mortar. However, due to the lower compressive strength of the SSC mortar than was expected, the flexural strength is 40% instead of the expected 25%.

However, it should be mentioned that there is a large dispersion in the values of the flexural strength tests done for the SSC mortar, especially for the values at 3 and 28 days. Therefore, it is hard to say if the average value is the true flexural strength of the material and it is advisable to do more tests to be able to get a clearer view of the average and the standard deviation of the flexural strength.

In addition a flexural strength test was done while measuring the horizontal deformation to get a clear view of the difference in behaviour of the materials. As expected the SSC mortar showed strain-hardening with large deformation, while the TC mortar broke brittle with very little deformation.

As said by the results the reach of the LVDTs was not large enough to get the complete deformation of the SSC mortar. Therefore it is advisable, when the test is done again, to use LVDTs with a larger reach to get the final deformation as well.

5.1.2. Permeability test

The results show that not only the permeability of the SSC mortar samples decreases faster than the TC mortar samples as expected, the SSC mortars start with a lower permeability as well.

Due to the fibers, it was not possible to completely split the SSC mortar samples. Therefore, it could be the case that the crack at the top and the bottom of the samples are larger than the crack in the middle of the samples or it might even be partially closed in the middle. Besides this, it was hard to get the spacers in the sample when it was not completely split, which made it hard to get similar crack widths for both materials.

The fibers also caused the material to have many micro cracks instead of one larger crack. The fact that these micro cracks change often direction and the size of the micro cracks will make it harder for the water to get through.

Something else that should be noted is that, as said by the results, sometimes the permeability of the samples increases after another two weeks of healing. This is probably caused by leakage during the tests. The leakage could be due to leaking pipes, but also by refilling the reservoirs on top of the samples water could be spilled easily, causing an increase in the amount water caught in the buckets below.

Due to the trouble with the splitting of the samples, defining the crack width and the relatively high chance of leaking, it is advised to research if there is a, more accurate method to determine the permeability or to come up with a new set up for this test.

5.1.3. Rapid chloride migration test

Uncracked samples

The results of the RCM test are mostly in agreement with the expectation. However, the migration coefficient of the Concrete is much lower than the migration coefficient of the mortars while the values were expected to be similar. This difference is caused by the CEM III in the mixture of the concrete. The concrete mixture with CEM III was chosen, because it was a standard mixture with a similar strength, used in practice.

When looking in the literature, one finds that the migration coefficient of concrete with CEM I 42,5 N is $13,4 \cdot 10^{-12} \text{ m}^2/\text{s}$ (Yu, 2015). This value is similar to the results found for the TC mortar and the SSC mortar, which is in agreement with the expectations.

Cracked samples

For the cracked samples, the migration coefficient of the SSC mortar samples at the uncracked surface is lower than the migration coefficient of TC mortar samples. This is in agreement with the expectation. However, the migration coefficient of the Concrete is even lower, which is against the expectations, although this is probably caused by the addition of CEM III as said earlier.

When comparing the results of the uncracked surface with the results of the uncracked samples, it can be seen that the migration coefficient of the SSC mortar and the Concrete has slightly decreased. The migration coefficient of the TC mortar has increased a lot, however, which was not expected. A possible explanation is that at some places in the sample the chlorides went completely through. In figure 19 it can be seen that at the location of the crack, the chlorides nearly reached the other side of the sample, which means it could have happened at other places in the sample due to the irregularity of the crack. This could cause a disruption in the difference in voltage between the sides of the samples.

When using the following formula with the aging factor:

$$D = D_0 * \left(\frac{t_0}{t}\right)^n$$

With:

- D = migration coefficient at wanted time (in this case 56 days)
- D_0 = migration coefficient at 28 days
- t_0 = 28 days
- t = wanted time (in this case 56 days)
- n = aging factor (in this case 0,178)

The formula and the value for the aging factor are found in a research by (Yu, 2015). Filling in this formula one finds $D = 12,1 \cdot 10^{-12} \text{ m}^2/\text{s}$. This value is slightly lower than the value of the uncracked sample. However, the value of the SSC samples decreased more. This suggests that it might be possible to decrease the cover depth. Although, as the difference is not very large, research should be done with longer healing periods.

In all materials clear peaks due to the cracks can be seen, in one SSC sample even multiple cracks showed, as was expected due to the fibers. Also, the migration coefficient of the SSC samples at the location of the cracks are lower than the migration coefficient of the TC mortar samples. Looking at the results, the migration coefficient of the SSC samples is lower, although this could be caused by the smaller crack width in the samples as well. The crack width of the SSC samples is smaller than the crack width of the TC mortar samples due to larger rebound effect after unloading. Still, the migration coefficient at the location of the cracks is much larger than the migration coefficient of the uncracked surface, while a smaller peak was expected. It could be the case that 28 days of healing is not enough to seal the cracks, therefore tests with longer healing periods should be performed to find out if this is the case.

The peaks at the location of the cracks show that the penetration perpendicular to the crack in the TC mortar samples is larger than is the case for the SSC samples ($D_{\text{nssm,SSC}} = 11,0$ vs. $D_{\text{nssm,TC}} = 7,2$ ($\cdot 10^{-12} \text{ m}^2/\text{s}$)).

As mentioned before, the presence of CEM III in the mixture of the Concrete causes the migration coefficient to be lower than the migration coefficient of the SSC samples. This, in combination with the differences in crack width, makes it difficult to compare the samples of the different materials.

Method

The cracking of the samples was very hard and took a lot of time. Especially the cracking of the traditional concrete was difficult, as a crack width of 200 μm was wanted and a few times the sample would break in two halves.

Besides that it was hard to get the same crack width for all the samples, especially for different materials. This was due to the difference in rebound, which was difficult to estimate and this led to different unloaded crack sizes.

If more research has to be done, especially with larger cracks, it is advised to use another set up for the cracking and possibly for the RCM test as well. For examples the wedge-splitting method can be used to create the cracks.

5.1.4. Frost/thaw cycle test

The results are as expected for the series of cycles before the healing period. The TC mortar scales more than the SSC mortar and the amount of scaling continues at the same rate over time.

However, as said in the results, some of the samples have a much lower scaling than the other samples of the same materials and cause a high standard deviation. This can be caused by the water level at the samples. When the water level is too low, there will be less or no scaling due to freeze/thaw cycles.

Another factor that can influence the scaling is the freeze/thaw chamber. The machine does not always work properly, which can decrease the amount of cycles. Due to problems with leaking, the samples were split in two batches to make sure the right method was used. This, in combination with the problems of the freeze/thaw chamber, can cause a difference in scaling as well, which can mean an increase in the standard deviation.

For the series of cycles after the healing period the TC mortar scales more than the SSC mortar as expected. However, it was also expected that the difference in scaling would increase. When looking at the results it can be seen that the difference has decreased after the healing period.

In this batch again large differences in values can be seen between the samples of the same material. This time the standard variation is even larger. Again, the water level on the samples is part of the cause. Together with problems of the freeze/thaw chamber. The increase of the standard deviation can be coupled to the increase of problems with the freeze/thaw chamber. When using the freeze/thaw chamber again it might be a good idea to use an external device to monitor what happens with the temperature, so the exact number of cycles is known, even after malfunctioning.

This test is mainly about the external damage of the materials due to frost/thaw cycles. No real data came forward about the amount of healing after the first series of cycles. It would be interesting to do tests or change the test in such a way that information about these aspects will be found as well.

5.1.5. Young's modulus in compression test

The results of the Young's modulus test are conform the expectations.

Officially the test should be done until a third of the compressive strength. However, the machine used could only go up to 10 kN instead of the 50-60 kN needed. Therefore, the Young's modulus is determined using the stress and strain over a smaller range. Those values were already in the straight part of the graphic. The only thing that could not be done, was to load the sample until failure to see if this value is comparable to the value of the compression test. So if loading the sample until failure is required, a machine with higher capacity should be used.

5.1.6. Shrinkage test

As mentioned in the results, the shrinkage values of the sample T1 are very large in comparison to the values of the other samples. When taking T1 into account, the shrinkage of the TC mortar samples on average is larger than the shrinkage of the SSC samples, which is against the expectations, although with a high standard deviation ($\sigma = 1,7 - 2,7$).

However, if the results of T1 are left out of the comparison, the shrinkage of the SSC mortar samples is larger than the shrinkage of the TC mortar samples, which is as expected. Also, the standard deviation decreases significantly ($\sigma = 0,1 - 0,4$). This can be seen in figure 29. Here the shrinkage development is shown again, although on the right, a graph is added where the results of T1 are left out.

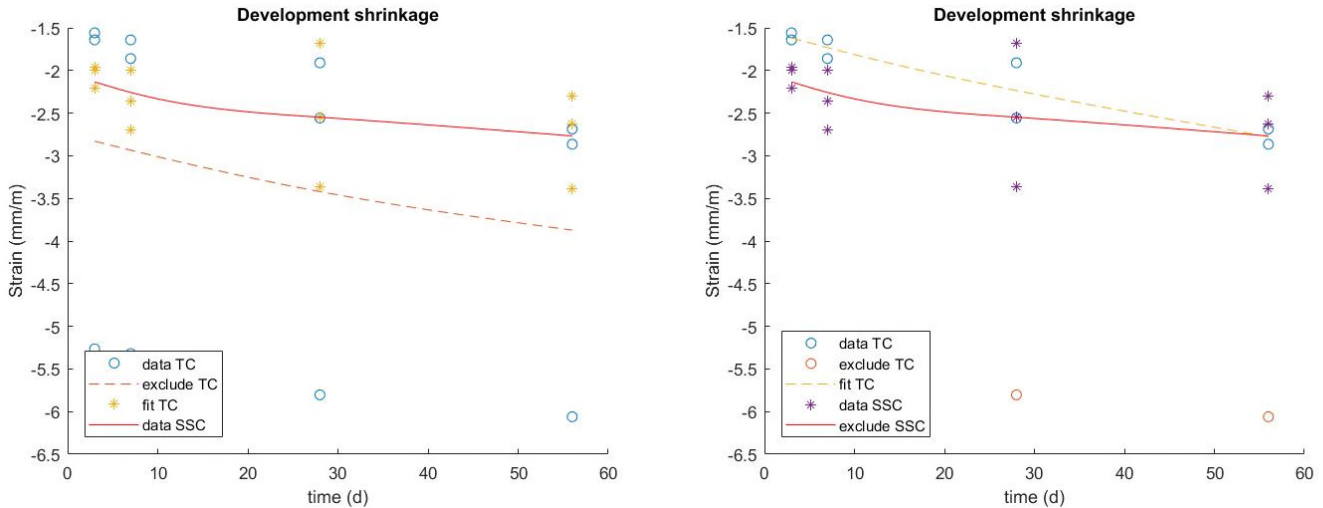


Figure 29: Development shrinkage: left – with T1; right – without T1

5.1.7. Absorption test

It was expected that the SSC samples would absorb more water than the TC mortar samples due to the added light weight aggregates. This difference can be seen in the results.

It can also be seen that the rate of absorption decreases over time for both materials. This is in agreement with the expectations as well. The decrease in rate of absorption is larger for the TC mortar samples, probably because the TC mortar is saturated faster than the SSC mortar.

5.2. Demonstrator Bridge

5.2.1. Design TC vs. SSC

Structural design

When comparing the designs for the bridge made with TC and SSC, one can see that, using the assumptions from the start of the report, the design made with SSC gives a more slender construction. The difference in slenderness can be seen most clearly in compressive and tensile bars of the truss.

The beams are also more slender. However, in case of the bridge deck, there is nearly no difference in thickness between the both materials, the deck of TC is even slightly thinner. This is due to the decreased stiffness of the SSC material compared to the TC material, caused by the smaller Young's modulus. Therefore more height is needed to get the same stiffness. It would be desirable if the Young's modulus of the SSC mortar can be increased by making some changes to the mixture.

The increased slenderness of the beams, the compressive and the tensile bars is mostly due to the decrease in needed cover for the SSC and the lack of extra reinforcement for crack width control.

Effect healing agent

When looking at the design, it is expected that the healing agent will have most influence on the bridge deck and the tensile bars of the truss.

The first point of influence of the healing agent on the bridge deck is caused by the fabrication method. It is chosen to use cold formed bending to produce the arched bridge deck. This process causes the deck to crack. The healing agent will be able to heal these cracks more quickly than the autogenous healing of the TC. The fibers that keep the cracks small help stimulate this as well. There will also be negative moments at the locations where the deck is supported by the trusses. At these locations the deck will crack under loading. This will happen above the compression bars of the truss as well (see figure 30, red circles).

For the beams and tensile bars of the trusses, the effect will be smaller. For these elements there will be much less chance of de-icing salt or chlorides to come close. The main risk here is humidity and oxygen causing the reinforcement to corrode (see figure 30, orange circles).

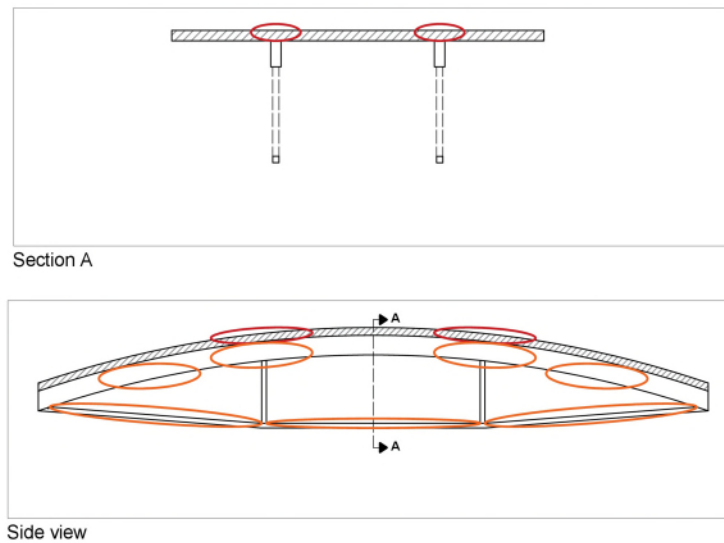


Figure 30: Locations corrosion due to cracks

However, in both cases the cracks will seal itself more quickly due to the combination of the healing-agent and fibers. Therefore, the chance for the chlorides (due to de-icing salt, etc.) to quickly reach the reinforcement through a crack is decreased and corrosion will be delayed compared to the structure designed with TC.

Costs

Here a qualitative comparison of the costs of the design made with TC and the design made with SSC will be made. For this comparison the following points will be taken into account:

- The costs for the transportation of the elements to the construction site
- The costs of the materials
 - o Concrete
 - o Steel
- The production costs
- The costs of the assembly
- The costs due to maintenance

Slightly more concrete is needed for the Demonstrator Bridge designed with TC than for the bridge designed with SSC (see table 22). Also, it can be seen that the bridge designed with TC needs more steel, the amount of steel needed is also shown per element. The increase in steel for the bridge designed with TC is probably due to the fact that for the bridge designed with SSC crack width is controlled by the added fibers, while the steel reinforcement has to do this for the design with TC.

Comparing the costs of the materials, one can see that the bridge designed with SSC is more expensive than the bridge designed with TC, as the elements of the SSC mixture are more expensive, especially the healing agent, the fibers and the plasticizer. The prices of all materials used can be found in appendix I.

Table 22: Needed materials and costs

		TC	SSC
Volume concrete (m³)		10,8	10,1
Weight steel	Deck (kg/m²)	3,0	2,4
	Beam (kg/m)	10,8	7,3
	Compressive bars (kg/m)	1,1	1,8
	Tensile bars (kg/m)	10,3	6,6
	Total (kg)	701	324
Total costs (€)		5.184	20.587

However, these are only the production costs of the bridge. Below, for all points the expected costs are compared to the costs for a bridge designed with TC. These points are also shown in comparison figure 31.

- Transportation – These costs are expected to be similar for the bridges designed with both materials.
- Materials – The costs for the material needed for the bridge designed with SSC is significantly higher than the costs for the bridge designed with TC.
- Production – The production costs are expected to be slightly higher for the bridge designed with SSC, as some new materials are added to the mixture.
- Assembly – The costs for the assembly of the bridge is expected to be similar for the design of both materials.
- Maintenance – The costs for maintenance are expected to be significant lower for the bridge designed with SSC compared to the bridge designed with TC due to the increased durability of SSC.

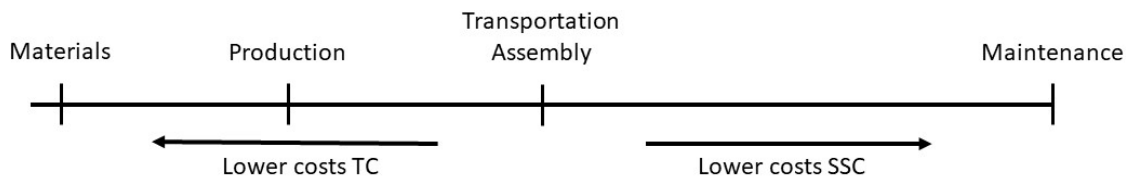


Figure 31: Comparison costs TC and SSC

Looking at figure 31 and the points named above, one can see immediately that the main difference in costs is found in the materials and the maintenance. Besides these points the differences are small. As the expectation is that the decrease in maintenance costs for the SSC bridge is larger than the increase in costs for materials, this overview suggests that the SSC bridge would be cheaper when looking at the whole lifespan.

5.2.2. Assumptions structural design

In this paragraph, first, the differences between the results and the assumed characteristics will be discussed. Afterwards a short calculation will be made with results of SSC to see how these influence the design.

Compressive strength

As mentioned earlier in the discussion about the results of the tests, the compressive strength of the SSC mortar is lower as expected: 32,5 MPa instead of the assumed 45 MPa. This will not have much effect on the dimensions of the structure of the bridge, only the height of the compressive zone (x_u) will increase which will cause a decrease in moment capacity. However, this is not expected to be a problem that cannot be solved without increasing the construction height significantly.

The results were only slightly lower for the TC mortar than expected and will not have noticeable effects.

Flexural strength

In both cases, the flexural strength is slightly higher than assumed. This means that both materials will crack under slightly higher loads. Besides that, it will not affect the design of the structure of the bridge.

Cover depth

The migration coefficient of the uncracked samples was similar for both materials, as was expected, and after healing, the migration coefficient of the SSC mortar was lower than the migration coefficient of the TC mortar. This strengthens the thought that the cover depth can be decreased.

However, after 28 days of healing a clear peak can still be seen at the location of the crack, which means that the crack is not sealed yet. The permeability test shows that the cracks in the SSC mortar were mostly sealed after 42 days. So to be sure whether the cover depth can be decreased, tests with longer healing periods should be done.

The test done for this thesis was focused on the difference between the TC mortar and the SSC mortar, although it does not show if and how much of the cracks are sealed. An option is to test cracked samples without healing period as well to get this information. When comparing the cracked samples without healing period with the cracked samples with healing period, one would be able to see the impact of the healing period.

To use the simplified model from the literature it is necessary to know the depth of the crack to be able to know if the cover depth can be decreased. However, with this testing method the depth of the crack is not known, so the model cannot be used. If there is a wish to use this model in the future, a method has to be used where the depth of the crack is known or can be known.

For now, it is not possible to say whether the cover depth can be decreased to 25 mm instead of 45 mm as more research is needed to see how much the effect of the healing capacity is and what period of healing is necessary to seal the cracks completely.

If the cover depth cannot be decreased for the SSC, the dimensions of the bridge will increase and will probably become larger than the design with TC due to the low Young's modulus of SSC. However, the results point in the direction of a better healing capacity, only more tests should be done to be sure.

Young's modulus

The assumed Young's modulus of both materials was slightly higher than the results from the test. However, the results and assumptions were of the same magnitude.

The lower value of the Young's modulus mainly influences the stiffness of the construction and therefore the deformation. It can be, that the height of the structural elements, mostly the bridge deck and the beams, have to be increased slightly.

Density

No test has been done to measure the density of the materials. However, the initial weight of the samples of the absorption test can be used to make an estimate of the density of the materials. The values can be found in the table below.

Table 23: Density TC and SSC mortar (sample size 40 x 40 x 160 mm³)

	Initial weight (g)	Density (kg/m ³)
TC mortar	560,3	2189
SSC mortar	455,1	1778

The values in the table show that for both materials the density is lower than the assumed value. This will cause the permanent load to decrease slightly, which will cause a small change in the internal forces and the deformation. However, the difference is not that big, so no large changes in the construction are expected.

Calculation results SSC

The assumptions made in chapter 3 are shown again together with the results from the tests in the table below:

Table 24: Assumed characteristics compared to results

Characteristic	SSC mortar - assumed	SSC mortar - results
<i>Compressive strength (MPa)</i>	45	32,5
<i>Flexural strength (MPa)</i>	11	13
<i>Cover depth (mm)</i>	25	25 (uncertain)
<i>Young's modulus (GPa)</i>	15	10,2
<i>Density (kg/m³)</i>	1860	1778

The dimension of the construction calculated with the results of the tests performed on SSC mortar are shown in table 24 together with the dimensions from the calculation based on the assumed characteristics.

Table 25: Dimensions based on assumptions and based on results

Structural element	SSC mortar - assumed	SSC mortar - results
<i>Bridge deck – h (mm)</i>	140	160
<i>Beam – b x h (mm²)</i>	140 x 350	140 x 400
<i>Compressive bar – b x h (mm²)</i>	85 x 85	85 x 85
<i>Tensile bar – b x h (mm²)</i>	85 x 120	85 x 120

Comparing the dimensions of the calculation made with the results with the dimensions of the calculation based on the assumed characteristics, one can see that the height of the bridge deck and the beams is increased. This increase is mainly due to the lower Young's modulus in the results than was expected.

6 Conclusions & recommendations

This final chapter will discuss conclusions based on the results and the discussion. Also, some recommendations will be made for further research and development of the SSC material.

6.1. Conclusions

During this thesis a structural design has been made for a TC mortar and a SSC mortar based on the expected characteristics of the materials. In this manner it was possible to research the effects of the characteristics of the SSC mortar on the structural design. Research on multiple characteristics was also performed to see if the assumptions made for the design were correct, looking at the results the following can be concluded:

Structural design

The structural elements of the bridge designed with SSC are more slender than the structural elements of the bridge designed with TC, except for the bridge deck. The bridge deck is slightly thinner in the design made with TC. The reason the bridge deck made with SSC cannot be more slender is because the low Young's modulus decreases stiffness of the material, which means more height is needed. The increased slenderness of the beams and bars of the truss are mainly caused by the decrease of needed cover depth and the lack of reinforcement needed for crack width control.

Structural characteristics

The results show that the main differences in the structural characteristics of the TC mortar and the SSC mortar are the compressive strength, the Young's modulus, and the shrinkage. The lower compressive strength and the increased shrinkage do not have a large influence on the structural design. The lower compressive strength only influences the height of the compressive zone and the increase in shrinkage is controlled by the added fibers. However, the lower Young's modulus does have significant influence on the construction. As mentioned before, the effect of the lower Young's modulus causes a decrease in stiffness.

Durability

Looking at the results of durability, one can see that, overall, the SSC mortar is more resistant to aggressive environments than the TC and that the SSC has an increased healing capacity. This suggests that it is possible to decrease the minimal cover depth. It is not possible to say how much the cover depth can be decreased, as the time needed to seal the cracks is not precisely known for now. It is expected that the increase in durability will be most visible at the locations where the structure cracks and the highest chloride concentration is found.

Costs

The production costs of both designs are also compared. It is found that the design with TC has lower production costs than the design with SSC. However, the expectation is that the bridge designed with TC will need maintenance and the SSC bridge can do mostly without maintenance. It is also expected that the bridge designed with SSC will have a longer live span. Taking the whole service life into account, one expects the SSC bridge will get less expensive compared to the TC bridge. After a long enough life span, it could even be cheaper. Although, as mentioned before, no numbers are known as no structures have been build using SSC yet.

6.2. Recommendations

This thesis gives an overall view of the characteristics of TC and SSC and the differences between the materials. In short the following about SSC can be said:

- It is possible to design a slender structure compared to a structure designed with TC.
- The cover can be decreased, although more research is needed to determine how much.
- SSC is more resistant to frost/thaw cycles in combination with de-icing salts.
- The fibers eliminate the need of additional reinforcement to control the crack width.
- The Young's modulus is very low and decreases the stiffness of the material.
- The production costs of the SSC bridge are higher than the TC bridge, however this is expected to be compensated by less maintenance and an increased lifespan.

It has to be mentioned that due to the amount of different tests in a relatively short time, all tests have been performed on quite small batches of samples and some results have a large dispersion. Therefore, it is advised to do more research with larger batches of samples, so proper statistics (average and standard deviation) can be used to determine the characteristics of the materials. For the performance of more research, it would be best to take a TC mortar with lower compressive strength which is similar to the compressive strength of the SSC mortar found in this research.

The results of the test show that there is a possibility to decrease the cover depth, although, still more research has to be done to determine how much the cover depth can be decreased.

An important point is to see whether there are possibilities to increase the Young's modulus of the SSC material by making some changes to the mixture composition, because at the moment this is a limiting factor if it comes to the height of the bridge deck and probably other larger spans with high deformations.

Also, it would be interesting to have a look at structures in which a TC and a SSC are combined in different layers. This is because the high costs of the SSC and, as concluded earlier, the main difference can be made in the top layer of the structure where the cracks occur and the chloride concentration is highest, while the effect in the other parts of the structure will be less significant.

Test methods

As already mentioned in the discussion, difficulties occurred during execution of some of the tests and it is advisable to make some changes in the procedure.

For the permeability test, the difficulty was the splitting of the samples. Due to the fibers in the SSC mortar it was not possible to completely split the samples. This caused problems with placing the spacers to control the crack width. Therefore, it is advisable to find another way of cracking the samples in which the crack width can be controlled. Also, due to the low permeability, the measurements were very sensitive for mistakes due to leakage by refilling the reservoirs. It would be recommendable to find a way to refill the reservoirs in a way that spilling can be prevented.

The RCM test had problems with creating the cracks as well, although in this case the problem was caused by failure of the TC mortar samples. To get a crack of 0,2 mm, quite often the sample completely got split and therefore unusable. Also, the process to create the cracks took 2 hours per sample and this time should be taken into account. Thus, it is advisable to search for another way to crack the samples or the height of the samples could be increased. The wedge splitting method and drilling out a core afterwards (Savija, 2014) is a good option. Changes should be made in the test, especially when larger cracks are required. Also, tests with longer healing periods should be done in combination with tests on cracked samples without healing. This way a good view of the impact of healing is obtained and one will be able to see how long it takes to seal the cracks enough to decrease the chloride penetration.

During the frost/thaw test only the external damage is researched by measuring the weight loss due to scaling. It is advised to measure the starting weight as well, to be able to see if and how much healing occurred before the second series of cycles after the healing period starts. Here, it is interesting to look at different lengths of healing periods as well. Also, the internal damage should be researched, as at the moment only knowledge about the external damage is gathered.

However, the best way to gather the missing knowledge, especially when looking at the durability and the need for maintenance, is to build the proposed or a similar bridge design using SSC and monitor the construction during a longer period of time.

Bibliography

- Blagojevc, A. (2016). *The influence of cracks on the durability and service life of reinforced concrete structures in relation to chloride-induced corrosion*. Delft: Ridderprint.
- Constructiebedrijf Hillebrand B.V. (2010). *Voetgangersbrug*. Retrieved 10 23, 2016, from Constructiebedrijf Hillebrand B.V.: <http://www.hillebrand.nu/nl/bruggenbouw/2/43/voetgangersbrug/3.htm>
- de Rooij, M., van Tittelboom, K., de Belie, N., & Schlangen, E. (2013). *Self-healing phenomena in cement-based materials*. Dordrecht: Springer.
- ENCI B.V. (2015). *Beton pocket 2016*. 's-Hertogenbosch: ENIC B.V.
- Farah, H., & Daamen, W. (2016). *Short note with respect to building bridges on the TU Delft campus as show case for innovative materials*. Delft: TU Delft.
- fib. (2006). fib Bulletin 34. *Model code for service live design*. Lausanne, Switzerland: Federation for structural concrete (fib).
- Jonkers, H., Schlangen, H., Schipper, H., & Lukovic, M. (2016, December 22). (C. Roghair, Interviewer)
- Li, M. (2009). *Multi-scale design for durable repair of concrete structures*. Ann Arbor: University of Michigan.
- Liu, X., Chia, K. S., & Zhang, M.-H. (2011). *Water absorption, permeability and resistance to ion-chloride penetration of lightweight aggregate concrete*. Singapore: Elsevier.
- Naaman, A. E. (2007). Tensile strain-hardening FRC composites: historical evolution since the 1960's. In A. E. Naaman, *Advances in construction materials* (pp. 181-202). Heidelberg: Springer.
- Pacheco Farias, J. (2015). *Corrosion in cracked concrete: chloride microanalysis and service life predictions*. Delft: TU Delft.
- Palin, D., Jonkers, H., & Wiktor, V. (2015). *Autogenous healing of sea-water exposed mortar: Quantification through a simple and rapid permeability test*. Delft: TU Delft.
- Savija, B. (2014). *Experimental and numerical investigation of chloride ingress in cracked concrete*. Delft: Haveka B.V.
- Sierra-Beltran, M. (2017, May 21). (C. Roghair, Interviewer)
- Sierra-Beltran, M., Jonkers, H., & Schlangen, E. (2014). *Characterization of sustainable bio-based mortar for concrete repair*. Delft: Elsevier.
- Tuutti, K. (1982). *Corrosion of steel in concrete*. Stockholm: CBI research.
- Yu, Z. (2015). *Microstructure Development and Transport Properties of Portland Cement-fly Ash Binary Systems: In view of service life predictions*. Delft: TU Delft.

Appendix

Appendix A: Test plan

RESEARCH PROJECT

Researchers: Charlotte Roghair
Supervisor: Henk Jonkers
Project Title: Self-healing concrete: Curved panels for a Demonstrator Bridge
Start Date: 05-09-2016
Current Date: 25-10-2016
Project code:

- **The project:** To show companies and other possible interested parties what possibilities the use of self-healing concrete gives when used, a 'demonstrator' bridge will be developed for the TU Delft campus. This bridge will show that applying strain hardening self-healing concrete (SSC) allows building an elegant bridge with less concrete used in comparison to a similar bridge designed with traditional concrete (TC).

At this moment little is known about characteristics such as strength and how the material works in combination with reinforcement. Therefore tests will be done to find the characteristics of SSC, which are necessary to calculate a pedestrian bridge. The tests will be performed on TC as well, so it will be possible to compare the results.

These tests will be performed on samples of mortar, which have similar characteristics as the concrete. This is done, because of the size of the samples that will be used. Only test 3: Rapid Chloride Migration test will be done on concrete as well.

- **Concrete mixtures:** The used concrete mixtures are given in the table below.

<i>Mixture composites (kg/m³)</i>	<i>Self-healing mortar (0-2 mm)</i>	<i>Mixture composites (kg/m³)</i>	<i>Traditional mortar (0-4 mm)</i>	<i>Mixture composites (kg/m³)</i>	<i>Traditional concrete (0-16 mm)</i>
<i>Cement I 42.5 N</i>	440	<i>Cement I 42.5 N</i>	464	<i>Cement III/B 42.5 N</i>	286
<i>Fly ash</i>	530	<i>Water</i>	232	<i>Cement I 52.5 R</i>	32
<i>Limestone powder</i>	410	<i>Sand 2-4 mm</i>	475	<i>Water</i>	182
<i>LWA*</i>	69,315	<i>Sand 1-2 mm</i>	350	<i>Sand 0-4 mm</i>	809
<i>Water</i>	375	<i>Sand 0.5-1 mm</i>	355	<i>Gravel 4-16 mm</i>	1057
<i>Super Plasticizer*</i>	14,4	<i>Sand 0.25-0.5 mm</i>	320		
<i>PVA fibres 8 mm</i>	22	<i>Sand 0.125-0.25 mm</i>	180		

*Lightweight aggregates (55 kg/m³) with carbon source (4 kg/m³), nutrient (0,3 kg/m³), bacteria (0,015 kg/m³) and healing agent (10 kg/m³).

** Cretoplast Col. 35% PL

- **Test 1: Compressive and flexural strength test**

Aim of test: The aim of the compressive and flexural strength test is to measure the compressive strength of the SSC mortar as well as the compressive strength of the TC mortar and compare the found results. The test is also meant to measure the flexural strength.

Test description: The test will be done on prisms of 160 x 40 x 40 mm. is placed in a concrete press with the finished side directed to the column.

First the prisms will be subjected to a three point bending test; thereafter the two halves will be subjected to a compression test.

Three point bending test

The prisms will be placed on two points with a span of 140 mm. In the middle of this span (the third point) a load will be applied to bend the prisms until failure. When failure occurs the load will be recorded. Using this load and the following formula's the tensile strength of the prism can be defined, this is about 50-75% of the flexural strength.

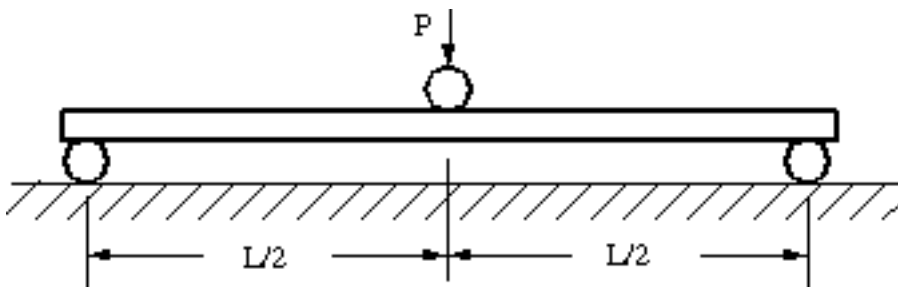
First the bending moment is calculated: $M = (1/4) * F * L$

Followed by the moment of inertia: $I = (1/12) * b * h^3$

Then the tensile stress can be calculated: $\sigma = (M * z) / I = (M * h) / (2 * I) = (3 * F * L) / (2 * h^3)$

- With:
- M = bending moment (Nmm)
 - F = applied load (N)
 - L = span of the prism (mm)
 - I = moment of inertia (mm⁴)
 - b = width of the prism (mm)
 - h = height of the prism (mm)
 - z = (1/2) * h (mm)

In the figure below a three point bending test can be seen.



<http://www.mech.utah.edu/~rusmeeha/labNotes/composites.html>

Also a three point bending test measuring the deformation will be done to get more information about the difference in behaviour of the materials.

The three point bending test will also be done while measuring the horizontal deformation.

Compression test

Both halves of the prism are placed in a press with the finished side directed to the column.

Until half of the estimated load, the load may be applied quickly to the cube, after this the applied load may be increased with a speed of 0.6 ± 0.04 MPa per second. The highest applied load on the cube should be recorded. Using the formula below the maximum compressive stress can be calculated.

$$\sigma_{\text{druk}} = F / A \quad (\text{MPa})$$

With: σ_{druk} = compressive stress (N/mm²)
F = highest applied force (N)
A = area of top cube (mm²)

The mortar of the uncracked cubes will be tested when 3, 7 & 28 days old.

Expected Results: The expectation is that the TC mortar will have a compressive strength of ± 45 MPa after 28 days. For the SSC mortar a compressive strength of ± 45 MPa is expected after 28 days of hardening as well. The flexural strength is normally about 10% of the compressive strength, though for the SSC mortar it is expected to be higher due to the fibre reinforcement, circa 25%.

Planning of the test: The mortar mixtures will be made and casted in the molds for the prisms. The prisms will be kept in the curing room. After 3 days of hardening the first prism of both SSC and TC mortar will be tested on bending and compression. After 7 days of hardening the next prisms of both mortar mixtures will be tested and after 28 days the last prisms will be tested. All the tests will be done until failure occurs. After 28 days the three point bending test with the measurement of the deformation will be performed.

Materials needed:

- Strain hardening self-healing mortar, 9 + 3 prisms (see above)
- Traditional mortar, 9 + 3 prisms (see above)

Equipment needed:

- Mold
- Compression machine
- Three point bending machine
- Equipment to make mortar mixtures

Assistance needed: Explanation about the use of equipment and machines and help to start up the test. (M. van Leeuwen)

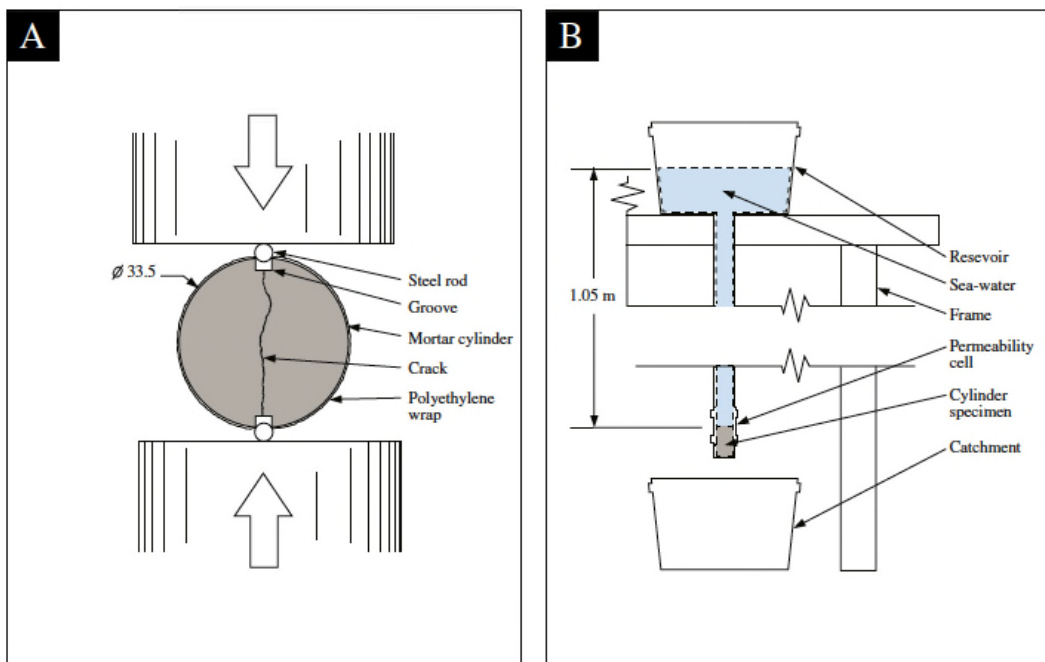
- **Test 2: Permeability test**

Aim of test: The aim of the permeability test is to investigate the healing capacity of the self-healing mortar and to compare this with the healing capacity of the traditional mortar.

Test description: The test will be executed on cylinders with a length of 60 mm and het diameter of 33.5 mm. After a 28-day period of hardening the cylinders were wrapped in polyethylene and steel rods were placed at the grooves before placing it in the compression machine. There a compressive load will be applied until the cylinders split. When cylinders are split, the polyethylene will be removed carefully and spacers will be placed to achieve crack widths of 0,2 mm.

Afterwards the permeability will be tested directly and a picture of the crack will be taken. This will be repeated after 14, 28 and 42 das after the first measurements.

The permeability will be tested by placing the cylinders in a fitting at the bottom of a column connected to a reservoir. Underneath it is a bucket and the weight of the water in the bucket will be recorded after 5 and 10 minutes. The sample should be saturated before the start of the test; otherwise the closing of the crack due to strain hardening self-healing. The water level of the column is 1 – 1.05 m, to give a constant water head of 0.1 bar. In the figures below the splitting setup and the permeability setup can be seen.



Expected results: The expected result of the test is that the permeability of the SSC and TC mortar will be similar at the start of the test, but that the permeability of SSC mortar will decrease much more than the traditional mortar due to the increased healing capacity.

Planning of the test: The mortar mixtures will be made and casted into the molds for the cylinders. The cylinders will be kept in the curing room until they have an age of 28 days.

When the age of 28 days is reached the cylinders will be split as is explained above and put together again using spacers, to ensure the right crack width. Directly afterwards, the first permeability test will be done and a picture of the crack will be taken.

When the permeability test is done, the cylinders will be kept in containers of water to heal until the next permeability test. The permeability test will be done every 14 days with a total of 4 tests. Every time a photo will be taken as well.

- Materials needed:**
- Strain hardening self-healing mortar, 6 samples (see above)
 - Traditional mortar, 6 samples (see above)
 - Water
 - Polyethylene

- Equipment needed:**
- Mold
 - Compression machine
 - Steel rods
 - Equipment to make mortar mixtures

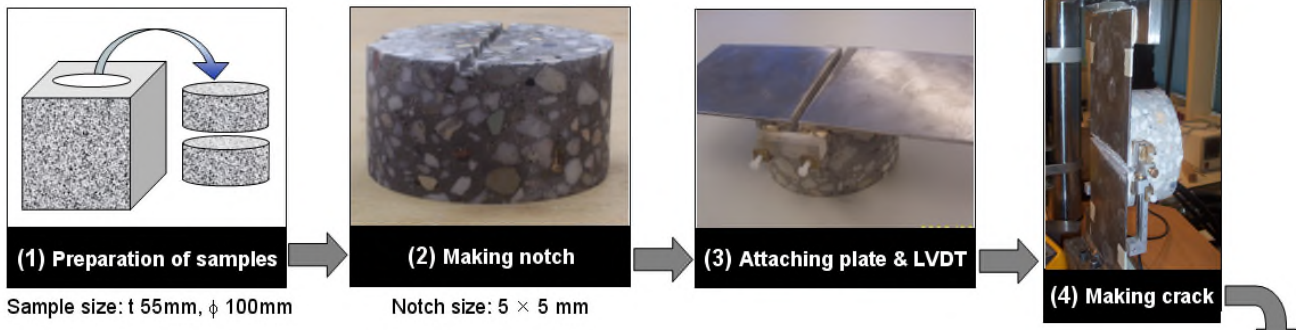
Assistance needed: Explanation about the use of equipment and machines and help to start up the test. (M. Megalla)

• **Test 3: Rapid chloride migration test**

Aim of test: The aim of the rapid chloride migration test is to be able to compare chloride migration of traditional and self-healing mortar, especially when both mortars are cracked and had time to heal. The test will be done at normal concrete as well.

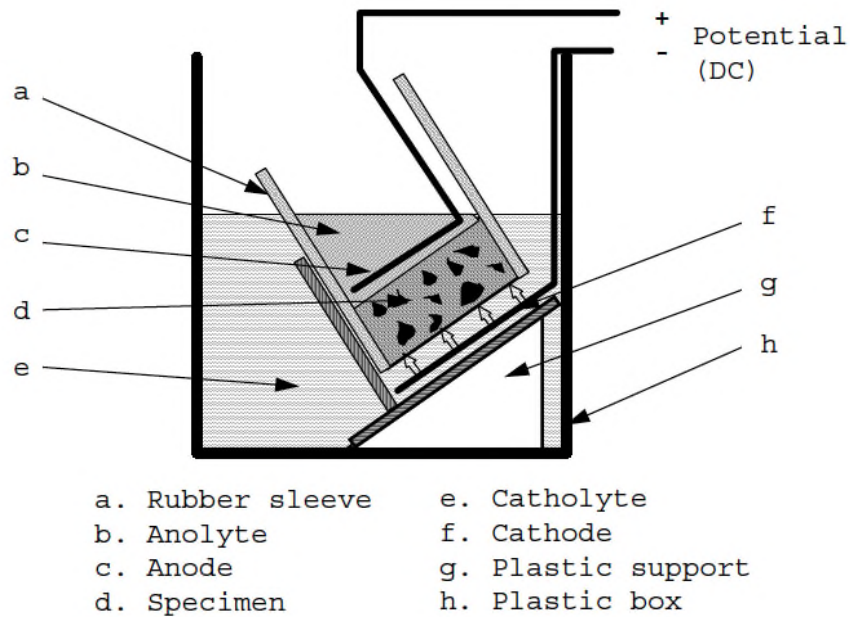
Test description: The rapid chloride migration test is done with a 50 mm thick slab of mortar with a diameter of 100 mm.

The samples will be cut from cubes with the size of 150 x 150 x 150 mm or cast in a cylindric mold with a diameter of 100 mm. From every cube/cylinder will be taken two or more slabs with a height of 55 mm. Then a notch of 5 mm will be made over the middle of the cylinder and two steel plates will be attached. After this it is possible to make a crack using a pulling machine. This can be seen in the figure below.

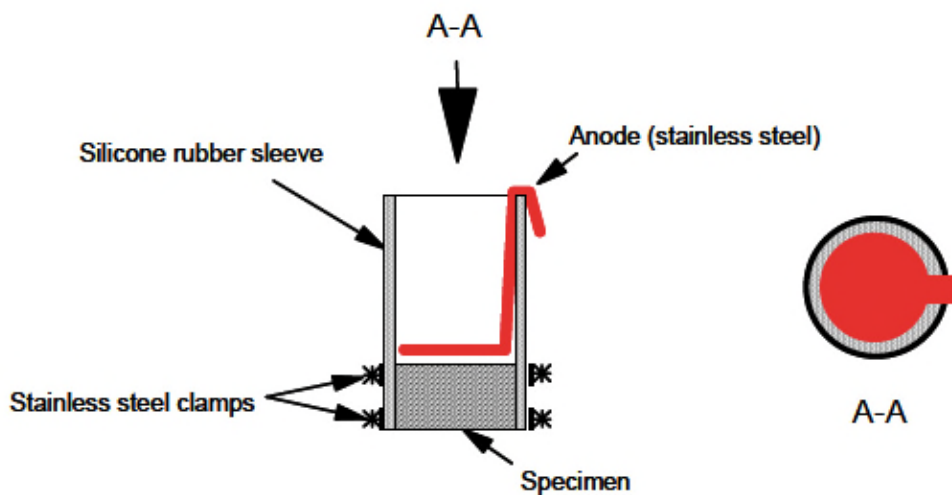


For both types of mortar the strain should be the same, so the TC mortar will have one crack while the SSC mortar is expected to have multiple cracks. The width of the cracks in the self-healing concrete should be 0.2 mm.

The samples will be subjected to a DC potential using the setup seen below.



The catholyte reservoir will be filled with 12 L of 10% NaCl solution. Then the rubber sleeve will be put on the sample and two clamps will be applied as seen in the next figure. If there are rough surface parts or defects on the curved surface, which could lead to significant leakage, a line of silicone should be applied to improve tightness.



Afterwards the samples should be placed in the plastic support in the catholyte reservoir with the end surface that was nearest to the as-cast surface exposed to the anolyte solution. In case of a cracked sample the cracked side should be exposed to the catholyte solution. The sleeve above the samples should be filled with 300 mL of the anolyte 0.3 M NaOH solution. Then the anode should be immersed in the anolyte solution and connected to the positive pole, while the cathode should be connected to the negative pole.

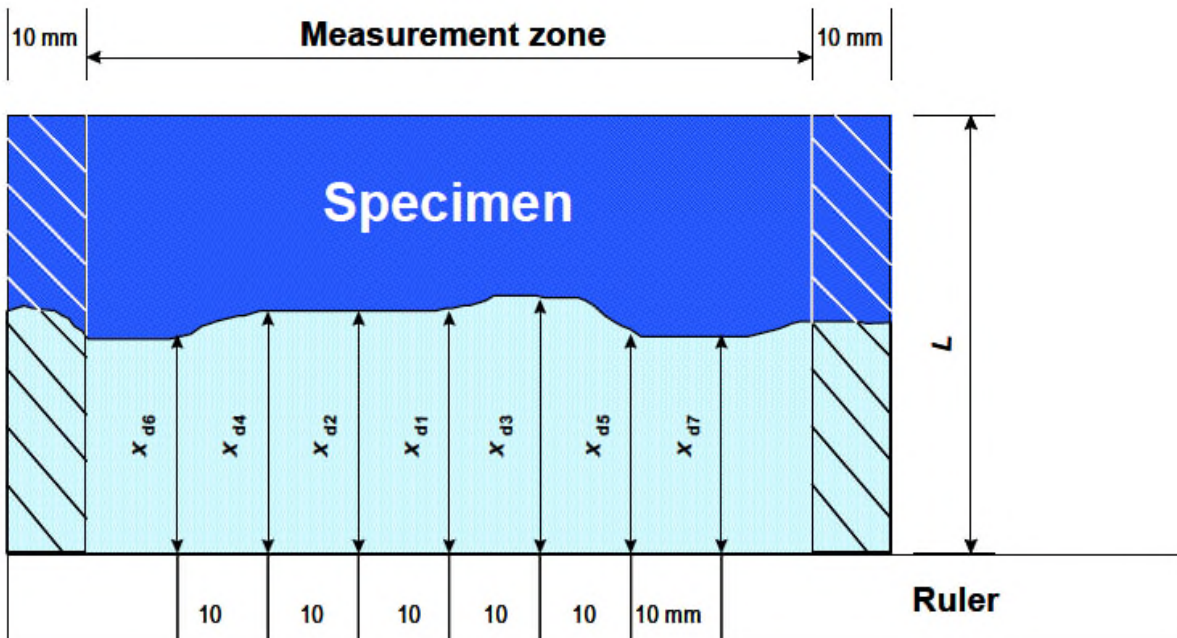
Turn on the power on 30 V and record the initial current through the sample. Adjust the voltage if necessary according to the table below.

Initial current I_{30V} (with 30 V) (mA)	Applied voltage U (after adjustment) (V)	Possible new initial current I_0 (mA)	Test duration t (hour)
$I_0 < 5$	60	$I_0 < 10$	96
$5 \leq I_0 < 10$	60	$10 \leq I_0 < 20$	48
$10 \leq I_0 < 15$	60	$20 \leq I_0 < 30$	24
$15 \leq I_0 < 20$	50	$25 \leq I_0 < 35$	24
$20 \leq I_0 < 30$	40	$25 \leq I_0 < 40$	24
$30 \leq I_0 < 40$	35	$35 \leq I_0 < 50$	24
$40 \leq I_0 < 60$	30	$40 \leq I_0 < 60$	24
$60 \leq I_0 < 90$	25	$50 \leq I_0 < 75$	24
$90 \leq I_0 < 120$	20	$60 \leq I_0 < 80$	24
$120 \leq I_0 < 180$	15	$60 \leq I_0 < 90$	24
$180 \leq I_0 < 360$	10	$60 \leq I_0 < 120$	24
$I_0 \geq 360$	10	$I_0 \geq 120$	6

After adjustment record the current again. Record the initial temperature as well, as shown by the thermometer and thermocouple. Choose an appropriate test duration using the current and the table above. Before terminating the test, record the final temperature and current. Disassemble the setup in opposite order of the procedure to build up.

Rinse the sample with tap water and wipe off the excess water of the surfaces of the sample. Split the sample in halves and choose the part with the most perpendicular split section to the edges of the sample for the penetration depth measurements.

Spray with 0.1 M silver nitrate solution on the freshly split section. After ± 15 minutes the chloride precipitation will be clearly visible on the surface and the penetration depth can be measured. The measurements will be taken at intervals of 10 mm starting at the center of the sample with an accuracy of 0.1 mm to obtain 7 depths. Do not make measurements in a zone of 10 mm to the edge. This can be seen in the figure below.



The non-steady-state migration coefficient can be calculated with the following simplified formula:

$$D_{nssm} = \frac{0.0239(273+T)L}{(U-2)t} \left(x_d - 0.0238 \sqrt{\frac{(273+T)L x_d}{U-2}} \right)$$

With:

- D_{nssm} = non-steady-state migration coefficient ($\times 10^{-12}$ m²/s)
- U = absolute value of applied voltage (V)
- T = average value of initial and final temperatures in the anolyte solution (°C)
- L = thickness of the sample (mm)
- x_d = average value of the penetration depths (mm)
- t = test duration (hour)

For more detailed information see NT-build-492-RCM-test.

The test will be done for uncracked samples and cracked samples. The cracked samples will have cracks with a width of 0,2 mm. The cracking of the samples will be done after 28 days of hardening and will heal in a container of water until they reach the age of 56 days.

Expected Results: It is expected that the uncracked samples of TC mortar and SSC mortar will have similar Chloride Penetration levels. For the cracked and healed samples it is expected that the SSC mortar will have a lower non-steady-state migration coefficient than the traditional concrete. This is due to the increased healing capacity, which closes the cracks. The TC mortar has a much lower healing capacity than the SSC mortar, so it will have more open cracks. For the TC mortar and the concrete similar results are expected.

Planning of the test: The needed mortar mixtures will be mixed and casted in the molds, which will be used. After 28 days of hardening in the curing room, 3 samples of the SSC mortar, 3 samples of the TC mortar and 3 samples of the concrete will be loaded until cracks with a width of 0.2 mm occur, as described above. When the samples are cracked they will be kept in containers of water for 28 days.

When the cracked samples healed for 28 days, they will be taken out of their containers of water and tested on chloride penetration in 4 following days.

When the other samples have an age of 56 days as well they will be tested on chloride penetration.

Materials needed:

- Strain hardening self-healing mortar, 6 samples (see above)
- Traditional mortar, 6 samples (see above)
- Traditional concrete C40/50, 6 samples
- 0.3 M NaOH solution
- 10% NaCl solution
- distilled or de-ionised water
- Calcium hydroxide Ca(OH)₂
- Silver nitrate AgNO₃

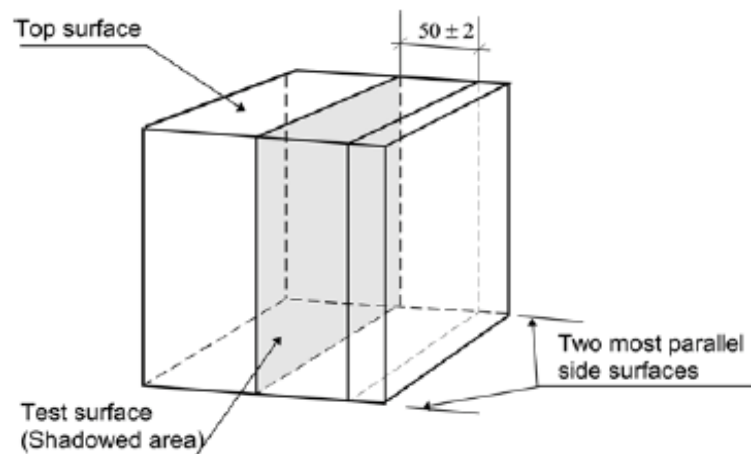
- Equipment needed:**
- Molds
 - Migration set-up
 - Equipment to make mortar mixtures
 - Water-cooled diamond saw
 - Vacuum container
 - Vacuum pump
 - Power supply
 - Ammeter
 - Thermometer or thermocouple
 - Device for splitting sample

Assistance needed: Explanation about the use of equipment and machines and help to start up the test. (M. van Leeuwen and B. Savija)

• **Test 4: Frost/thaw cycle test:**

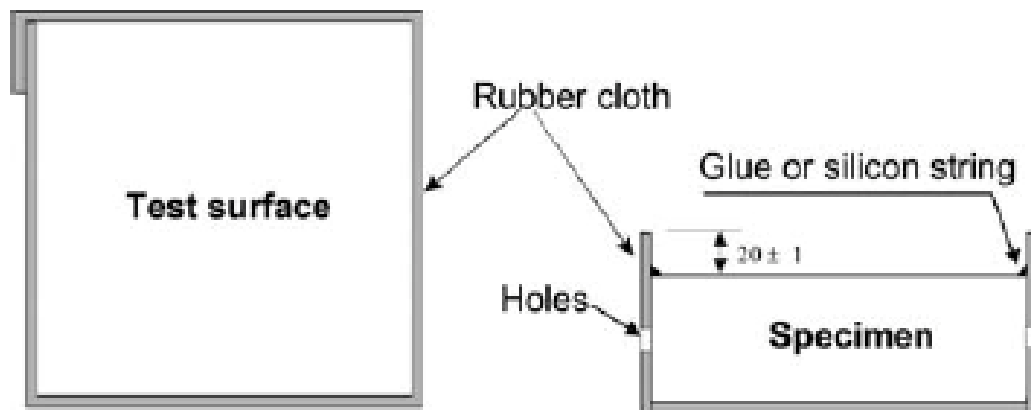
Aim of test: The aim of the test is to research if the healing capacity of the SSC mortar is affected by frost/defrost cycles and how resistant it is in the first place to frost/thaw cycles. This reaction will be compared with the reaction of TC mortar.

Test description: The samples will be slabs of 50 ± 2 mm thick, cut out of cubes of 150 x 150 x 150 mm. During the first day after casting, the cubes will be kept in a room of 20 ± 2 °C. After 24 hours the molds will be removed from the cubes and the cubes will be placed in a bath of tap water with a temperature of 20 ± 2 °C. 7 days later the cubes are taken out of the baths and are placed in a climate chamber with a temperature of 20 ± 2 °C and a relative humidity of 65 ± 5 %. When the cubes have an age of 21 days, the slabs will be cut out in a way that one cut surface is at the centre of the cube, this will be the test surface (see figure below).



Directly after sawing, the sample will be washed with tap water, the excess tap water will be wiped of and the sample will be placed back in the climate chamber directly. The test surface will be vertically exposed to the air and an in between distance of at least 50 mm.

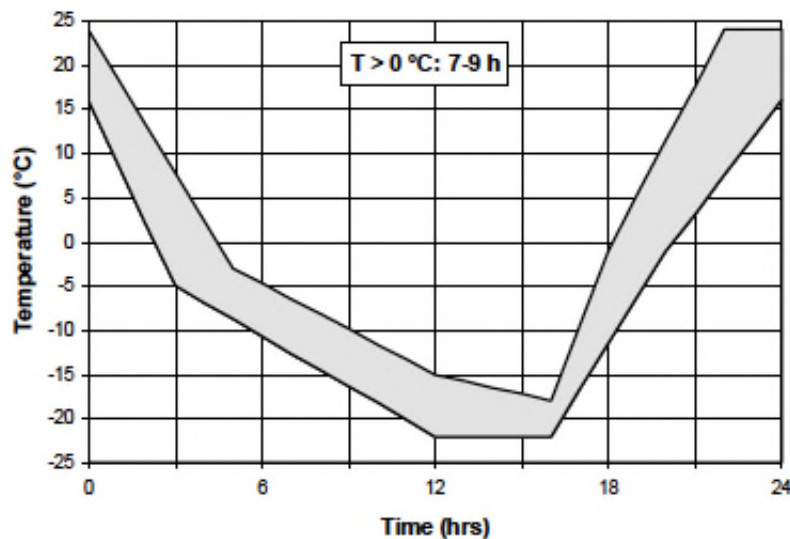
When the samples have an age of 25 days two rubber cloths should be cut for every sample, one of 150 x 150 mm and one of 630 x 73 mm. Apply adhesive evenly to all concrete and rubber surfaces except for the test surface. First glue the square cloth and afterwards the rectangular cloth to the sample. An extra line of glue/silicon is applied at the edge of the test surface in the corner between the rubber cloth and the concrete, see figure below.



The samples should be placed back in the climate chamber directly with the test surface exposed horizontally to the air.

At the age of 28 days an layer of water with a thickness of 3 mm should be poured onto the test surface, this is about 67 mL of water. The water should have a temperature of 20 ± 2 °C. When the concrete is 31 days old (this is 72 hours after pouring the water on the sample) the water should be removed.

Directly after removing the samples from the climate chamber the freezing medium should be poured onto the sample with a thickness of 3 mm with a temperature of 20 ± 2 °C. Then all the sides, except the test surface, should be insulated with 20 ± 1 mm polystyrene cellular plastic. Quickly after the pouring of the freezing medium (max. 15 minutes) the samples will be placed in a freezing chamber. The freezing medium used will be 3% NaCl as it has to imitate an environment with de-icing salt. A thick polyethylene film will prevent the medium from evaporating. The samples will be subjected to the repeated freezing and thawing according to the cycle seen below. The samples will be placed at time 0 ± 0.5 hour.



After 7 and 14 cycles the loss of weight due to scaling will be measured, to do this the freezing medium will be poured through a filter and more tap water and a brush are used to remove all scales. Afterwards the scales are put in an oven of 110°C for 24 hours and then the weight can be measured. After 14 cycles the measurement will be repeated and if enough scaling has happened the samples will be placed in containers of water for 28 days. Afterwards the samples will be measured again before undergoing more cycles. If weight loss isn't big enough the samples will be undergo another 7 cycles.

If the weight loss is big the samples will be put underwater for 28 days to heal. After this period the above described procedure will be repeated.

Using the following formulas the mass loss related to the test area can be calculated:

$$m_{s,n} = m_{s,before} + (m_{v+s(+f)} - m_{v(+f)})$$

$$S_n = \frac{m_{s,n}}{A} \cdot 10^3$$

With:

- $m_{s,n}$ = cumulative mass of dried scaled material after n freeze-thaw cycles (g)
- $m_{s,before}$ = cumulative mass at the previous measurement (g)
- $(m_{v+s(+f)} - m_{v(+f)})$ = mass of the scaled material of the current measurement (g)
- S_n = mass of the scaled material related to the area of the test surface (kg/m²)
- A = Area of the test surface, after glue is applied (mm²)

Expected Results: The results will show that the SSC mortar will lose less weight due to scaling than the TC mortar. This is expected due to the fibers in the SSC mortar. After the healing period, the difference is expected to be even larger.

Planning of the test: The mixtures for both mortar types will be made and casted in the molds. After 25 days of hardening in a climate chamber as described above the samples will be sawn, after 28 days the samples will be put under water and after 31 days the frost/thaw test will start.

Materials needed:

- Strain hardening self-healing mortar, 6 samples (see above)
- Traditional mortar, 6 samples (see above)
- Polystyrene cellular plastic
- 3% NaCl

Equipment needed:

- Molds
- Climate chamber
- Equipment to make mortar mixtures
- Self-adhesive paper labels
- Rubber cloth
- Contact adhesive
- Polyethylene film
- Freezing chamber
- Filters

Assistance needed: Explanation about the use of equipment and machines and help to start up the test. (M. van Leeuwen)

- **Test 5: Compression test E-modulus**

Aim of the test: The aim of the test is to determine the E-modulus of the self-healing and the traditional mortar.

Test description: A prism of size 40 x 40 x 160 mm will be loaded under compression. During the test both the compressive load and the strains will be recorded. By dividing the difference between the basic and the upper stress by the according strains the E-modulus will be calculated, see formula below.

$$E_c = \frac{\sigma_a - \sigma_b}{\varepsilon_a - \varepsilon_b}$$

Expected results: The expectation is that the self-healing mortar will deform more, but will have higher failure strength. Therefore the expectation is that the E-modulus of the SSC mortar will be lower than the E-modulus of the TC mortar.

Planning of the test: The test starts with casting the samples, 3 of each kind of mortar. When the mortar has hardened for 28 days the measurements will be taken. Before testing the samples should be kept under water for at least 12 hours.

The sample should be placed in the machine vertically in the center, with the measuring instruments or fixing points attached axially (see figure below). Apply the basic stress of 0,5 N/mm² (MPa) (σ_b), maintain it for 60 seconds and measure and record the strain gauge readings afterwards, taken at each measurement line.



Increase the compressive strength with a constant speed (0,1 kN/s) until it equals 9 kN.

Maintain the stress for 60 s and measure and record the strain readings during the following 30 seconds at each measurement line. When the value of the individual strains are not in a range of $\pm 20\%$ of the mean value σ_a , centre the sample again and repeat the test.

When the sample is placed good enough to the center the load should be reduced to the basic stress, this should be done at the same speed as the loading happened. Repeat the preloading cycle at least two more time using the same speed for loading and unloading and maintain the stresses σ_b and σ_a for 60 seconds. After finishing the last cycle, keep the basic stress for 60 more seconds and afterwards measure and record the basic strain, ϵ_b , at the measurement lines during the following 30 seconds.

Reload the specimen till the σ_a at the same speed and maintain it for 60 seconds. In the 30 seconds afterwards measure and record the strain, ϵ_a .

Materials needed:

- 3 samples strain hardening self-healing mortar
- 3 samples traditional mortar

Equipment needed:

- Instron
- Molds
- Mixing equipment

Assistance needed: Explanation about the use of equipment and machines and help to start up the test. (M. van Leeuwen)

- **Test 6: Shrinkage test**

Aim of the test: This test is aiming to measure the free drying shrinkage of both kinds of mortar, to see if it influences the design.

Test description: The shrinkage test will be done on samples with the size of 40 x 40 x 160 mm; at the ends of the samples studs will be placed to be able to measure the length. The shrinkage is determined by measuring the length of the samples. In the beginning the length will be measured more often, due to the expectation that the shrinkage will be faster directly after casting in comparison to later on in the process.

The strain will be calculated using the following formula:

$$\text{Strain} = \frac{\Delta L \times 1\,000}{L_g} \text{ [mm/m]}$$

Expected results: Expected is that the SSC mortar will have more shrinkage than the TC mortar based on articles of MG. Sierra-Beltran and H.M. Jonkers.

Planning of the test: First the samples shall be casted and the studs will be placed at the ends of the samples. One day after casting the samples will be removed from their molds and will be kept the climate room with 50% RH. The samples should be stored with a distance of at least 100 mm in between. The first measurement will be taken 1 day after demoulding. Further measurements will be taken after 3, 7, 28, 56 days after demoulding.

Materials needed:

- 3 samples strain hardening self-healing mortar
- 3 samples traditional mortar

Equipment needed:

- Equipment to mix concrete
- Molds
- Studs
- Measure equipment.

Assistance needed: Explanation about the use of equipment and machines and help to start up the test. (M. van Leeuwen)

- **Test 7: Water absorption test**

Aim of the test: Using this test, it will be aimed to determine the water absorption of the mortars due to capillary action. This way the porosity of the samples can be determined.

Test description: The test will be done on prisms of 40 x 40 x 160 mm. To determine the water absorption of both mortars, the samples of both mortars will be placed in two separate trays of water. The mortar with bacteria should be kept separate from the traditional mortar. While the samples are in the water, once in a while the weight of the samples will be determined.

Using the weight and the following formula the capillary absorption will be determined.

$$C_A = \frac{M_j - M_o}{1600}$$

With:

- C_A = Capillary absorption (g/mm²)
- M_j = mass of the sample after certain absorption time (g)
- M_o = mass of the sample after curing (g)

Expected results: The absorption of the SSC mortar will be higher than the absorption of the TC mortar, due to the light weight aggregates (Liu, Chia, & Zhang, 2011). Though it is expected that the rate of absorption will decrease over time for both materials.

Planning of the test: First the mortar mixtures will be made and cast in the molds. After 7 days the first series of the test will be taken from the curing room and placed in a ventilated oven of 40°C for 24 hours, afterwards the test will start. The prisms will be weighted and placed in a receptacle containing water at constant level. The water level should be kept 3 ± 1 mm above the base of the specimen. The specimens will be weighted after 1 and 7 days in the water.

For the samples, which are cured for 42 days, the samples with weighted after 1, 7 and 28 days in contact with the water.

Materials needed:

- 6 samples strain hardening self-healing mortar
- 6 samples traditional mortar
- Water

- Equipment needed:**
- Molds
 - Mixing equipment
 - Receptacle
 - Balance

Assistance needed: Explanation about the use of equipment and machines and help to start up the test. (M. van Leeuwen)

Reviewer:

Date:

Suggestions / comments:

Appendix B: Explanation type construction

Choosing the type of construction for the bridge one requirement was important: the construction should crack during production or due to tensile forces during the service live. The idea is that the SSC will be able to seal the cracks and increase the durability. This will result in a slender bridge design, while this is not possible using TC.

For this reason it was chosen to use an arched bridge deck made using cold formed bending. By this method the deck is casted as a straight slab and bend when the concrete is partially hardened. When using an arched bridge deck a logical step is to look at a compressive arch with tensile bar construction (see figure 32). Although to get an arch with only compressive forces and no bending the arch will needs quite a large height, which will be negative for the users. Also the large curvature will be a problem when using cold formed bending.

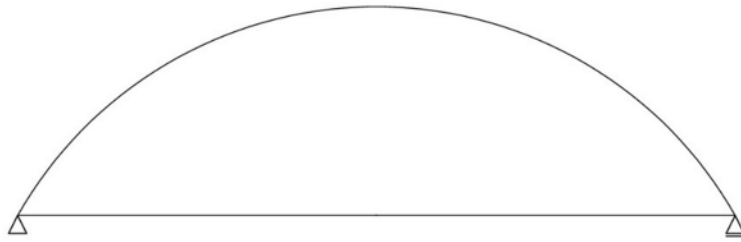


Figure 32: Compressive arch with tensile bar

Another structural option, which works with normal forces, is the under tensioned beam (see figure 33). In this case the beam has two extra supports (however, not completely stiff). These extra supports take part of the load and bring this to the supports at the sides of the bridge through normal forces (compression and tensile). Although the beam is flat, so cold formed bending cannot be used.



Figure 33: Under tensioned beam

A third option is to use a box girder or double T beam (see figure 34). However these type of constructions are mostly used in combination with pre-tensioning, which will prevent the construction from cracking. Also this type of construction is mostly used for large spans.

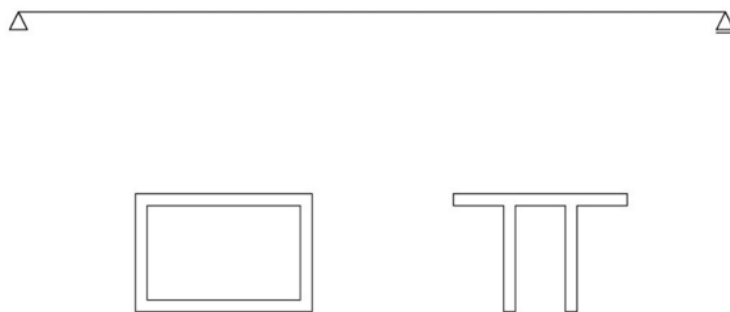


Figure 34: Box girder or double-T beam

The last option is to use a truss (see figure 35). However, this type of construction is like the box girder and double T beam, mostly used for large spans.

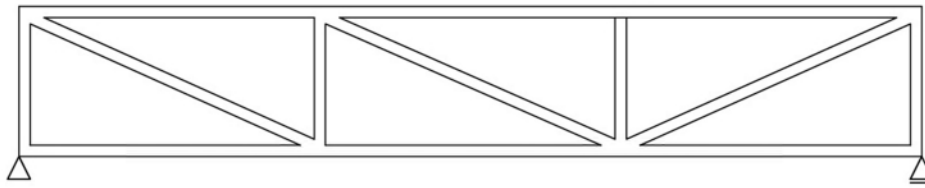


Figure 35: Truss

Looking at the construction types described above it is chosen to combine the compressive arch with the under tensioned beam. This way the arch does not have to be a perfect compressive arch and the curvature can be decreased. Also the under tensioning will decrease the moments and deformation which will occur in the construction.

The final construction will be made of two under tensioned beams supporting the bridge deck, as can be seen in figure 36.



Figure 36: Chosen construction type

Appendix C: Calculation Demonstrator Bridge

First the calculation for the design of the bridge with SSC will be explained. Afterwards the same will be done for the design with TC.

For both designs a global calculation will be done, to get an good view on the differences between the designs made with the materials. Therefore, it is decided to only look at load combinations with distributed loads. The point loads due to cyclist and service vehicles are left out.

The same is done with the snow load, wind load and shrinkage, because these elements are expected to be very small. This is due to the dimensions of the bridge and the fact that they are secondary loads.

Also, for the calculation, the value of the Young's modulus of a cracked concrete profile $1/3^{\text{th}}$ of the Young's modulus of an uncracked concrete. At the end of the calculation this value will be checked using the Eurocode 1992-1-1.

Design with SSC

The bridge can be split in three elements:

- A deck
- Two beams supporting the deck and
- Two trusses supporting the beams.

In this calculation only one load combination is looked at. An evenly spread load on the whole construction.

First the deck will be calculated by simplifying it to a beam on two supports in the middle, see figure 37. Afterwards the calculation will be optimized using excel.



Figure 37: Structural scheme deck

For the beams first a calculation will be made by hand, assuming it is a straight beam on four supports. Also this calculation will be optimized using excel.

As the beams can be seen as part of the truss as well, the next step is to put the whole trusses into matrixframe, including the beams. Therefore an estimate has to be made of the tensile and compressive bars. When all profiles are known, matrixframe can calculate the moments, normal forces and deformation. If one of the values do not satisfy the requirements, the profiles will be adjusted and matrixframe will be used to calculate again. This process will be repeated until all requirements are satisfied.

When the dimensions of all elements are determined in such a way that they fulfil both ULS and SLS, finally a look will be taken at the crack width control.

The deck

For the deck two options will be calculated with a different position of the reinforcement.

- By the first option the supports will be placed a such a distance from each other that the moment at the supports is the same as the biggest field moment. Therefore the reinforcement will be placed in the middle of the deck (see figure 38, left).

- The distance between the supports of the second option will be chosen to ensure there only will be a negative moment in the beam, so the field moment of the middle span will be 0. In this case the reinforcement will be placed at the top of the deck (see figure 38, right). It is an unrealistic situation, but interesting to look at.

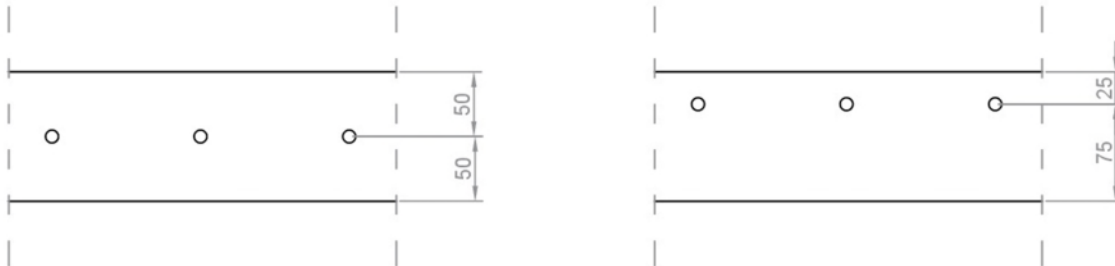


Figure 38: Location reinforcement option 1 & 2

For both options 5 different load combinations will be calculated. These 5 combinations are shown in the figure below.

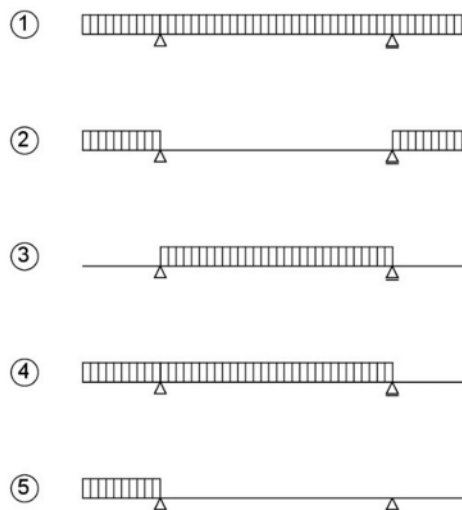


Figure 39: Load combinations

Below only the calculation of the first load combination is written out completely. The calculations of the other load combinations are done in a similar manner. At the end of the option the dimensions needed to fulfil the requirements for all load combinations are given.

Option 1: Reinforcement in the middle

As said above the first option has the reinforcement in the middle, which would work optimal, when the maximum positive and negative moment are the same. The distance between the supports is calculated by setting the moment at the support caused by the cantilever at the same value as the wanted value caused by the middle span. This gives the following formula:

$$\frac{1}{16} * q * L_B^2 = \frac{1}{2} * q * L_A^2$$

Solving this formula gives: $L_A = 1,0$ m (sides) and $L_B = 3,0$ m (middle), the structural scheme and the M-line can be seen in figure 40.

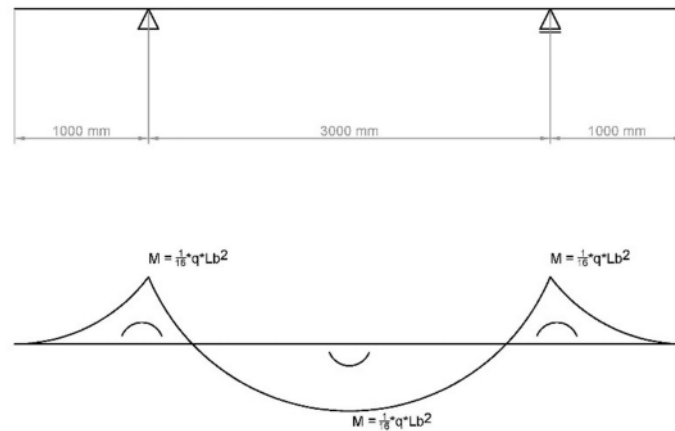


Figure 40: Structural scheme and M-line option 1

To start the calculation a beam is taken with $b = 1000$ mm and $h = 100$ mm. Due to the location of the reinforcement the following can be said: $d = 0,5 * h$.

For the reinforcement and the SSC the following strengths and loads are used:

- $E = 15000$ MPa
- $E_{cracked} = E/3 = 5000$ MPa
- Cover = 25 mm
- $f_{cd} = 45 / 1,5 = 30$ MPa
- $f_{yd} = 500 / 1,15 = 435$ MPa
- $q_G = 0,1 * 1 * 20 = 2$ kN/m
- $q_Q = 4$ kN/m
- $q_{G,d} = 2 * 1,2 = 2,4$ kN/m
- $q_{Q,d} = 4 * 1,5 = 6$ kN/m

$E_{cracked}$ is used in elements where bending or tensile forces occur.

Ultimate Limit State

First the moments due to the applied loads are calculated:

$$M_{E,d,negative} = \frac{1}{2} * (2,4 + 6) * 1^2 = 4,1 \text{ kNm}$$

$$M_{E,d,positive} = 4,2 - \left(\frac{1}{8} * (2,4 + 6) * 3^2 \right) = -5,1 \text{ kNm}$$

As $M_{E,d,field}$ has the largest absolute value, it will be used in the ULS calculation, for $M_{E,d,support}$ the calculation is the same and will be shown in the excel.

The percentage of reinforcement (ρ) should be between 0,19% and 2,7%. For the reinforcement is chosen for 5 bars with a diameter of 10 mm. This gives the following area and percentage of reinforcement:

$$A_s = 5 * \pi * r^2 = 5 * \pi * 5^2 = 392,7 \text{ mm}^2$$

$$\rho = \frac{A_s}{b * d} * 100\% = \frac{392,7}{1000 * 50} * 100\% = 0,79\%$$

The moment caused by the load on the beam is taken by a compressive force in the concrete and a tensile force in the steel, which cause a counteracting moment. The forces can be seen in the figure below.

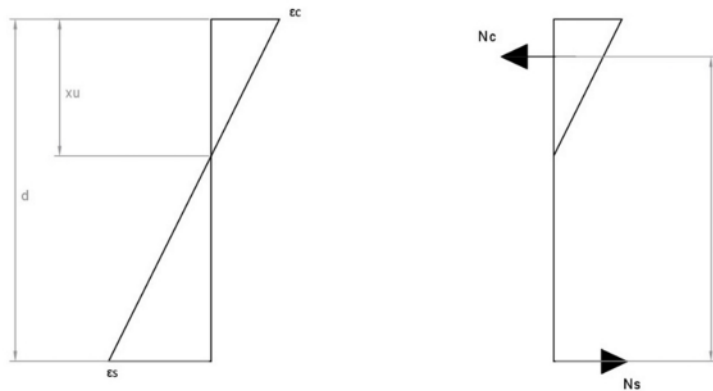


Figure 41: Deformation and stresses in elastic phase

The following is known:

$$\begin{aligned}
 N_c &= \frac{3}{4} * x_u * f_{cd} * b \\
 N_s &= A_s * f_{yd} \\
 N_c &= N_s \\
 x_u &= \frac{A_s * f_{yd}}{\frac{3}{4} * f_{cd} * b} \\
 z &= d - 0,39 * x_u \\
 M_{R,d,field} &= N_s * z = A_s * f_{yd} * d * \left(1 - 0,52 * \rho * \frac{f_{yd}}{f_{cd}} \right) = 8,0 \text{ kNm} > M_{E,d,field}
 \end{aligned}$$

This requirement is fulfilled.

Serviceability Limit State

The maximal allowable deformation is $w_{max} = 0,004 * L$

$$\begin{aligned}
 w_{max,A} &= 0,004 * L_A = 4 \text{ mm} \\
 w_{max,B} &= 0,004 * L_B = 12 \text{ mm}
 \end{aligned}$$

Using forget-me-not's the deformation due to the load can be calculated with the following formula:

$$\begin{aligned}
 w_A &= \frac{q * L_A^4}{8 * EI} - \left(\frac{q * L_B^3}{24 * EI} \right) * L_A + \left(\frac{M_{support} * L_B^2}{6 * EI} \right) = 10,5 \text{ mm} \gg 4 \text{ mm} \\
 w_B &= \frac{5}{384} * \left(\frac{q * L_B^4}{EI} \right) - 2 * \left(\frac{M_{support} * L_B^2}{16 * EI} \right) = 6,9 \text{ mm} < 12 \text{ mm} \\
 M_{support} &= \frac{1}{2} * q * L_A^2 = \frac{1}{2} * 6 * 1^2 = 3 \text{ kNm} \\
 EI &= E * \frac{1}{12} * b * h^3 = 5000 * \frac{1}{12} * 1000 * 100^3 = 4,17 * 10^{11} \text{ Nmm}^2
 \end{aligned}$$

Not all requirements are fulfilled.

Optimization with excel

Using excel to optimize the construction of the bridge deck the following values are found:

- $h = 140 \text{ mm}$
- $b = 1000 \text{ mm}$
- 4 bars, diameter = 10 mm
- $L_A = 1,30\text{m}$
- $L_B = 2,40 \text{ m}$
- $M_{E,d,negative} = 7,9 \text{ kNm} < 9,2 \text{ kNm} = M_{R,d,support}$
- $M_{E,d,positive} = 7,9 \text{ kNm} < 9,2 \text{ kNm} = M_{R,d,field}$
- $w_A = 4,7 \text{ mm} < 5,2 \text{ mm} = w_{max,A}$
- $w_B = 3,6 \text{ mm} < 9,6 \text{ mm} = w_{max,B}$

With these values the construction fulfils the requirements for all load combinations shown in figure 39.

Option 2: Reinforcement on top

By the second option the reinforcement will be at the top of the cross section, which would work optimal, when there is only a negative moment. The distance between the supports is calculated by setting the moment at the support caused by the cantilever at the same value as the wanted value caused by the middle span with a field moment of 0 kNm.

This gives the following formula:

$$\frac{1}{8} * q * L_B^2 = \frac{1}{2} * q * L_A^2$$

Solving this formula gives: $L_A = 1,25 \text{ m}$ and $L_B = 2,5 \text{ m}$, the structural scheme and the M-line can be seen in figure 42.

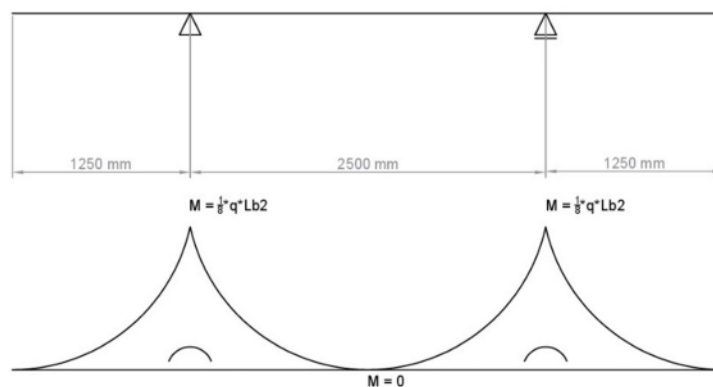


Figure 42: Structural scheme and M-line option 2

To start the calculation a beam is taken with $b = 1000 \text{ mm}$ and $h = 100 \text{ mm}$. Due to the location of the reinforcement and the minimal cover (c) of 20 mm the following is known: $d = h - c = 80 \text{ mm}$.

For the reinforcement and the SSC of this option the same values are used as for the first option:

- $f_{cd} = 45 / 1,5 = 30 \text{ MPa}$
- $f_{yd} = 500 / 1,15 = 435 \text{ MPa}$
- $q_G = 0,1 * 1 * 20 = 2 \text{ kN/m}$
- $q_Q = 4 \text{ kN/m}$
- $q_{G,d} = 2 * 1,2 = 2,4 \text{ kN/m}$
- $q_{Q,d} = 4 * 1,5 = 6 \text{ kN/m}$

Ultimate Limit State

First the moments due to the applied loads are calculated:

$$M_{E,d,negative} = \frac{1}{2} * (2,4 + 6) * 1,25^2 = 6,4 \text{ kNm}$$

$$M_{E,d,positive} = 6,56 - \left(\frac{1}{8} * (2,4 + 6) * 2,5^2 \right) = 0 \text{ kNm}$$

As $M_{E,d,support}$ has the largest absolute value, it will be used in the ULS calculation, for $M_{E,d,field}$ the calculation is the same and will be shown in the excel.

The percentage of reinforcement (ρ) should be between 0,19% and 2,7%. For the reinforcement is chosen for 5 bars with a diameter of 10 mm. This gives the following area and percentage of reinforcement:

$$A_s = 5 * \pi * r^2 = 5 * \pi * 5^2 = 392,7 \text{ mm}^2$$

$$\rho = \frac{A_s}{b * d} * 100\% = \frac{392,7}{1000 * 75} * 100\% = 0,52\%$$

Using the same method as for option 1 the formula below can be found.

$$M_{R,d,field} = N_s * z = A_s * f_{yd} * d * \left(1 - 0,52 * \rho * \frac{f_{yd}}{f_{cd}} \right) = 12,3 \text{ kNm} \gg M_{E,d,field}$$

This requirement is fulfilled with a large margin.

Serviceability Limit State

The maximal allowable deformation is $w_{max} = 0,004 * L$

$$w_{max,A} = 0,004 * L_A = 5 \text{ mm}$$

$$w_{max,B} = 0,004 * L_B = 10 \text{ mm}$$

Using forget-me-not's the deformation due to the load can be calculated with the following formula:

$$w_A = \frac{q * L_A^4}{8 * EI} - \left(\frac{q * L_B^3}{24 * EI} \right) * L_A + \left(\frac{M_{support} * L_B^2}{6 * EI} \right) = 1,4 \text{ mm} < 5 \text{ mm}$$

$$w_B = \frac{5}{384} * \left(\frac{q * L_B^4}{EI} \right) - 2 * \left(\frac{M_{support} * L_B^2}{16 * EI} \right) = 1,4 \text{ mm} \ll 12 \text{ mm}$$

$$M_{support} = \frac{1}{2} * q * L_A^2 = \frac{1}{2} * 6 * 1,25^2 = 4,7 \text{ kNm}$$

$$EI = E * \frac{1}{12} * b * h^3 = 5000 * \frac{1}{12} * 1000 * 100^3 = 4,17 * 10^{11} \text{ Nmm}^2$$

The requirement of deformation is not fulfilled.

Optimization with excel

Using excel to optimize the construction of the bridge deck the following values are found:

- h = 140 mm
- b = 1000 mm
- 4 bars, diameter = 8 mm
- L_A = 1,30 m
- L_B = 2,40 m
- M_{E,d,negative} = 7,7 kNm < 9,9 kNm = M_{R,d,support}
- M_{E,d,positive} = 6,6 kNm < 9,9 kNm = M_{R,d,field}
- w_A = 4,6 mm < 5,2 mm = w_{max,A}
- w_B = 3,5 mm < 9,6 mm = w_{max,B}

With these values the construction fulfils the requirements for all load combinations.

Both options have the same height to fulfil the requirements. However, for option 1 only one net of reinforcement is needed, while for option 2 two reinforcements nets are needed. Therefore it is chosen to go on with option 1.

Beam

The beams are bend according to the arch of the bridge deck. Although this is difficult to calculate by hand. Therefore at first the beams are assumed to be straight beams on four supports (see figure 43) to make an estimate of the height of the beams, also using excel to optimize an I-profile. Afterwards it will be checked and optimized in matrixframe for the bend situation. As this is an estimation only the load combination with an spread load everywhere is checked.

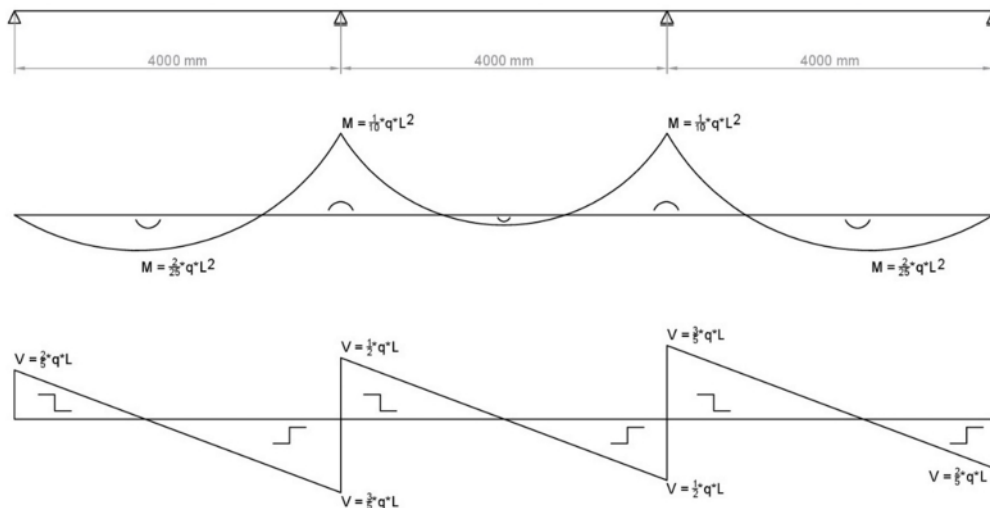


Figure 43: Structural scheme, m- & v-line beams

The m- and v- line are calculated using the force method. The location of the maximum field moment is calculated using the zero-point on the v-line.

To start the calculation a beam is taken with $b = 200$ mm and $h = 300$ mm. Due to the location of the reinforcement (bottom or top) and the minimal cover (c) of 25 mm the following is known: $d = h - c = 275$ mm.

For the reinforcement and the SSC the following strengths and loads are used:

- $f_{cd} = 45 / 1,5 = 30$ MPa
- $f_{yd} = 500 / 1,15 = 435$ MPa
- $q_G = 0,3 * 0,2 * 20 = 7,6$ kN/m
- $q_Q = ((2 + 4) * 5) / 2 = 10$ kN/m
- $q_{G,d} = 1,2 * 7,6 = 9,1$ kN/m
- $q_{Q,d} = 1,5 * 10 = 15$ kN/m

Ultimate Limit State

First the moments due to the applied loads are calculated:

$$M_{E,d,negative} = \frac{1}{10} * (9,1 + 15) * 4^2 = 38,6 \text{ kNm}$$

$$M_{E,d,positive} = \frac{2}{25} * (9,1 + 15) * 4^2 = 30,9 \text{ kNm}$$

As $M_{E,d,support}$ has the largest absolute value, it will be used in the ULS calculation, for $M_{E,d,field}$ the calculation is the same and will be shown in the excel.

The percentage of reinforcement (ρ) should be between 0,19% and 2,7%. For the reinforcement is chosen for 3 bars with a diameter of 12 mm. This gives the following area and percentage of reinforcement:

$$A_s = 3 * \pi * r^2 = 3 * \pi * 6^2 = 339,3 \text{ mm}^2$$

$$\rho = \frac{A_s}{b * d} * 100\% = \frac{339,3}{1000 * 275} * 100\% = 0,62\%$$

Using the same method as for the bridge deck the formula below can be found.

$$M_{R,d,field} = N_s * z = A_s * f_{yd} * d * \left(1 - 0,52 * \rho * \frac{f_{yd}}{f_{cd}}\right) = 38,7 \text{ kNm} > M_{E,d,field}$$

This requirement is fulfilled.

Serviceability Limit State

The maximal allowable deformation is:

$$w_{max} = 0,004 * L = 16 \text{ mm}$$

Using matrixframe the deformation due to the load can be calculated with the following formula:

$$w_A = 0,0069 * \frac{q * L^4}{EI} = 13,8 \text{ mm} < 16 \text{ mm}$$

$$w_B = 0,0005 * \frac{q * L^4}{EI} = 1,0 \text{ mm} \ll 16 \text{ mm}$$

$$EI = E * \frac{1}{12} * b * h^3 = 5000 * \frac{1}{12} * 200 * 300^3 = 2,25 * 10^{12} \text{ Nmm}^2$$

The requirement of deformation is fulfilled.

Shear resistance

To know how much area can be taken away to create an I-profile, it has to be known what the shear resistance is and if shear reinforcement is necessary. In the Eurocode NEN-EN 1992-1-1 the following formulas are found:

$$V_{Rd,c} = \left[C_{Rd,c} * k * (100 * \rho_l * f_{ck})^{\frac{1}{3}} + k_1 * \sigma_{cp} \right] * b_w * d = v_{min} * b_w * d$$

$$V_{Ed} = v_{Ed} * b_w * d$$

$$v_{min} = 0,035 * k^{\frac{3}{2}} * f_{ck}^{\frac{1}{2}}$$

$$k = 1 + \sqrt{\frac{200}{d}} \leq 2,0$$

$$\rho_l = \frac{A_{sl}}{b_w * d} \leq 0,02$$

With:

- $V_{Rd,c}$ = Design value shear resistance
- $C_{Rd,c} = 0,18/\gamma_c$
- f_{ck} = compressive strength
- $k_1 = 0,15$
- $\sigma_{cp} = N_{Ed}/A_c < 0,2 f_{cd}$
- b_w = smallest width of cross section
- d = effective height cross section
- N_{Ed} = axial force in cross section
- A_c = concrete area

As $V_{Ed} < V_{Rd,c}$, the following can be said:

$$v_{Ed} \leq v_{min}$$

$$v_{min} = 0,035 * 1,85^{\frac{3}{2}} * 40^{\frac{1}{2}} = 0,56 \text{ N/mm}^2$$

V_{Ed} is taken at a distance d from the support, this is because the load close to the support is taken directly by the support. This gives the following formula:

$$V_{Ed} = \frac{\frac{1}{2}L - \frac{1}{2}s - d}{\frac{1}{2}L} * R_{Ed} = \frac{2000 - 40 - 275}{2000} * 106,1 = 89,4 \text{ kN}$$

With:

- s = width of the support
- R_{Ed} = force at support (see V-line figure 43)

This gives:

$$v_{Ed} = \frac{V_{Ed}}{b_w * d} = \frac{89400}{200 * 275} = 1,63 > 0,56 = v_{min}$$

So shear reinforcement is necessary.

For the calculation of the minimal needed shear reinforcement the following formula is given by the Eurocode:

$$\frac{A_{sw}}{s} = \frac{V_{Ed}}{z * \cot \theta * f_{ywd}} = \frac{89400}{269 * 2,5 * 435} = 0,306 \text{ mm}^2/\text{mm}$$

With:

- z = arm of the moment couple
- θ = the angle between the horizontal beam and the compression diagonals
- f_{ywd} = design strength of the steel

Taking two bars of $\varnothing 8$ mm every 300 mm one gets:

$$\frac{A_{sw}}{s} = \frac{100,5}{300} = 0,335 \text{ mm}^2/\text{mm} > 0,305 \text{ mm}^2/\text{mm}$$

Closer to the support s could be increased, although for simplicity s is kept the same.

Also the shear resistance of the compressive diagonals have to be checked with the following formula:

$$V_{Rd,max} = b_w * z * v * f_{cd} / (\cot \theta + \tan \theta) = 200 * 269 * 0,504 * \frac{40}{1,5} / (2,5 + 0,4) = 249,4 \text{ kN}$$

With:

$$v = 0,6 * \left(1 - \frac{f_{ck}}{250}\right) = 0,504$$

This is more than enough, even for $b_w = 140 \text{ mm}$ $V_{Rd,max} = 174,5 \text{ kN}$, which is the smallest width needed to be able to place the shear reinforcement.

Optimization with excel

Using excel to optimize the construction of the bridge deck the following values are found:

- $h = 300 \text{ mm}$
- $b = 140 \text{ mm}$
- Reinforcement top and bottom: 3 bars, diameter = 12 mm
- $M_{E,d,negative} = 38,0 \text{ kNm} < 38,6 \text{ kNm} = M_{R,d,negative}$
- $M_{E,d,positive} = 35,4 \text{ kNm} < 38,6 \text{ kNm} = M_{R,d,positive}$
- $w = 19,4 \text{ mm} < 48 \text{ mm} = w_{max}$

With these values the construction fulfils the requirements.

Truss

Before the truss can be calculated in matrixframe, the profiles of the different elements should be known. For the beam the profile calculated above is used as start. For the truss the same load combinations as defined for the bridge deck are calculated (see figure 39).

Compressive bar

For the first estimate the force in the supports in the will be taken as a guide. The following formulas are found in the code:

$$A = \frac{F_{support}}{\sigma_{R,d,max}} = \frac{106040}{14,76} = 7184 \text{ mm}^2$$

$$\sigma_{R,d,max} = 0,6 * v' * f_{cd} = 14,76 \text{ N/mm}^2$$

$$v' = 1 - \frac{f_{ck}}{250} = 0,82$$

This gives a square profile of at least $85 \times 85 = 7225 \text{ mm}^2$. Which gives:

$$F_{support,max} = A * \sigma_{R,d,max} = 7225 * 14,76 = 106,6 \text{ kN}$$

Although it is a compressive bar, reinforcement is needed according to the codes.

Therefore the following formulas are used.

$$A_{s,min} = \max \left\{ \frac{0,1 * N_{E,d}}{f_{yd}}; 0,002 * A_c \right\} = \max \left\{ \frac{0,1 * 76120}{435}; 0,002 * 7225 \right\} = \max \{17,4; 14,5\}$$

$$= 17,4 \text{ mm}^2$$

This gives the smallest diameter (6 mm) with $A_s = 28 \text{ mm}^2$.

Tensile bar

In case of the tensile bar, the complete force is taken by the reinforcement and the concrete is used as protection. Using trigonometric the forces in the tensile bars can be determined. Giving the following formulas and values:

$$F_{T,diagonal} = \frac{F_{support}}{\sin \alpha} = 369,0 \text{ kN}$$

$$F_{T,x} = \frac{F_{support}}{\tan \alpha} = 353,5 \text{ kN}$$

$$\alpha = \tan^{-1} \frac{1,2}{4} = 16,7^\circ$$

It can be seen that $F_{T,diagonal}$ has the largest value, therefore this will be the base of the estimate. Using the following formula the needed area of steel is calculated.

$$A_s = \frac{F_{T,diagonal}}{f_{yld}} = \frac{369000}{435} = 848,3 \text{ mm}^2$$

Therefore is chosen for a bar with a diameter of 34 mm (should be a bundle) is chosen, which gives $A_s = 908 \text{ mm}^2$. This gives:

$$F_T = A_s * f_{yd} = 908 * 435 = 395 \text{ kN}$$

Optimization with matrixframe

In the figure below the structural scheme of the truss can be seen.

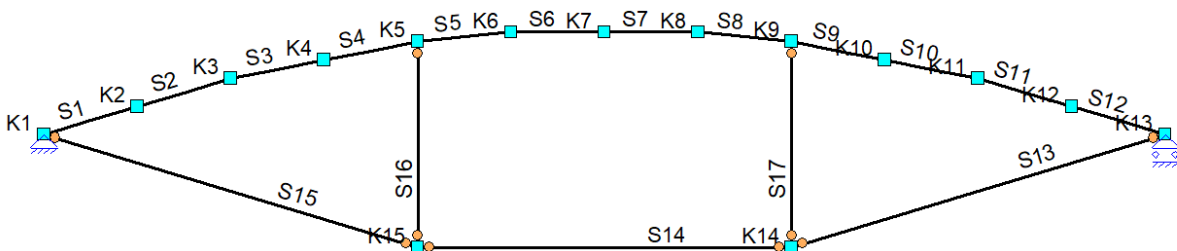


Figure 44: Structural scheme truss

$F_{support} = N_{E,d,comp}$ and $F_{T,diagonal} = N_{E,d,tens}$.

When the profiles estimated above are put into matrixframe, you get the following results:

- $M_{E,d,positive} = 46,5 \text{ kNm} > 39,4 \text{ kNm} = M_{R,d,positive}$
- $M_{E,d,negative} = 39,6 \text{ kNm} > 39,4 \text{ kNm} = M_{R,d,negative}$
- $N_{E,d,comp} = 52,9 \text{ kN} \ll 106,6 \text{ kN}$
- $N_{E,d,tens} = 184,1 \text{ kN} \ll 349,7 \text{ kN}$
- $w = 52,3 \text{ mm} > 48 \text{ mm} = w_{max}$

It can be seen that the moments are just above the requirements, this can be solved by increasing the reinforcement of the beam. The compressive and tensile forces fulfil the requirement with quite a lot of capacity left. However, the deformation is too large as well, so the stiffness of the construction should be increased. This can be done by increasing the stiffness of the beam by increasing the height of the flanges.

After optimization calculations in matrixframe the values below give the optimal construction:

- $h = 300 \text{ mm}$
- $b = 200 \text{ mm}$
- Reinforcement top: 2 bars with a diameter of 16 mm
- Reinforcement bottom: 2 bars with a diameter of 16 mm
- Reinforcement compressive bars: 1 bar with a diameter of 6 mm
- Dimensions compressive bars: $85 \times 85 \text{ mm}^2$
- Reinforcement tensile bars: a bundle of 4 bars with a diameter of 16 mm
- Dimensions tensile bars: $85 \times 85 \text{ mm}^2$
- $M_{E,d,negative} = 39,3 \text{ kNm} < 39,4 \text{ kNm} = M_{R,d,negative}$
- $M_{E,d,positive} = 46,5 \text{ kNm} < 51,7 \text{ kNm} = M_{R,d,positive}$
- $N_{E,d,comp} = 52,6 \text{ kN} \ll 106,6 \text{ kN}$
- $N_{E,d,tens} = 183,1 \text{ kN} \ll 349,7 \text{ kN}$
- $w = 47,4 \text{ mm} < 48 \text{ mm} = w_{max}$
- Shear reinforcement: 2 bars, diameter 8 mm, every 300 mm

It can be seen that this way the construction fulfils all requirements. When only looking at the compressive and tensile bars, those seem to be over dimensioned. However, these dimensions are needed to create enough stiffness to stay under the maximum allowable reinforcement. In the figures below, the M-line, N-line and deformation of the load combination 1 are shown. If load combination 1 has not the highest value, the combination with the highest value or the envelope is shown as well.

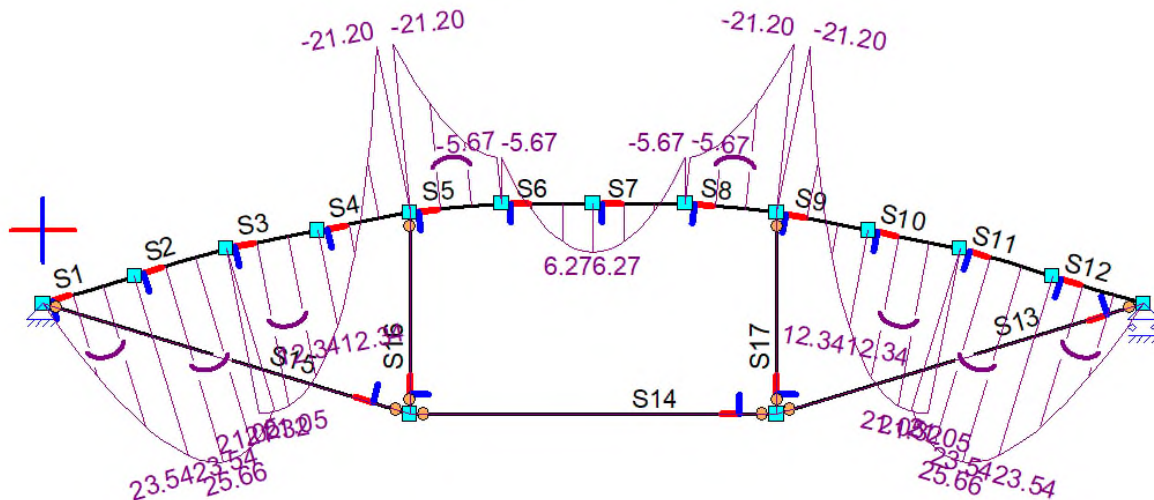


Figure 45: M-line load combination 1 SSC

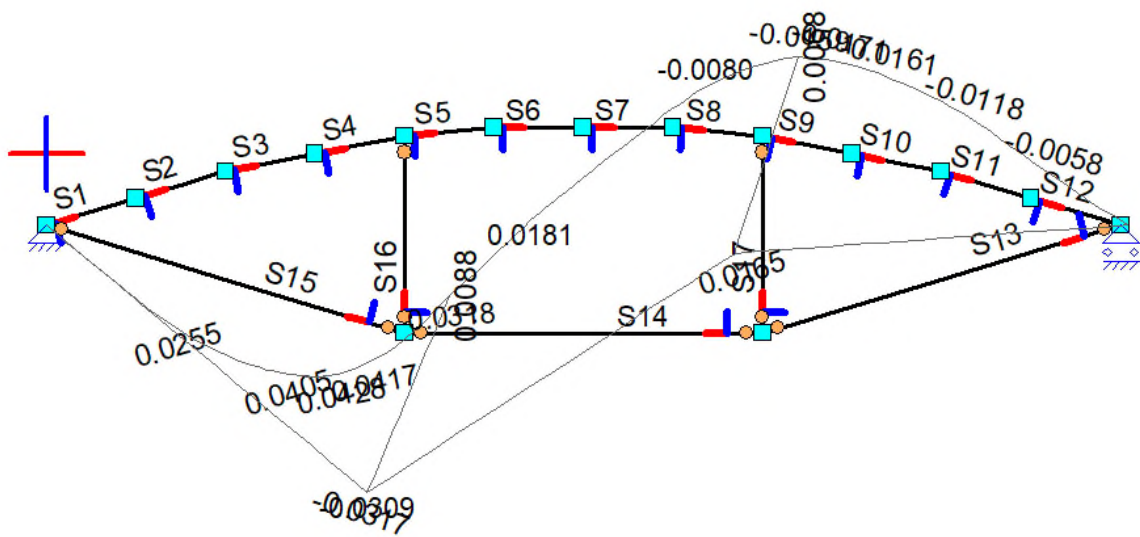


Figure 49: Deformation line load combination 5 SSC - highest value

Crack width control

In case of the bridge designed with SSC, the fibers in the mixture will take care of the crack width control. Due to the fibers the cracks will not increase further than 0,1 mm. This is below the boundary in the NEN-EN 1992-1-1, which is 0,3 mm.

Details

For the calculation it was assumed that the connection of the truss were hinges and could take no moments. However the connections have some moment resistance. This gives the following moments:

- Compressive bars $M = 3,1 \text{ kNm} \rightarrow \text{bar } \varnothing_{\min} = 10 \text{ mm}$
- Tensile bars $M = 4,1 \text{ kNm} \rightarrow \text{bar } \varnothing_{\min} = 20 \text{ mm}$

Also some overlap of reinforcement bars is needed for the connections, this means the dimensions of the tensile bars will increase slightly. These changes can be seen in the details. It is assumed that after the increase of reinforcement and other dimensions the structure still will fulfil the requirements.

Design with TC

The calculation for the design of the bridge with TC is done with the same method as for the calculation for the bridge designed with SSC, therefore only the results will be shown. However, there is a difference in the part about crack width control.

Most of the characteristics are the same, except the few named below:

- $E = 35000 \text{ MPa}$
- $E_{\text{cracked}} = E/3 = 11667 \text{ MPa}$
- Cover = 40 mm

The deck

After optimization for ULS and SLS in excel the following results are found for option 1 and 2:

Option 1: Reinforcement in the middle

- $h = 130 \text{ mm}$
- $b = 1000 \text{ mm}$
- 4 bars, diameter = 10 mm
- $L_A = 1,30\text{m}$
- $L_B = 2,40 \text{ m}$
- $M_{E,d,negative} = 8,2 \text{ kNm} < 8,6 \text{ kNm} = M_{R,d,negative}$
- $M_{E,d,positive} = 3,0 \text{ kNm} < 8,6 \text{ kNm} = M_{R,d,positive}$
- $w_A = 2,7 \text{ mm} < 5,2 \text{ mm} = w_{\text{max},A}$
- $w_B = 2,0 \text{ mm} < 9,6 \text{ mm} = w_{\text{max},B}$

Option 2: Reinforcement on top

- $h = 130 \text{ mm}$
- $b = 1000 \text{ mm}$
- Top: 5 bars, diameter = 8 mm
- Bottom: 2 bars, diameter = 8 mm
- $L_A = 1,30\text{m}$
- $L_B = 2,40 \text{ m}$
- $M_{E,d,negative} = 8,5 \text{ kNm} < 8,6 \text{ kNm} = M_{R,d,support}$
- $M_{E,d,positive} = 3,0 \text{ kNm} < 4,1 \text{ kNm} = M_{R,d,field}$
- $w_A = 2,2 \text{ mm} < 5,2 \text{ mm} = w_{\text{max},A}$
- $w_B = 1,7 \text{ mm} < 9,6 \text{ mm} = w_{\text{max},B}$

Due to the slightly smaller height of option 1, it is chosen to continue with this option.

Beam

After optimization for ULS, SLS and shearforce the following results came out:

- $h = 300 \text{ mm}$
- $b = 180 \text{ mm}$
- Reinforcement top : 2 bars, diameter = 16 mm
- Reinforcement bottom: 2 bars, diameter 20 mm
- $M_{E,d,negative} = 33,1 \text{ kNm} < 41,6 \text{ kNm} = M_{R,d,negative}$
- $M_{E,d,positive} = 41,4 \text{ kNm} < 41,6 \text{ kNm} = M_{R,d,positive}$
- $w = 7,1 \text{ mm} < 16 \text{ mm} = w_{max}$
- Shear reinforcement: 2 bars, diameter 8 mm, every 250 mm

This result is used to start the calculation with matrixframe.

Truss

After optimization in matrixframe for the ULS and SLS the following results are found:

- Beam: $h = 300 \text{ mm}$
- Beam: $b = 200 \text{ mm}$
- Reinforcement top: 2 bars with a diameter of 16 mm
- Reinforcement bottom: 2 bars with a diameter of 20 mm
- Dimensions compressive bars: $120 \times 120 \text{ mm}^2$
- Reinforcement compressive bars: 1 bar with a diameter of 6 mm
- Dimensions tensile bars: $120 \times 120 \text{ mm}^2$
- Reinforcement tensile bars: a bundle of 4 bars with a diameter of 12 mm
- $M_{E,d,negative} = 34,7 \text{ kNm} < 46,3 \text{ kNm} = M_{R,d,negative}$
- $M_{E,d,positive} = 49,0 \text{ kNm} < 70,0 \text{ kNm} = M_{R,d,positive}$
- $N_{E,d,comp} = 53,2 \text{ kN} \ll 212,5 \text{ kN}$
- $N_{E,d,tens} = 185,0 \text{ kN} < 196,7 \text{ kN}$
- $w = 28,2 \text{ mm} < 48 \text{ mm} = w_{max}$

It can be seen that the compressive force is much smaller than allowed. Still the dimensions of the structural elements cannot be decreased due to the minimal cover of 45 mm.

In the figures below, the M-line, N-line and deformation of the load combination 1 are shown. If load combination 1 is not the combination with the highest value, the line with the highest value or the envelope is shown as well.

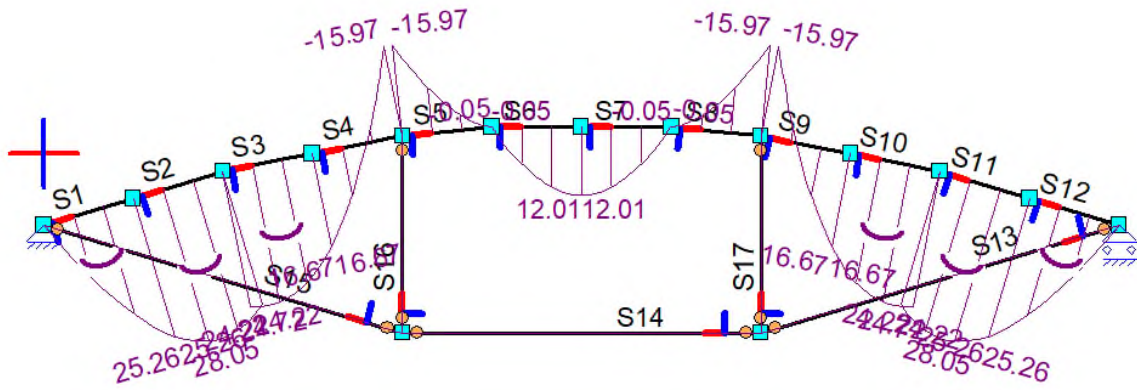


Figure 50: M-line load combination 1 TC

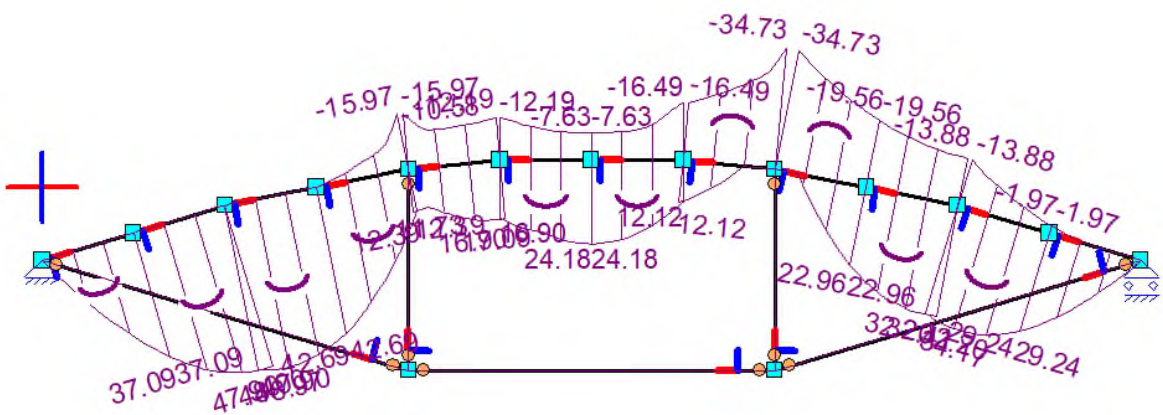


Figure 51: M-line envelope TC

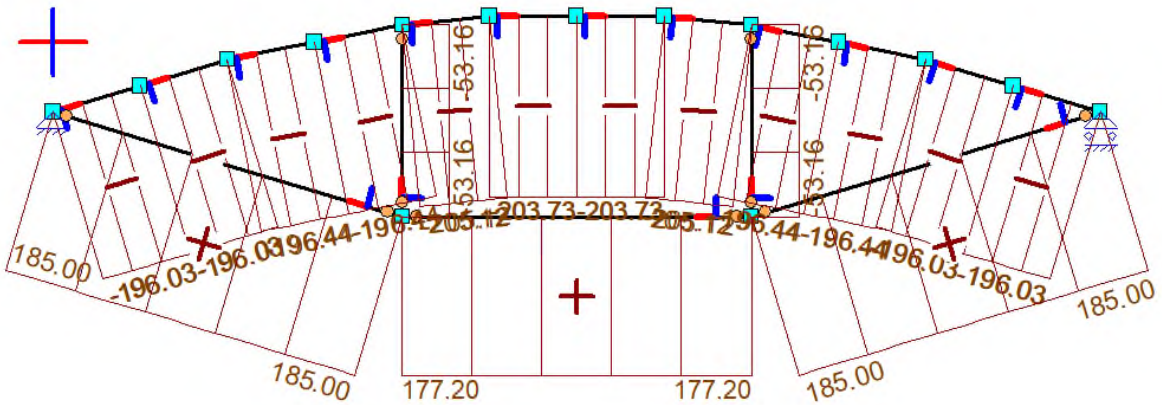


Figure 52: N-line load combination 1 TC - highest compressive and tensile value

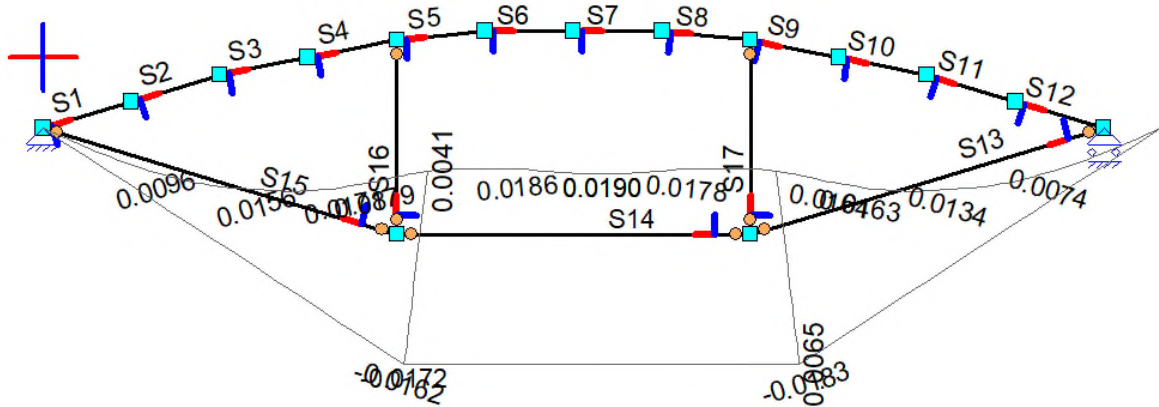


Figure 53: Deformation line load combination 1

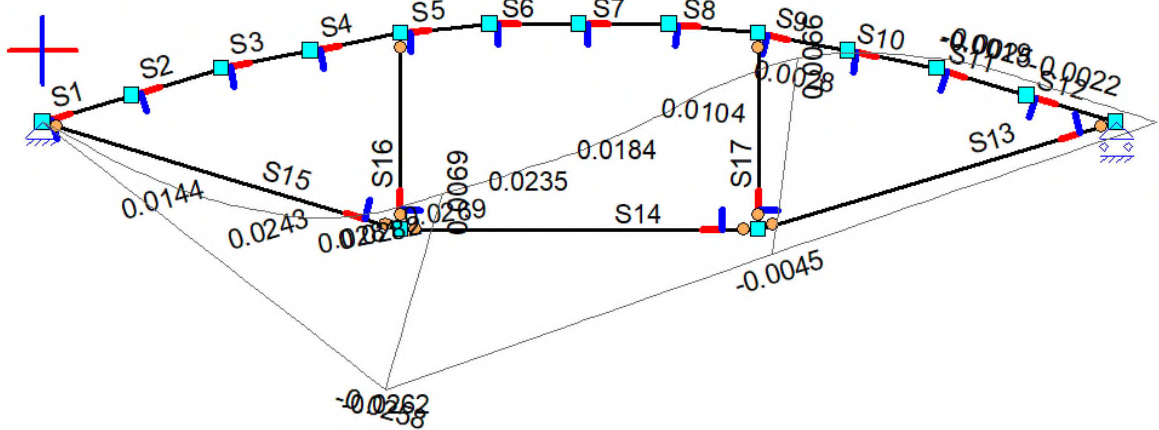


Figure 54: Deformation line load combination 4 TC - highest value

Crack width control

As said earlier by the calculation of the bridge designed with SSC, the maximum allowable crack width is 0,3 mm. All elements will be discussed separately.

The deck

As the cover is thicker than the minimum necessary the cracks at the surface will be larger than 0,3 mm. As the cracks increase linear over the thickness of the cover depth the crack width at the surface will be 0,4 mm, which is allowable for aesthetics and people to feel safe.

First the minimal area of steel has to be calculated with the following formulas and values:

$$A_{s,min} = \frac{k_c * k * f_{ct,eff} * A_{ct}}{\sigma_s} = 285,1 \text{ mm}^2$$

$$k_c = 0,4 * \left[1 - \frac{\sigma_c}{k_1 * (h/h^*) * f_{ct,eff}} \right] = 0,29 \leq 1$$

$$\sigma_c = \frac{N_{Ed}}{b * h} = 1,51 \text{ N/mm}^2$$

$$\begin{aligned}
k_1 &= 1,5 \\
h^* &= h = 300 \text{ mm} \\
f_{ct,eff} &= 3,51 \text{ N/mm}^2 \\
k &= 1 \\
A_{ct} &= b * (h - x) = 123900 \text{ mm}^2 \\
\sigma_s &= 435 \text{ N/mm}^2
\end{aligned}$$

For the reinforcement net the maximum bending moment is 8,2 kNm. Using the following formulas and values the maximum crack width in the concrete is calculated:

$$\begin{aligned}
w_{k,max} &= s_{R,max} * (\varepsilon_{sm} - \varepsilon_{cm}) = 0,20 \text{ mm} < 0,30 \text{ mm} \\
\sigma_s &= \frac{M}{z * A_s} = \frac{8,2 * 10^6}{99,6 * 314,2} = 262,1 \text{ MPa} \\
(\varepsilon_{sm} - \varepsilon_{cm}) &= \frac{\sigma_s - k_t * \frac{f_{ct,eff}}{\rho_{p,eff}} * (1 + \alpha_e * \rho_{p,eff})}{E_s} = 0,000329 \\
s_{R,max} &= k_3 * c + (k_1 * k_2 * k_4 * \phi) / \rho_{p,eff} = 600,0 \text{ mm} \\
\rho_{p,eff} &= \frac{A_s}{A_{c,eff}} = \frac{A_s}{b * \frac{h-x}{3}} = 41300 \text{ mm}^2 \\
k_1 &= 0,8 \\
k_2 &= 1 \\
k_3 &= 3,4 \\
k_4 &= 0,425 \\
c &= 45 \text{ mm} \\
\phi &= 10 \text{ mm}
\end{aligned}$$

The formulas show that the maximum crack width stays below 0,3 mm with the chosen reinforcement based earlier calculations.

The following is found:

- 4 bars with $\phi_s = 10 \text{ mm}$
- spacing = 250 mm
- $\sigma = 262,1 \text{ MPa}$

Beam

For the beam the calculation for crack width control will be done in the same way. Only this time the positive and negative moment are not the same, so the reinforcement in the top will be different from the reinforcement at the bottom.

Bottom reinforcement:

$M_{\text{positive}} = 49,0$ kNm using the same formula as for the deck, see below:

$$A_{s,\min} = \frac{k_c * k * f_{ct,eff} * A_{ct}}{\sigma_s} = 63,8 \text{ mm}^2$$

$$k_c = 0,4 * \left[1 - \frac{\sigma_c}{k_1 * (h/h^*) * f_{ct,eff}} \right] = 0,15 \leq 1$$

$$\sigma_c = \frac{N_{Ed}}{b * h} = 3,27 \text{ N/mm}^2$$

$$w_{k,max} = s_{R,max} * (\varepsilon_{sm} - \varepsilon_{cm}) = 0,27 \text{ mm} < 0,30 \text{ mm}$$

$$\sigma_s = \frac{M}{z * A_s} = \frac{49 * 10^6}{254,1 * 314,2} = 306,9 \text{ MPa}$$

$$(\varepsilon_{sm} - \varepsilon_{cm}) = \frac{\sigma_s - k_t * \frac{f_{ct,eff}}{\rho_{p,eff}} * (1 + \alpha_e * \rho_{p,eff})}{E_s} = 0,001326$$

$$s_{R,max} = k_3 * c + (k_1 * k_2 * k_4 * \phi) / \rho_{p,eff} = 201,7 \text{ mm}$$

In this case the requirements for crack width are fulfilled as well. So the following is found:

- 2 bars with $\phi_s = 20$ mm
- Spacing: 24 mm
- $\sigma = 306,9$ MPa
- $b = 200$ mm

Top reinforcement:

$M_{\text{negative}} = 34,7$ kNm.

At the same manner as for the reinforcement at the top the needed reinforcement is calculated and leads to the following:

- 2 bars with $\phi_s = 20$ mm
- Spacing: 24 mm
- $\sigma = 217,3$ MPa
- $b = 200$ mm

Truss

Tension bars

Again the same formulas and values are used, except for the steel stress and factor k_c . $F_{\text{tensile}} = 185,0$ kN and $A_s = 452,4$ mm². Using the same method the following value appears:

$$A_{s,\min} = \frac{k_c * k * f_{ct,eff} * A_{ct}}{\sigma_s} = 116,2 \text{ mm}^2$$

$$k_c = 1$$

$$\sigma_c = \frac{N_{Ed}}{b * h} = 13,6 \text{ N/mm}^2$$

$$w_{k,max} = s_{R,max} * (\varepsilon_{sm} - \varepsilon_{cm}) = 1,18 \text{ mm} \gg 0,30 \text{ mm}$$

$$\sigma_s = \frac{F}{A_s} = 408,9 \text{ MPa}$$

$$(\varepsilon_{sm} - \varepsilon_{cm}) = \frac{\sigma_s - k_t * \frac{f_{ct,eff}}{\rho_{p,eff}} * (1 + \alpha_e * \rho_{p,eff})}{E_s} = 0,004158$$

$$s_{R,max} = k_3 * c + (k_1 * k_2 * k_4 * \emptyset) / \rho_{p,eff} = 282,9 \text{ mm}$$

This gives a crack width which is too large. When changing to more bars with smaller diameters the following is found:

- 4 bars with $\emptyset_s = 20 \text{ mm}$
- Spacing: 20 mm
- $\sigma = 325,4 \text{ MPa}$
- $b = 150 \text{ mm}$

Details

For the calculation it was assumed that the connection of the truss were hinges and could take no moments. However the connections have some moment resistance. This gives the following moments:

- Compressive bars $M = 1,0 \text{ kNm} \rightarrow \text{bar } \emptyset_{\min} = 8 \text{ mm}$
- Tensile bars $M = 1,0 \text{ kNm} \rightarrow \text{bar } \emptyset_{\min} = 8 \text{ mm}$

Also some overlap of reinforcement bars is needed for the connections, this means the dimensions of the tensile bars will increase slightly. These changes can be seen in the details. It is assumed that after the increase of reinforcement and other dimensions the structure still will fulfil the requirements.

Young's modulus

SSC

In Eurocode 1992-1-1 in paragraph 5.8.5 one finds table 26 to calculate the fictional Young's modulus (E_f). As the assumed strength of the SSC is C40/50 the following formulas can be used to calculate E_f :

$$E_f = [2,35 + 445 * \rho + (26,5 - 235 * \rho) * \alpha_n] * 1000 = 12101 \text{ MPa}$$

$$\rho = \frac{A_{st} + A_{sc}}{A_c} = 0,016$$

$$\alpha_n = \frac{N_{Ed}}{f_{cd} * A_c + (A_{st} + A_{sc}) * f_{yd}} = 0,108$$

One can see that this value is significantly higher than the assumed value of $E/3$. This can be due to the fact that the Eurocode is written for TC and not for SSC. Therefore, the value $E/3$ is kept in the calculation. Also, it is recommended to research the effect of cracks on the Young's modulus of SSC. Especially when the cracks are healed, as this could have a positive effect on this value.

Table 26: Fictional Young's modulus

E_f MPa			
Sterkte- klasse	Buiging en normaalkracht, symmetrisch gewapende rechthoekige doorsnede		Buiging zonder normaalkracht; excentrisch gewapende rechthoekige doorsnede
	$\alpha_n \leq 0,45$	$0,45 < \alpha_n \leq 0,9$	
C12/15	$[1,30 + 410\rho + (9,0 - 130\rho)\alpha_n]10^3 \geq 2900$	$(6,8 + 517\rho)(1 - 0,5\alpha_n)10^3$	$(2,20 + 490\rho)10^3 \geq 2900$
C16/20	$[1,45 + 415\rho + (11,5 - 145\rho)\alpha_n]10^3 \geq 3250$	$(8,5 + 514\rho)(1 - 0,5\alpha_n)10^3$	$(2,35 + 520\rho)10^3 \geq 3250$
C20/25	$[1,60 + 420\rho + (14,0 - 160\rho)\alpha_n]10^3 \geq 3600$	$(10,0 + 510\rho)(1 - 0,5\alpha_n)10^3$	$(2,50 + 550\rho)10^3 \geq 3600$
C25/30	$[1,75 + 425\rho + (16,5 - 175\rho)\alpha_n]10^3 \geq 3950$	$(11,7 + 506\rho)(1 - 0,5\alpha_n)10^3$	$(2,65 + 580\rho)10^3 \geq 3950$
C30/37	$[1,96 + 432\rho + (20,0 - 196\rho)\alpha_n]10^3 \geq 4450$	$(14,0 + 501\rho)(1 - 0,5\alpha_n)10^3$	$(2,85 + 620\rho)10^3 \geq 4450$
C35/45	$[2,20 + 440\rho + (24,0 - 220\rho)\alpha_n]10^3 \geq 5000$	$(16,7 + 495\rho)(1 - 0,5\alpha_n)10^3$	$(3,10 + 670\rho)10^3 \geq 5000$
C40/50	$[2,35 + 445\rho + (26,5 - 235\rho)\alpha_n]10^3 \geq 5350$	$(18,3 + 491\rho)(1 - 0,5\alpha_n)10^3$	$(3,25 + 700\rho)10^3 \geq 5350$
C45/55	$[2,50 + 450\rho + (29,0 - 250\rho)\alpha_n]10^3 \geq 5700$	$(20,0 + 487\rho)(1 - 0,5\alpha_n)10^3$	$(3,40 + 730\rho)10^3 \geq 5700$
C50/60	$[2,65 + 455\rho + (31,5 - 265\rho)\alpha_n]10^3 \geq 6050$	$(21,6 + 484\rho)(1 - 0,5\alpha_n)10^3$	$(3,55 + 760\rho)10^3 \geq 6050$
C55/67	$[2,86 + 462\rho + (34,6 - 258\rho)\alpha_n]10^3 \geq 6400$	$(23,8 + 480\rho)(1 - 0,5\alpha_n)10^3$	$(3,70 + 790\rho)10^3 \geq 6400$
C60/75	$[3,10 + 470\rho + (37,0 - 170\rho)\alpha_n]10^3 \geq 6400$	$(25,5 + 480\rho)(1 - 0,5\alpha_n)10^3$	$(3,70 + 790\rho)10^3 \geq 6400$
C70/85	$[3,10 + 470\rho + (41,5 - 170\rho)\alpha_n]10^3 \geq 6400$	$(28,1 + 480\rho)(1 - 0,5\alpha_n)10^3$	$(3,70 + 790\rho)10^3 \geq 6400$
C80/95	$[3,10 + 470\rho + (46,5 - 170\rho)\alpha_n]10^3 \geq 6400$	$(31,1 + 480\rho)(1 - 0,5\alpha_n)10^3$	$(3,70 + 790\rho)10^3 \geq 6400$
C90/105	$[3,10 + 470\rho + (51,0 - 170\rho)\alpha_n]10^3 \geq 6400$	$(33,7 + 480\rho)(1 - 0,5\alpha_n)10^3$	$(3,70 + 790\rho)10^3 \geq 6400$
	waarin: $\rho = (A_{st} + A_{sc})/A_c$ $\alpha_n = N_{Ed}/(f_{cd} A_c + (A_{st} + A_{sc}) f_{yd})$ A_{st} is de oppervlakte van de wapening aan de meest getrokken zijde A_{sc} is de oppervlakte van de wapening aan de meest gedrukte zijde		waarin: $\rho = A_{st}/A_c$

TC

For TC the same formulas are used and give the following:

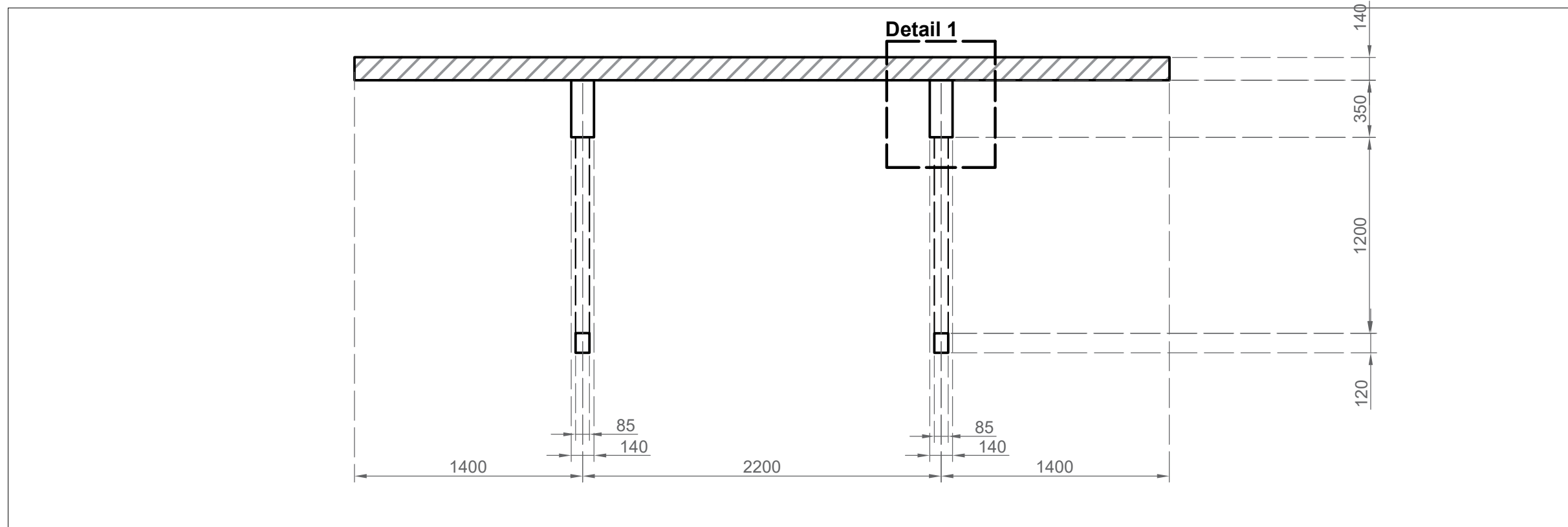
$$E_f = [2,35 + 445 * \rho + (26,5 - 235 * \rho) * \alpha_n] * 1000 = 12831 \text{ MPa}$$

$$\rho = \frac{A_{st} + A_{sc}}{A_c} = 0,017$$

$$\alpha_n = \frac{N_{Ed}}{f_{cd} * A_c + (A_{st} + A_{sc}) * f_{yd}} = 0,087$$

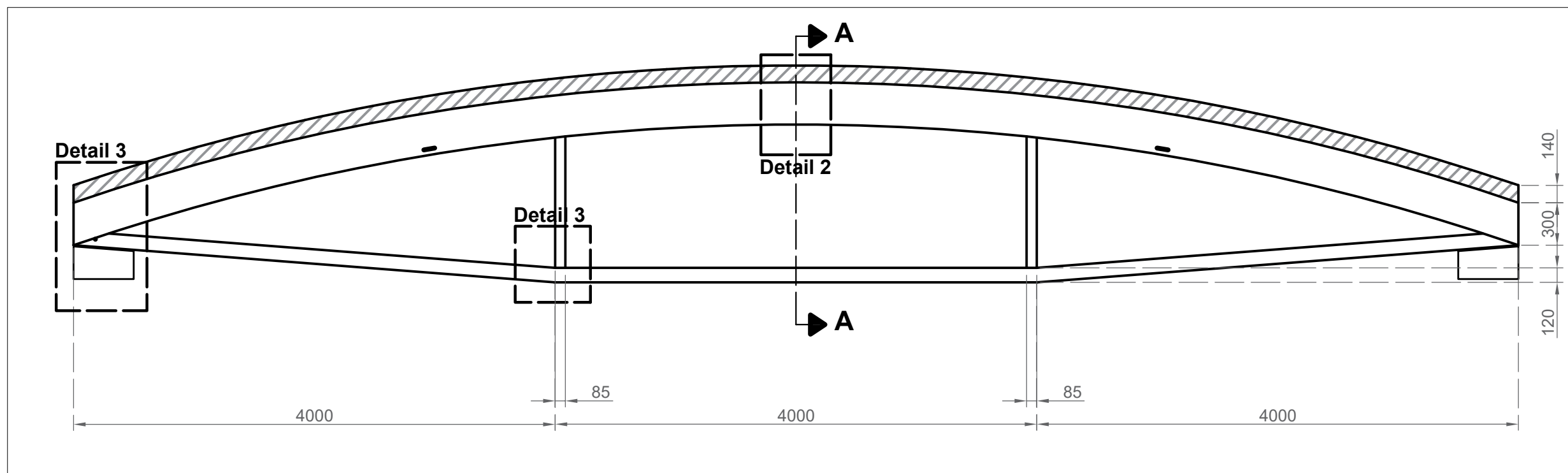
As expected is the value of the Young's modulus found with the Eurocode for TC close to the estimated value E/3 used for the calculation. The found value is slightly larger, which means that slightly smaller deformations will occur than calculated.

Appendix D: Drawings design bridge with SSC



Section A

Scale - 1:20

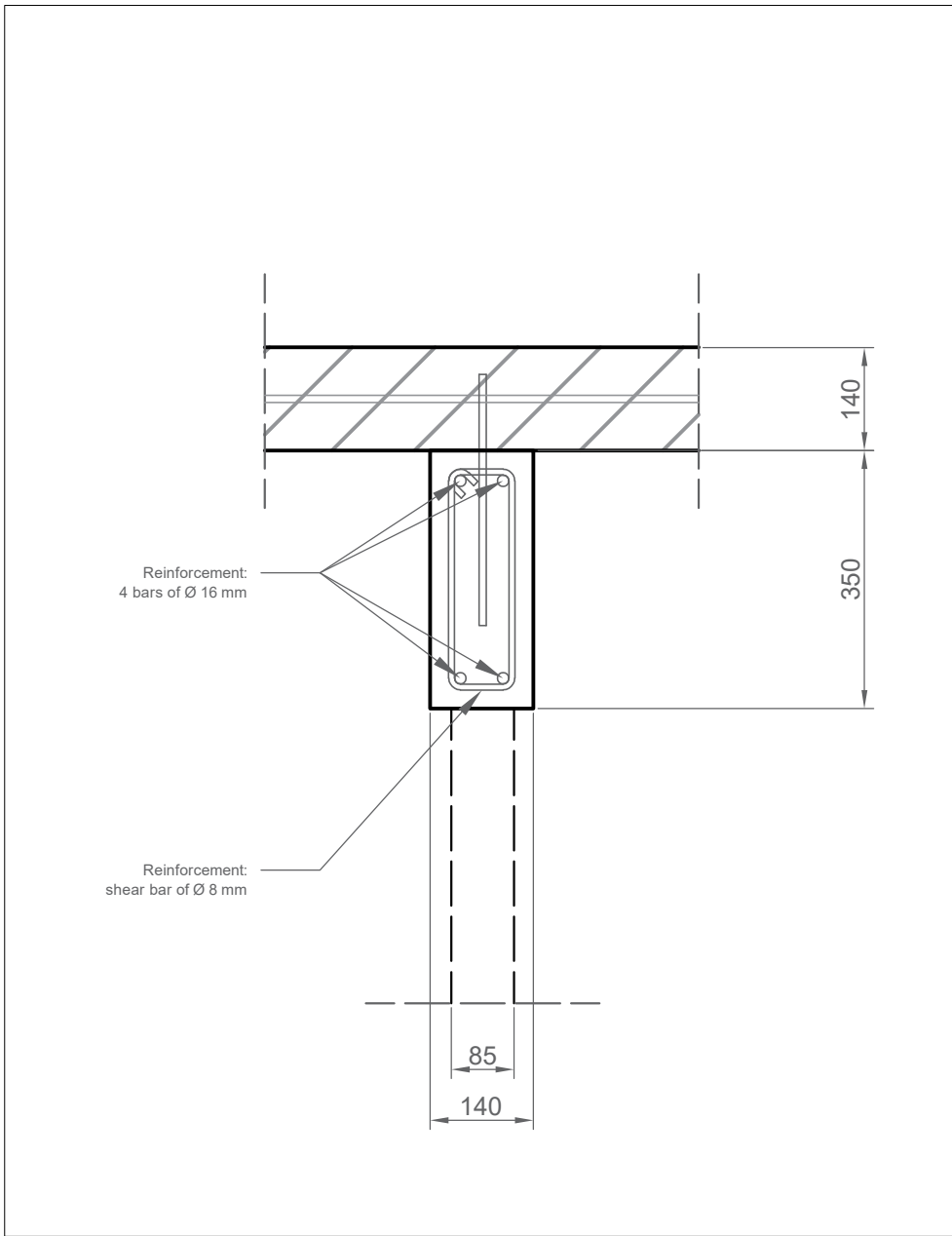


Side view

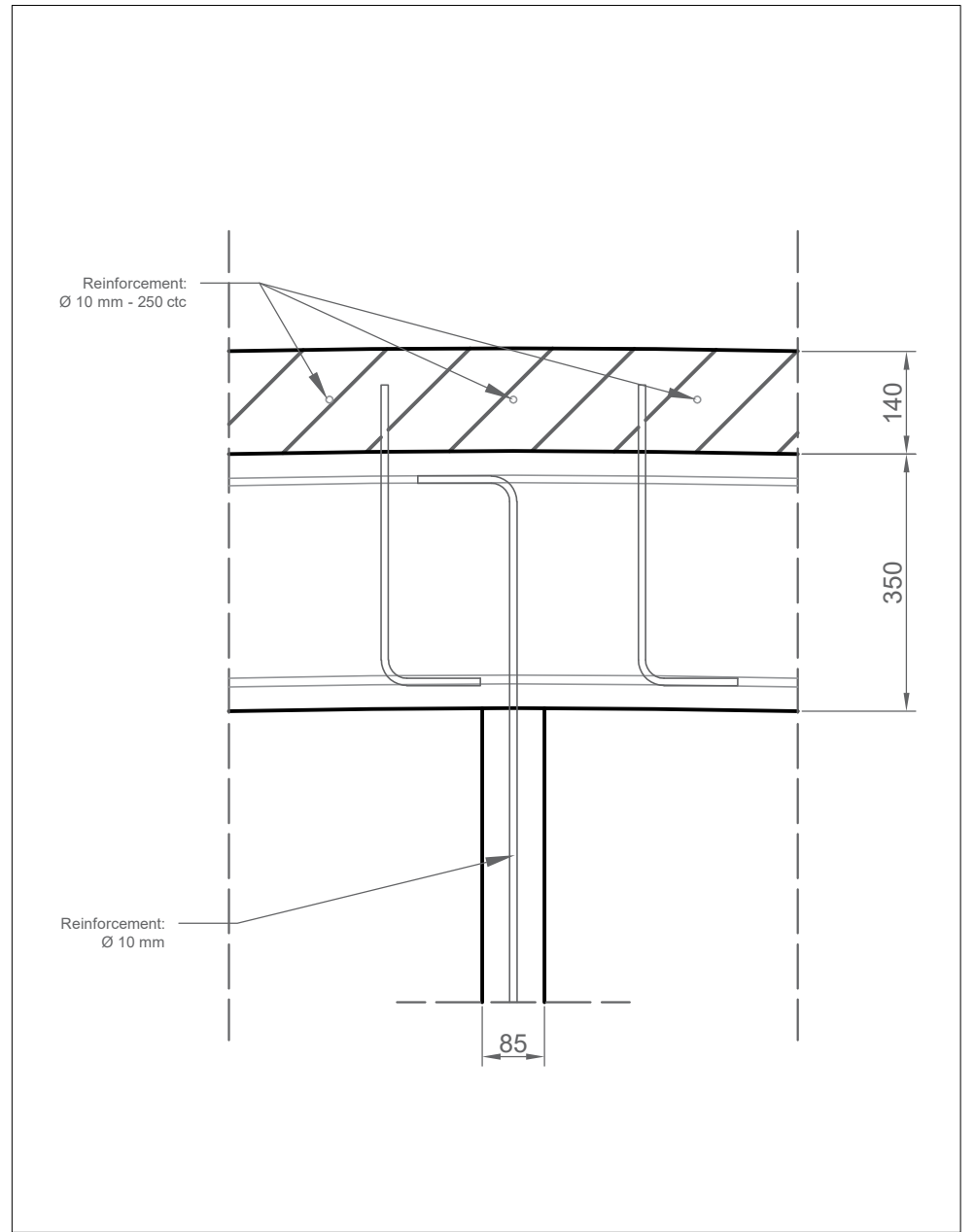
Scale - 1:40

Demonstrator bridge SSC

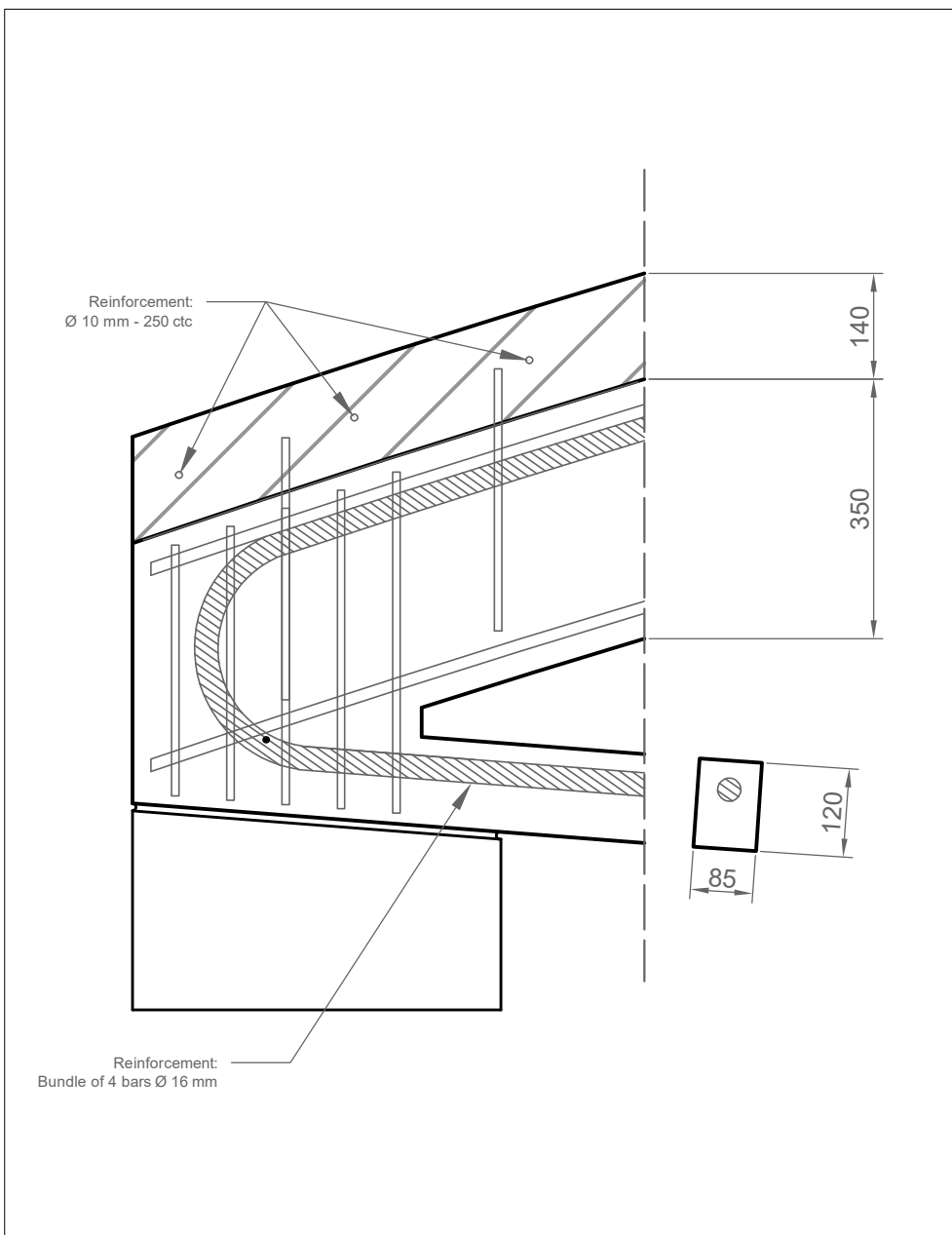
Sizes in mm



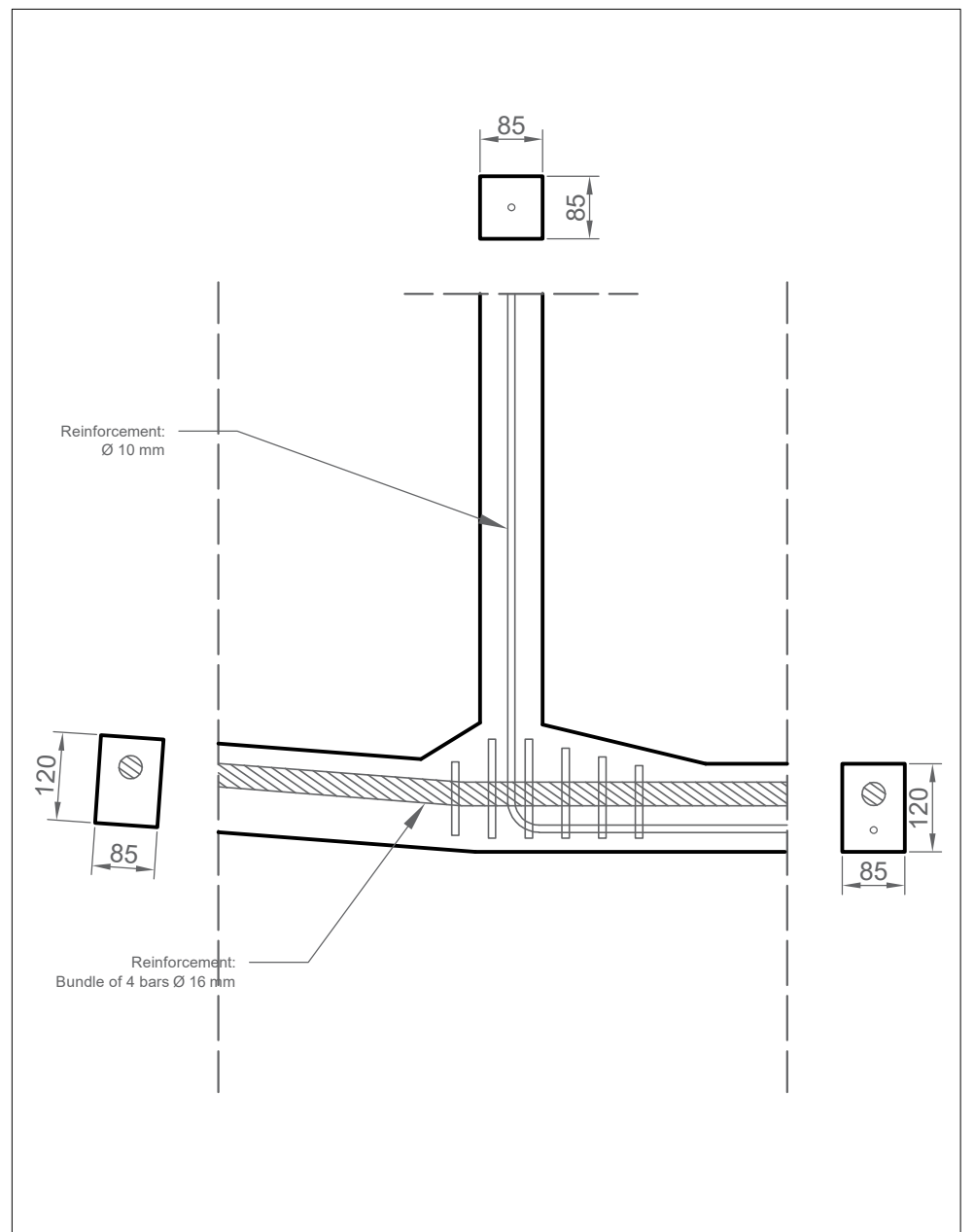
Detail 1



Detail 2



Detail 3

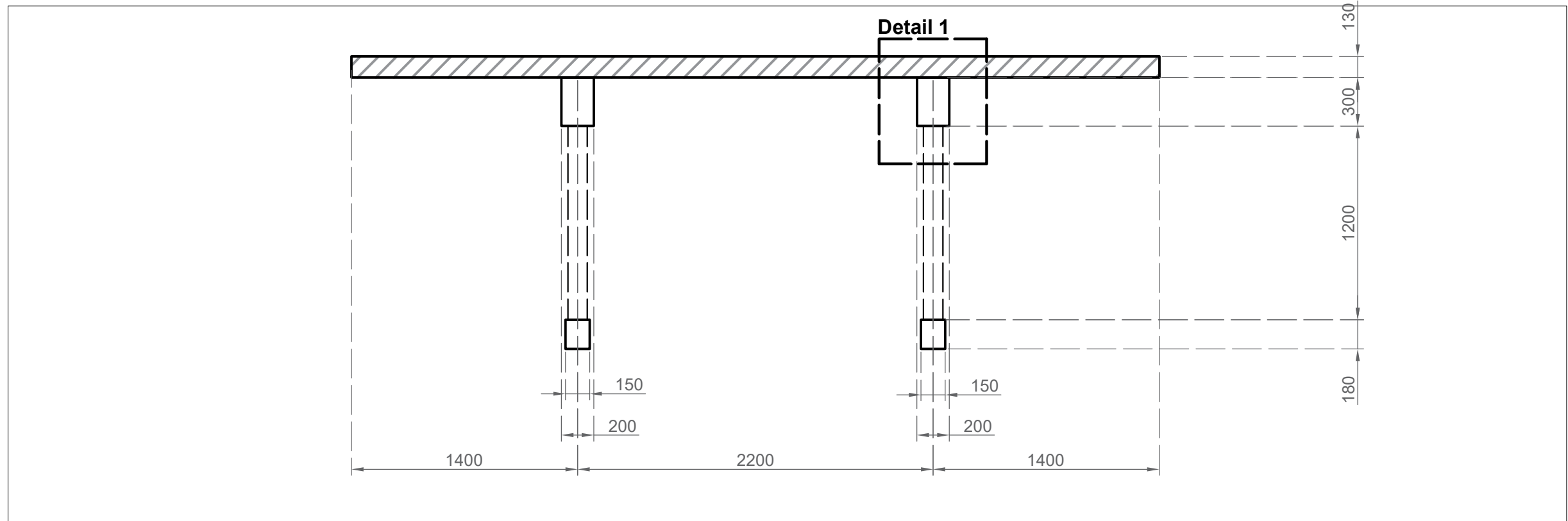


Detail 4

Details Demonstrator Bridge SSC

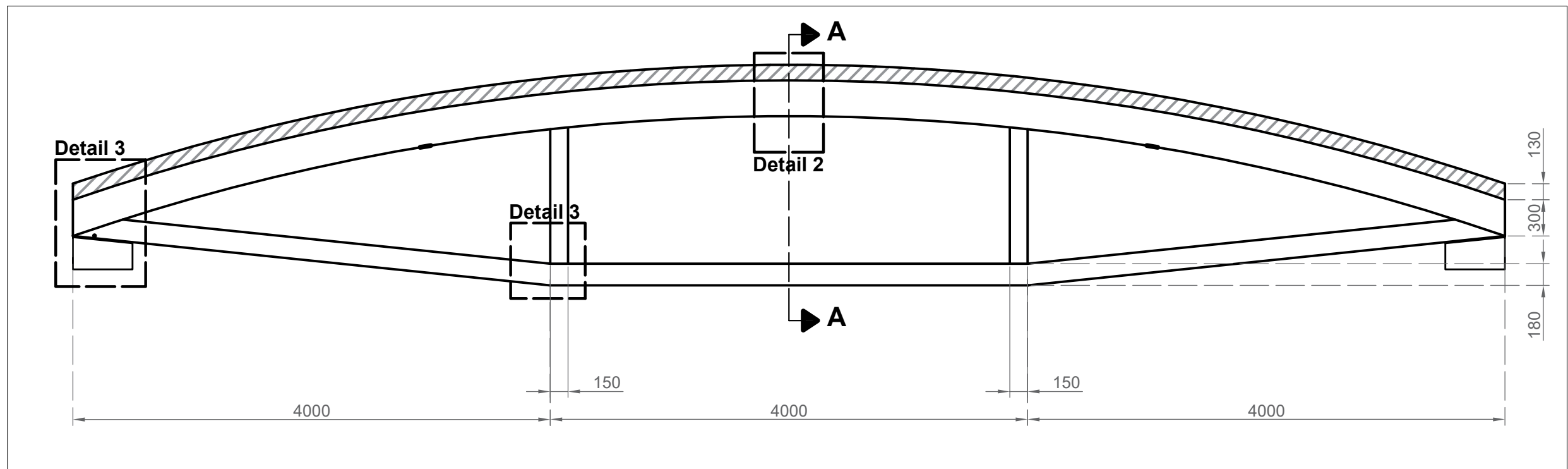
Scale - 1:10
 Sizes in mm

Appendix E: Drawings design bridge with TC



Section A

Scale - 1:20

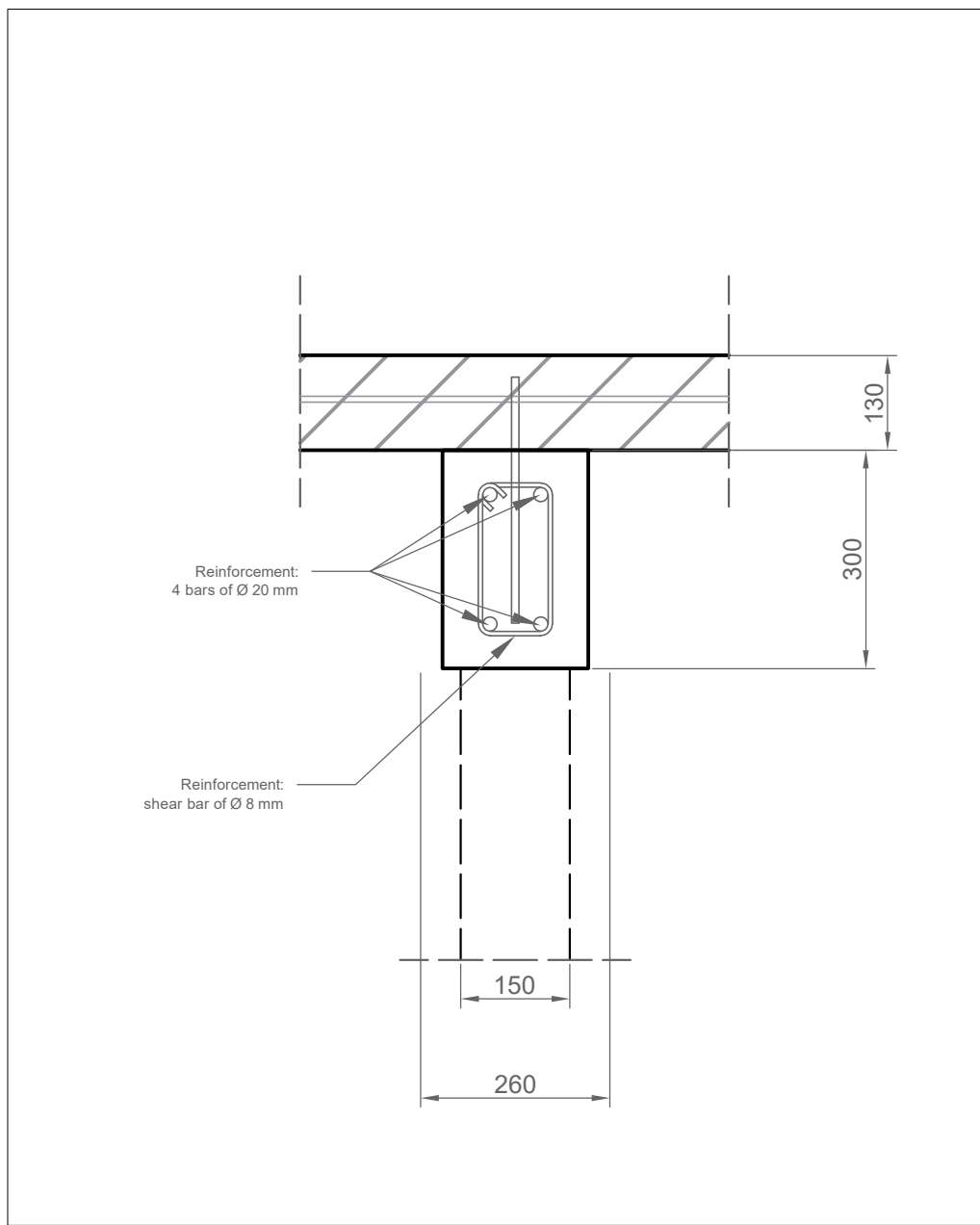


Side view

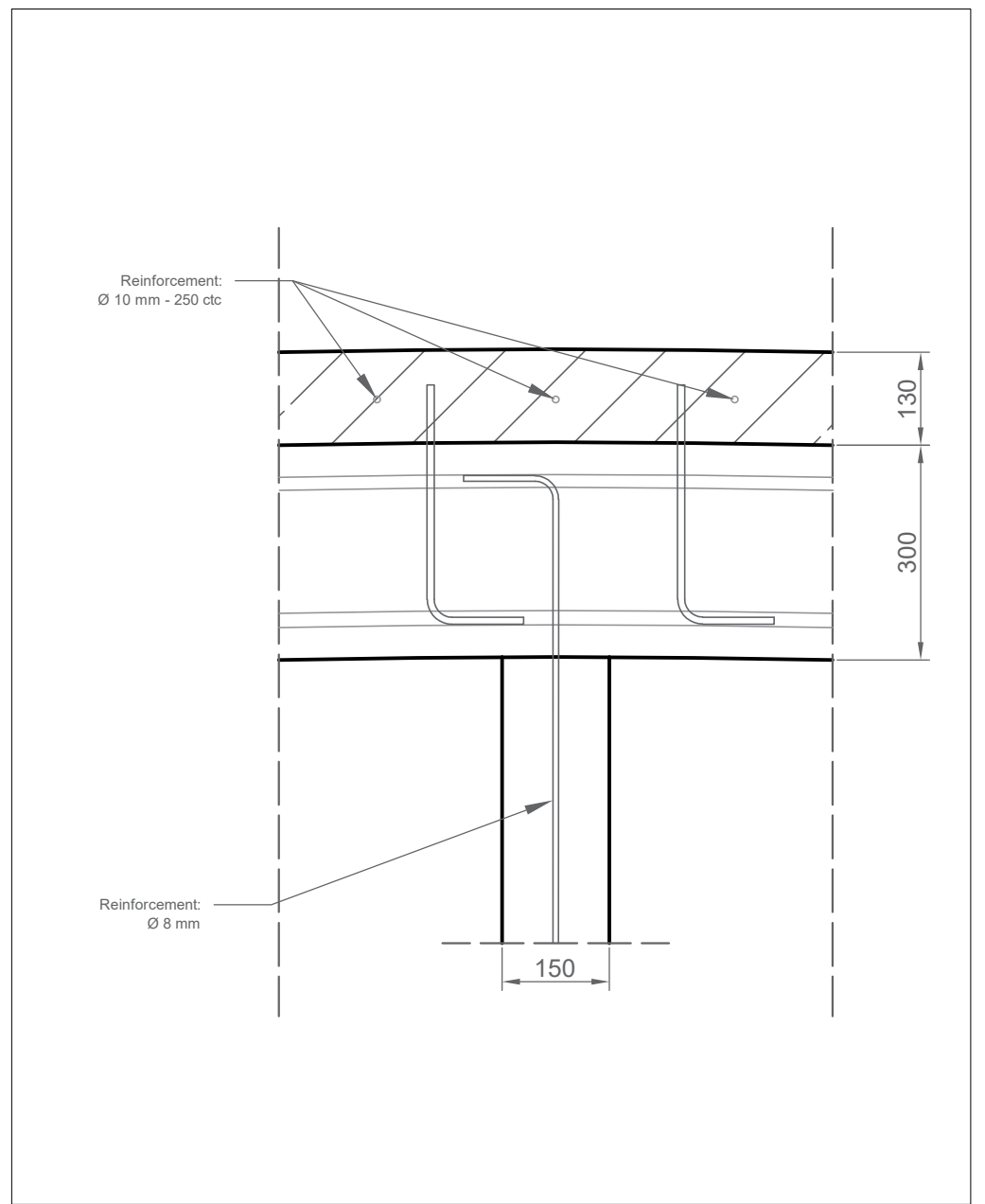
Scale - 1:40

Demonstrator bridge TC

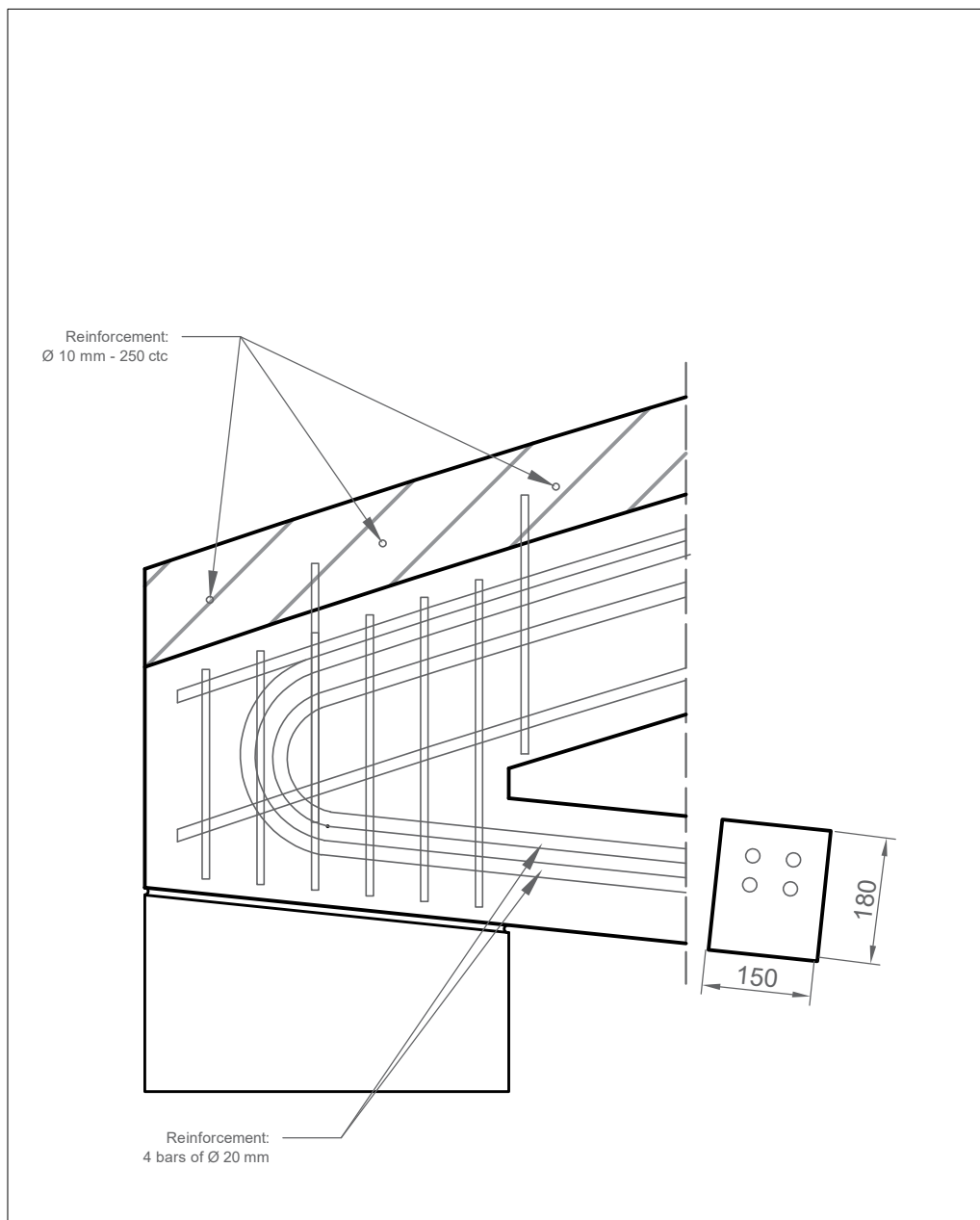
Sizes in mm



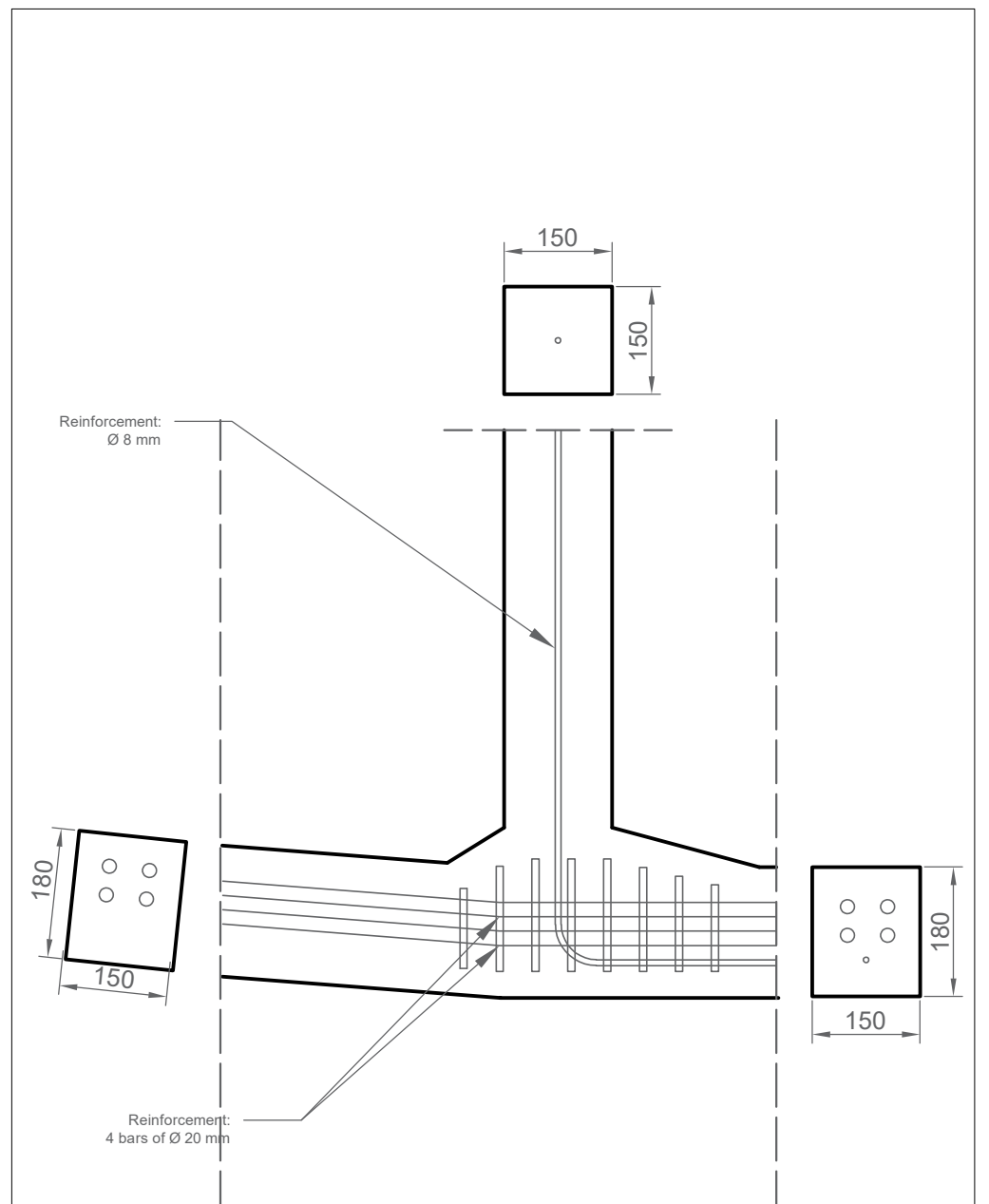
Detail 1



Detail 2



Detail 3



Detail 4

Details Demonstrator Bridge TC

Scale - 1:10
 Sizes in mm

Appendix F: Bar graphs permeability test

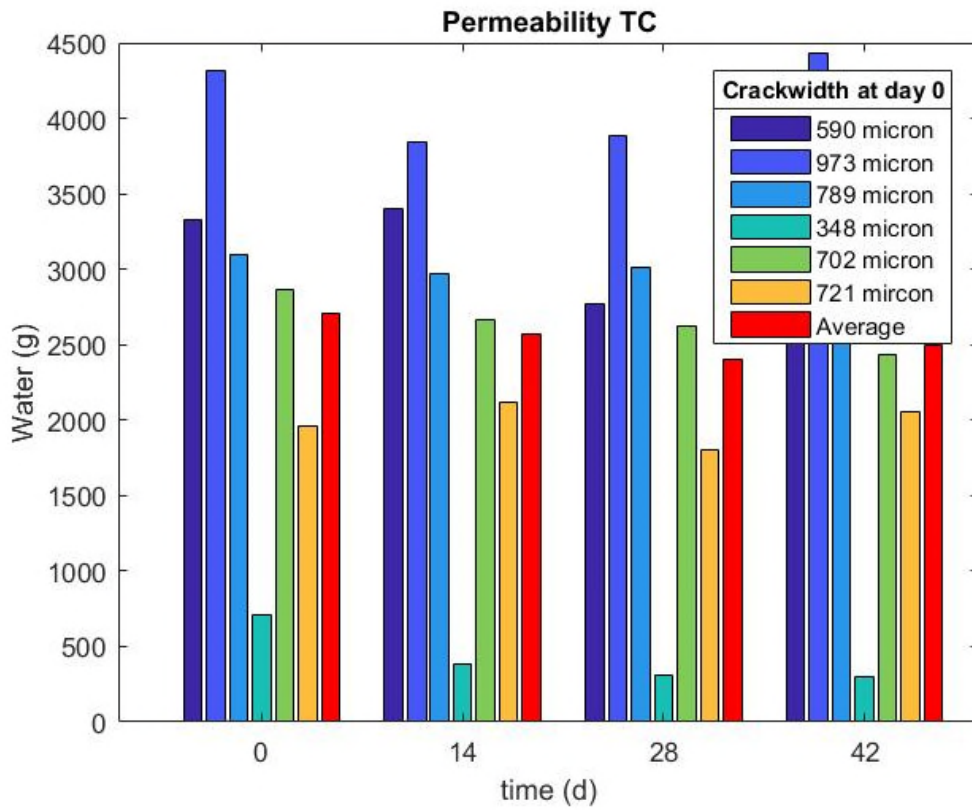


Figure 55: Development permeability TC mortar samples

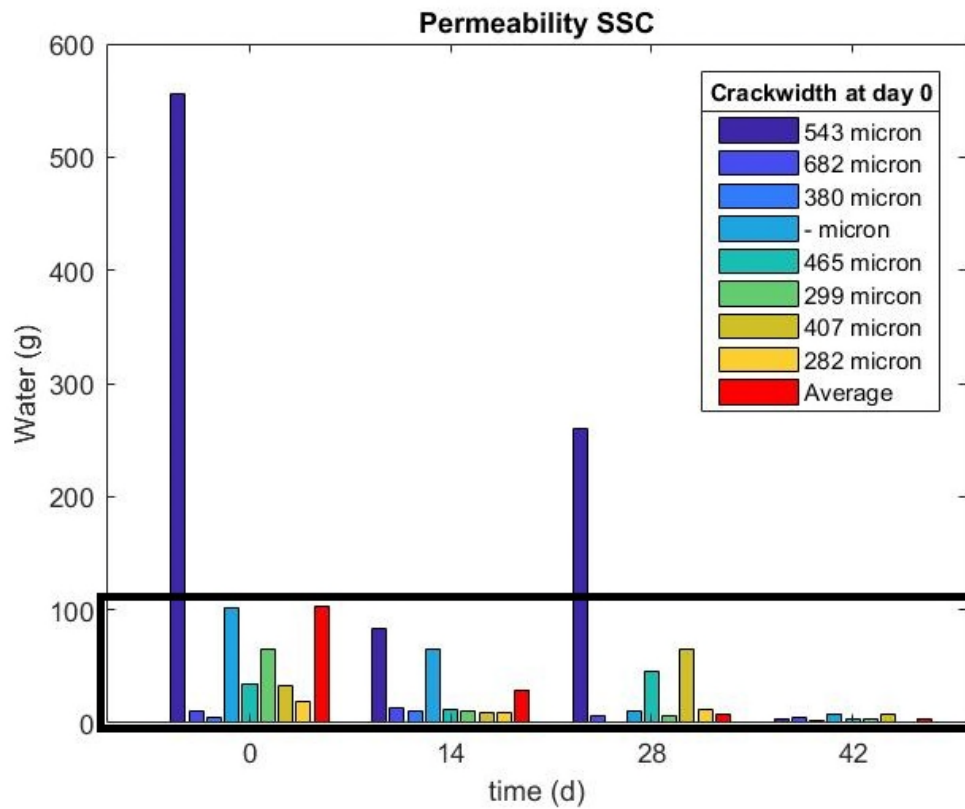


Figure 56: Development permeability SSC samples

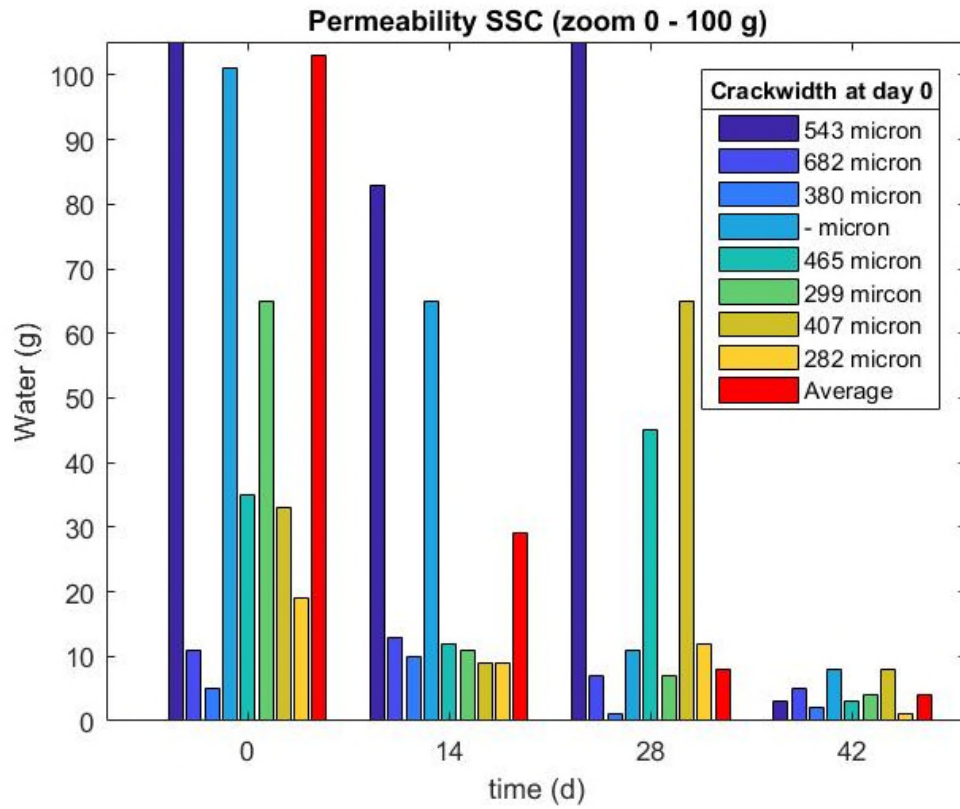


Figure 57: Zoom in development permeability SSC samples

Appendix G: Pictures permeability test

SSC samples

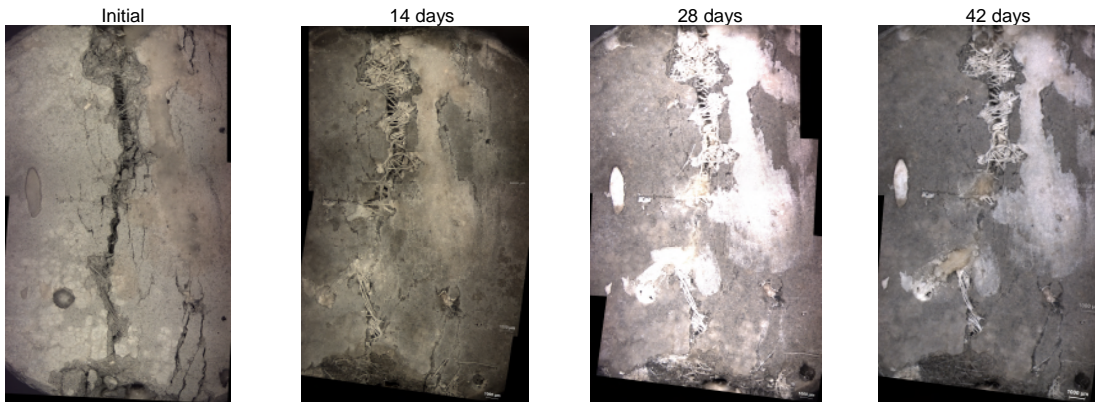


Figure 58: Pictures development permeability S2

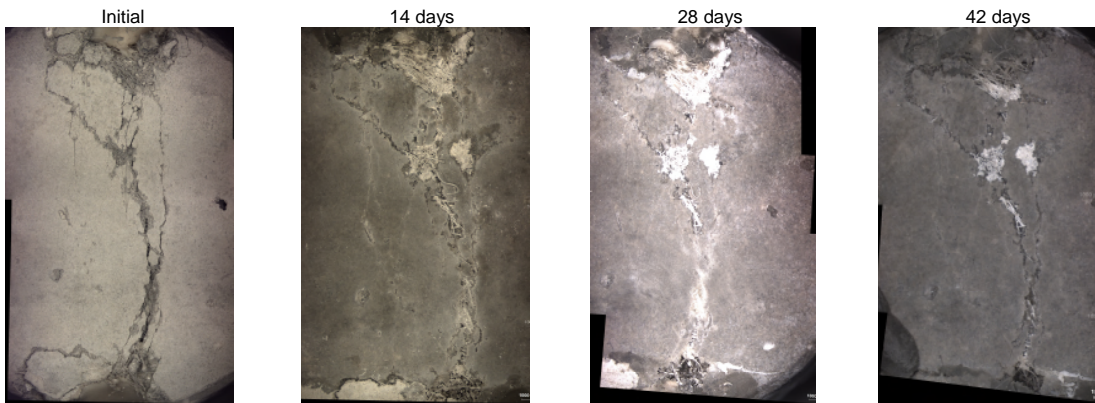


Figure 59: Pictures development permeability S3

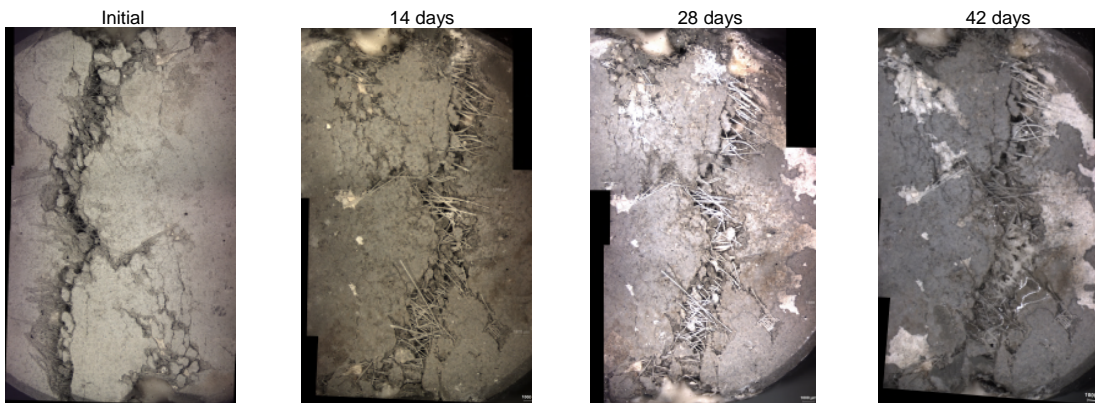


Figure 60: Pictures development permeability S4

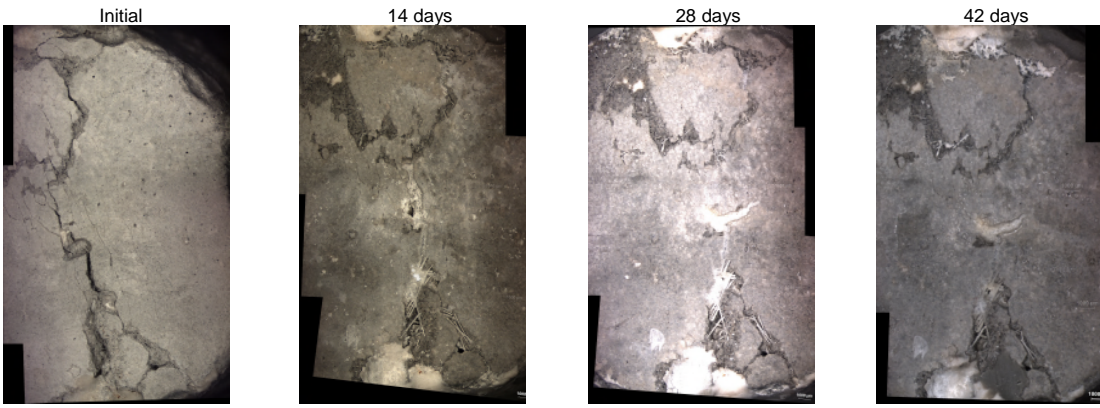


Figure 61: Pictures development permeability S5

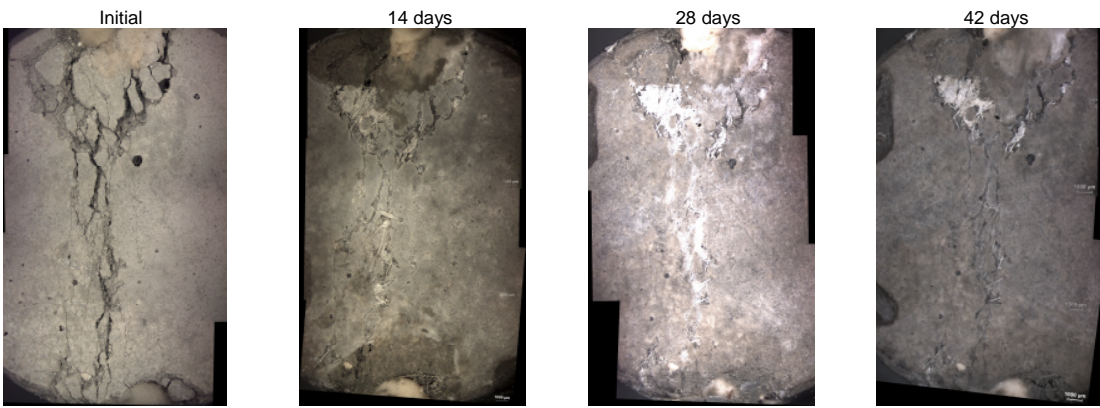


Figure 62: Pictures development permeability S6

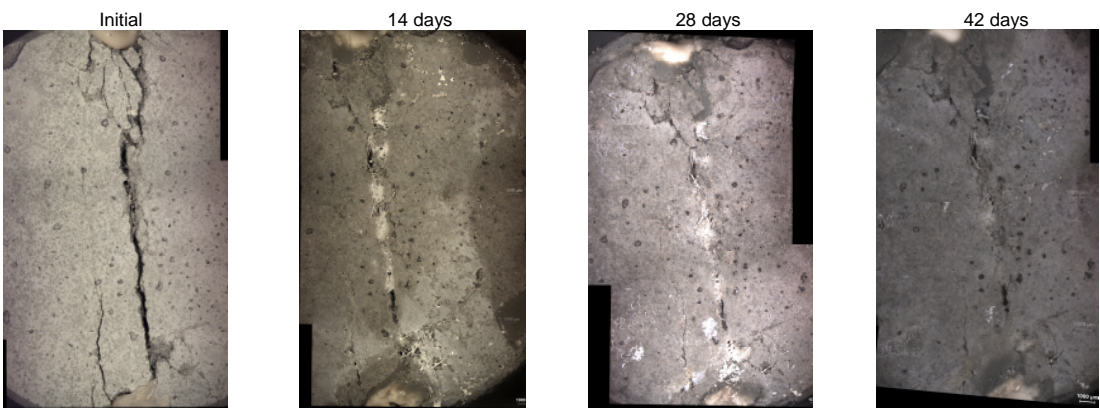


Figure 63: Pictures development permeability S7

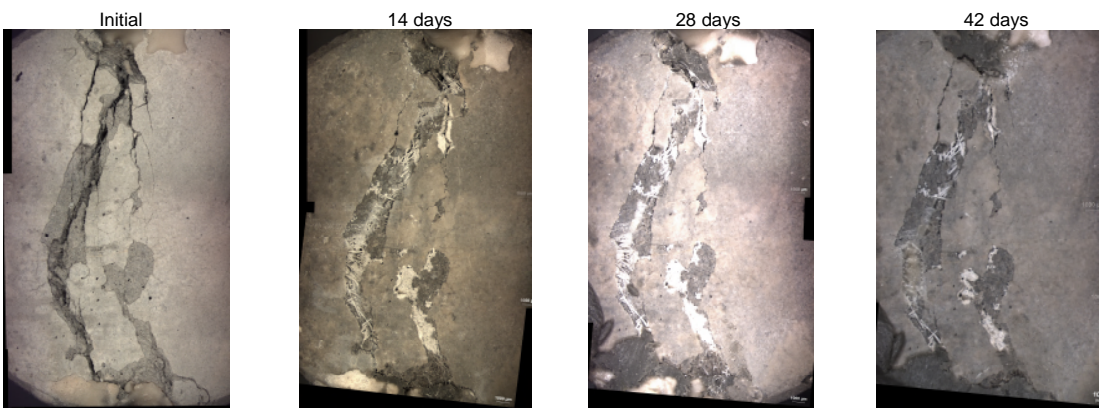


Figure 64: Pictures development permeability S8

TC mortar samples

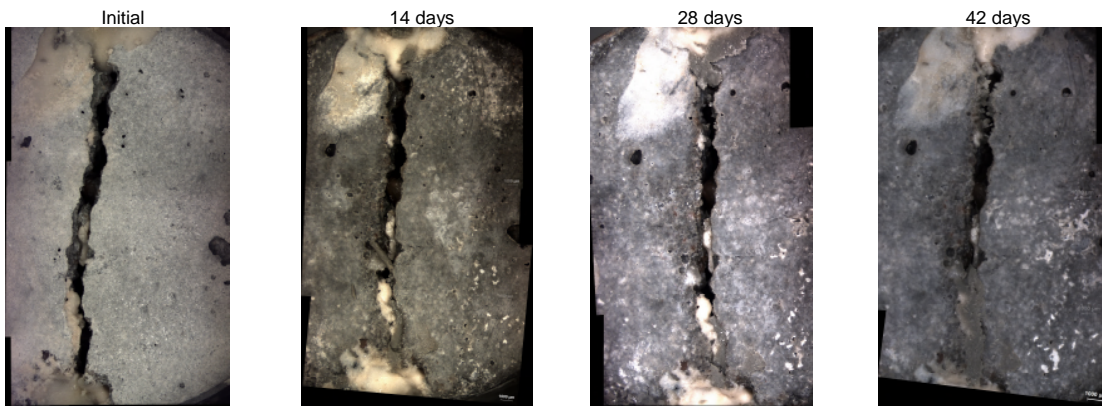


Figure 65: Pictures development permeability T2

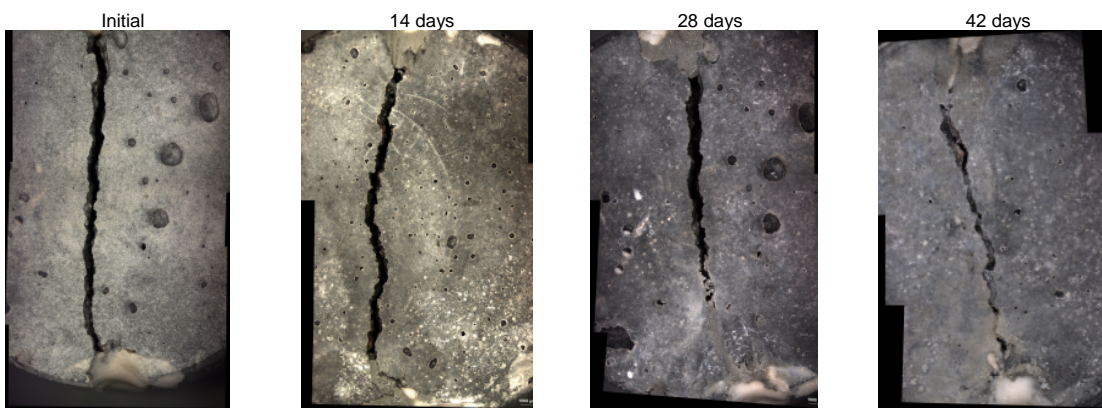


Figure 66: Pictures development permeability T3

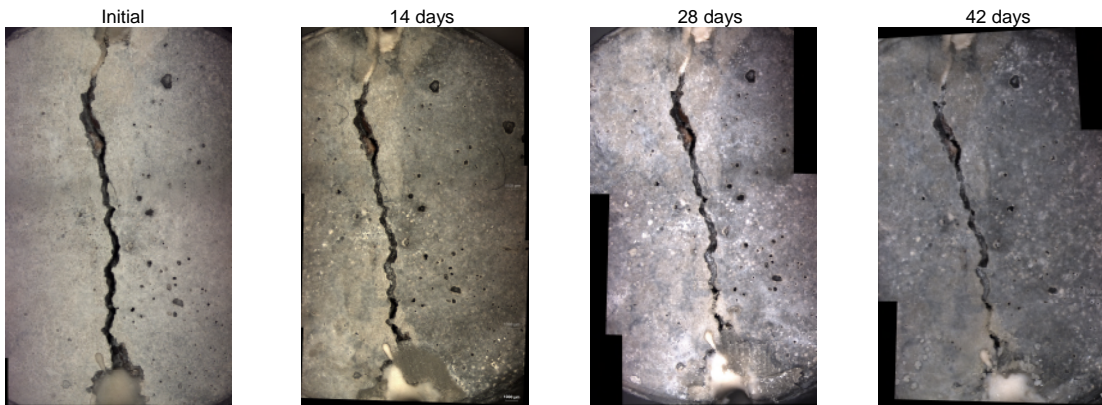


Figure 67: Pictures development permeability T4

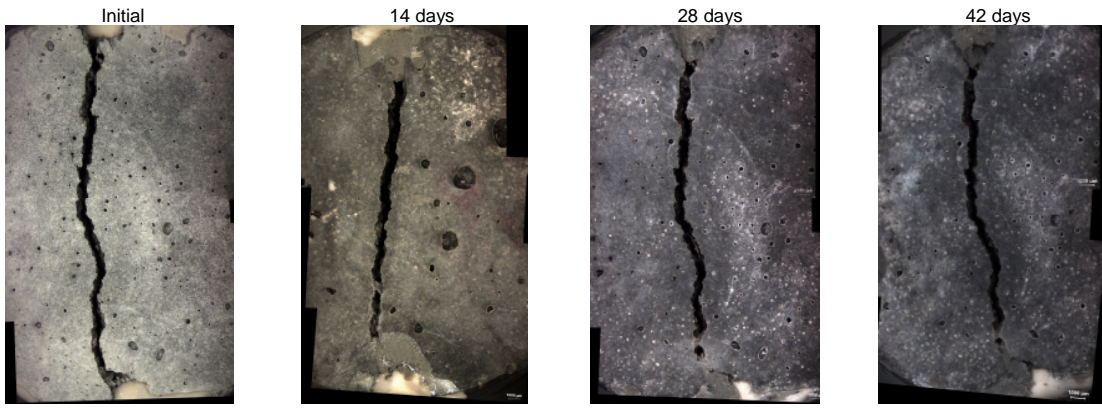


Figure 68: Pictures development permeability T5

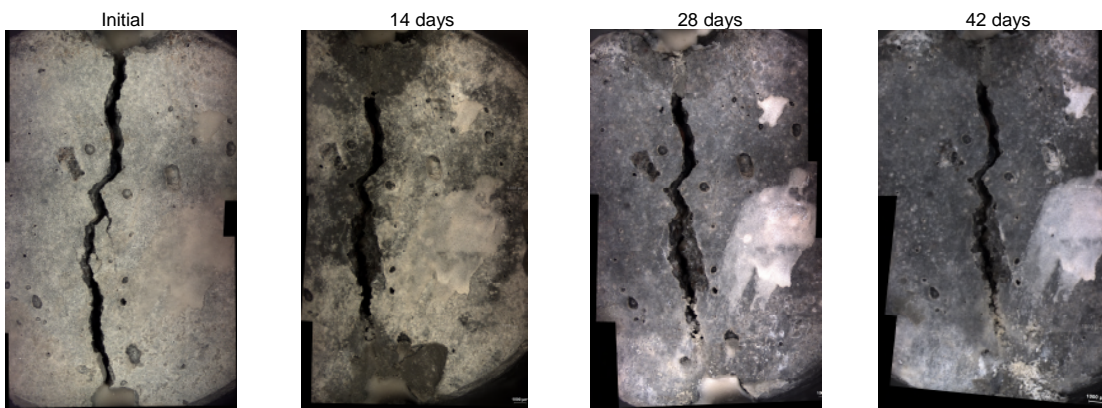


Figure 69: Pictures development permeability T6

Appendix H: Pictures RCM test

Uncracked samples



Figure 70: Chloride penetration uncracked TC mortar samples



Figure 71: Chloride penetration uncracked SSC samples



Figure 72: Chloride penetration uncracked Concrete samples

Cracked samples

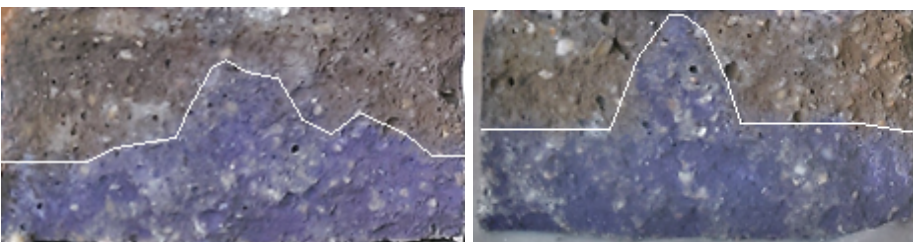


Figure 73: Chloride penetration cracked TC mortar samples



Figure 74: Chloride penetration cracked SSC samples



Figure 75: Chloride penetration cracked Concrete samples

Appendix I: Prizes materials in concrete

Table 27: Costs mixture composites and steel

Mixture composites	(€/kg)	Steel needed	(€/m)
<i>CEM I 42.5</i>	0,49 ¹	<i>Steel diameter 6</i>	0,35 ⁸
<i>Fly ash</i>	1,39 ²	<i>Steel diameter 8</i>	0,34 ⁸
<i>Limestone powder</i>	0,85 ³	<i>Steel diameter 10</i>	0,31 ⁸
<i>LWA*</i>	6,00 ⁴	<i>Steel diameter 12</i>	0,29 ⁸
<i>Plasticizer</i>	6,21 ⁵	<i>Steel diameter 16</i>	0,28 ⁸
<i>PVA fibers</i>	10,00 ⁶	<i>Steel diameter 20</i>	0,28 ⁸
<i>Sand 2-4 mm</i>	0,14 ⁷		
<i>Sand 1-2 mm</i>	0,14 ⁷		
<i>Sand 0,5-1 mm</i>	0,14 ⁷		
<i>Sand 0,25-0,5 mm</i>	0,14 ⁷		
<i>Sand 0,125-0,25 mm</i>	0,14 ⁷		

* Lightweight aggregates (55 kg/m³) with carbon source (4 kg/m³), nutrient (0,3 kg/m³), bacteria (0,015 kg/m³) and healing agent (10 kg/m³).

The prices are from the following suppliers: ¹ ENCI; ² Vliegas Unie; ³ Carmeuse; ⁴ Basilisk; ⁵ BASF; ⁶ Kuraray Europ GMBH; ⁷ Dekker grondstoffen; ⁸ Bressers metaal B.V.